Report No. FHWA-RD-79-88

ERMINATION OF THE IN SITU PERMEABILITY BASE AND SUBBASE COURSES

May 1979
Final Report

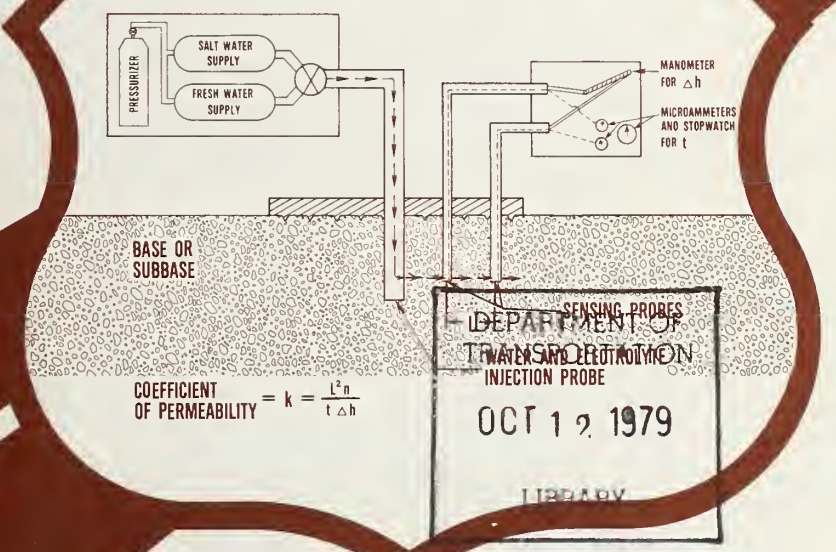

Document is available to the public through the National Technical Information Service, Springfield, Virginia 22161

Prepared for
FEDERAL HIGHWAY ADMINISTRATION
Offices of Research & Development
Materials Division
Washington, D.C. 20590

FOREWORD

This report describes the design, construction and evaluation of devices and procedures for measuring the in-situ permeability of base and subbase courses. The report will be of interest to engineers concerned with subsurface drainage.

This is the report of the study conducted by West Virginia University for the Federal Highway Administration, Office of Research, Washington, D.C., under contract DOT-FH-11-9060. This report covers the research completed May 31, 1979. Based on the results of the study, it was concluded that the field permeability testing device provides a convenient means for the determination of the in-situ coefficient of permeability with satisfactory accuracy and reproducibility. The device utilizes electrical conductivity probes to measure the velocity of flow through the granular material. The probes also serve as pressure taps for head measurements.

FHWA appreciates the assistance of the Kentucky, Maryland, Michigan, North Carolina, Ohio, Pennsylvania, and Tennessee Departments of Transportation and the West Virginia Department of Highways, in making field sites available and in providing other assistance to the researchers.

The report will be sent to members of the TRB Committee on Subsurface Drainage and members of the FCP team, including engineers in the State and FHWA field offices, who were involved in the field testing program.

Additional copies are available from the National Technical Information Service (NTIS), Department of Commerce, 5285 Port Royal Road, Springfield, Virginia 22161. A small charge is imposed for copies provided by NTIS.

Charles F. Scheffey
Director, Office of Research
Federal Highway Administration

NOTICE

Technical Report Documentation Page

1. Report No.	2. Government Accession No.	3. Recipient's Catalog No.
FHWA-RD-79-88		

4. Title and Subtitle	5. Report Date
Determination of the In Situ Permeability of Base and Subbase Courses	May 1979
	6. Performing Organization Code
	8. Performing Organization Report No.
7. Author(s)	
Lyle K. Moulton and Roger K. Seals	CES-4003
9. Performing Organization Nome and Address	10. Work Unit No. (TRAIS)
Department of Civil Engineering West Virginia University Morgantown, West Virginia	FCP 34F1273
	11. Contract or Grant No.
	DOT-FH-11-9060
12. Sponsoring Agency Nome and Address	13. Type of Report and Period Covered
Federal Highway Administration U.S. Department of Transportation Washington, D.C. 20590	Final Report May 25, 1976 - May 31, 1979
	14. Sponsoring Agency Code

15. Supplementary Notes

FHWA Contract Manager: J. R. Blystone

16. Abstract

The development of a prototype in situ test device, designated the field permeability testing device (FPTD), for determination of the permeability of highway base and subbase courses is described and discussed. The research consisted of two phases. Phase I involved the development and laboratory investigation of feasible in situ permeability measurement techniques, which led to the selection of the velocity method of in situ permeability determination for further development. Phase II involved the construction of a prototype field permeability test device (FPTD) and an extensive program of laboratory and field evaluations of this equipment. Based on the results of these studies, it was concluded that the prototype field permeability test device (FPTD) developed during this project satisfies project objectives and provides a convenient means for the determination of the in situ coefficient of permeability of highway bases and subbases with reasonable accuracy and reproducibility.

This device permits the consideration in design of saturated hydraulic conductivity (permeability) of bases and subbases and also permits the development of construction specifications for the permeability of these materials, since it makes available, for the first time, a mechanism for the evaluation and control of permeability during construction.

17. Key Words	18. Distribution Statement
Permeability tests, In Situ tests, Permeability coefficients, Highway bases and subbases	No restrictions. This document is available to the public through the National Technical Information Service, Springfield, VA 22161

19. Security Classif. (of this report)	20. Security Classif. (of this page)	21. No. of Pages	22. Price
Unclassified	Unclassified	157	

PREFACE

The authors wish to express their sincere appreciation to the Federal Highway Administration and to the many individuals and agencies that provided assistance during the course of this research effort. In particular, the authors wish to thank Mr. Jerome R. Blystone of FHWA, who served as project manager throughout the project. His technical and administrative contributions were very valuable.

The successful completion of the project would not have been possible without the cooperation of Dr. William J. Wilhelm, Chairman of the West Virginia University Department of Civil Engineering, and without the hard work and devotion of Graduate Research Assistants Chandrashaker Savant, Ran-Jay Chen, Kantilal Patel, and particularly John Kent and John Wallace, who played key roles in the development and testing of the field permeability test device (FPTD). The authors are particularly grateful to Michael Poling for his efforts in readying the FPTD for field testing and for his hard work during that phase of the project.

The field testing of the FPTD was made possible by the whole-hearted cooperation of the various state highway and transportation agencies who participated in the evaluation program. Included among those who either arranged for the field visits or actually assisted during the testing are: Robert C. Deen and Donald C. Newberry of the Kentucky Department of Transportation; William B. Greene and Robert K. Taylor of the Maryland Department of Transportation; K. A. Allemeier, Thomas A. Coleman and Rich Ostrowski of the Michigan Department of State Highways and Transportation; R. W. Spangler and Carl Auvil of the North Carolina Department of Transportation; Leon O. Talbert and R. E. Bashore of the Ohio Department of Transportation; Wade L. Gramling ; and Charles Churilla of the Pennsylvania Department of Transportation; Billy D. Evans and Luther Kite of the Tennessee

Department of Transportation; and Thomas Dugan and Donald Long of the West Virginia Department of Highways.

Finally, the authors are grateful to the West Virginia University Department of Civil Engineering secretarial staff for their efforts throughout the project, and particularly to Linda Sutherland, who typed the Phase I Interim Report, and especially to Ellen Hans for her untiring efforts in the preparation of the Final Report manuscript.

TABLE OF CONTENTS

LIST OF TABLES

LIST OF FIGURES

LIST OF FIGURES (cont.)

LIST OF FIGURES (cont.)

INTRODUCTION

There is some evidence that even the earliest road builders were aware of the need for adequate subsurface drainage (96,97). Certainly by the middle of the 18th century, it was understood that appropriate subsurface drainage was absolutely necessary for the satisfactory long term performance of roadways. The subsequent introduction of 'french drains' and the pavement systems of Tresaquet and MacAdam shows not only an understanding of the problem, but an attempt to incorporate into the roadway design formal measures for the satisfactory removal of water from the pavement structure and subgrade (87,96). In the years following these early beginnings, the number of published accounts of research dealing with highway subsurface drainage has undergone a substantial growth (33,34). In addition, there has been a steady growth in the knowledge and availability of solutions to problems of fluid flow through porous media (4, 32,45, 59,92,101). Consequently, we now recognize and understand many of the problems that can be created by excessive moisture in the subgrade and pavement structural section, and we have the means available to provide for satisfactory removal of this moisture. Therefore, it is indeed enigmatic that only relatively recently has it been clearly demonstrated that current pavement design procedures and construction specifications do not always provide for the adequate removal of water from the pavement structural section (33,35,42,108, 114).

Over the years, many highway agencies, in an effort to improve the strength of their pavement systems, have adopted specifications that require that bases and subbases be constructed of densely compacted, well graded, granular materials. While these materials have high strength when they are unsaturated, they have relatively low permeability, especially when they contain any significant quantity of material passing the No. 200 sieve (7,33,35). Thus, even

though these granular layers may be properly outletted, they often cannot carry away the water that gets into them from groundwater and/or surface infiltration fast enough to prevent saturation (33,35,108). If such a pavement structural section and its subgrade becomes saturated, its normal ability to transmit the dynamic loading imposed by traffic can be greatly impaired (8,33,35,60). The result is often pavement cracking, increased maintenance, reduced pavement life, and occasionally, complete failure of the pavement.

In an effort to minimize such problems, rational procedures have been developed (33,35,108) for estimating the amount of water that gets into the pavement structural section and for designing drainage layers (permeable bases and/or subbases) to rapidly remove this water. As part of these procedures, it is necessary that the coefficient of permeability of the base, subbase and subgrade be known so that its influence on drainage characteristics can be evaluated and considered in design. Furthermore, in order for the resulting design of drainage layers to be effective, it is necessary that a certain minimum coefficient of permeability be specified for the granular drainage layers. To this end, subgrade soils and prospective drainage layer materials can be sampled, and their coefficients of permeability can be determined in the laboratory after they have been compacted to the densities that it is anticipated will be achieved in the field. These laboratory methods are well known and are considered to be reliable (6,7,75,124,149). However, there is ample evidence that relatively small variations in gradation and density, such as those normally encountered in construction, can produce large changes in the coefficient of permeability (7,75,76,116,119). Thus, the field permeabilities of these materials may be quite different than the values determined in the laboratory. Therefore, it appears logical to consider the in situ determination of the coefficient of permeability of base, subbase and subgrade materials. In fact, proven and reliable methods for such determinations must be available before the

coefficient of permeability can be routinely specified in construction contracts in order to provide for control of materials and construction practices.

It has long been recognized that a knowledge of the coefficient of permeability is a vitally important factor in the solution of practical problems involving seepage in porous media. This is evidenced by the large volume of literature dealing with permeability and its determination (see for example the bibliographies on this subject in References 34, 67, and 133). However, relatively little information appears in the literature pertaining to the permeability of highway base and subbase materials. The works of Barber and Sawyer (7), Smith, Cedergren and Reyner (116), and Strohm, Nettles and Calhoun (119) are among the notable exceptions. Moreover, with the exception of the scheme proposed by Maytin (86), little or no effort appears to have been devoted to devising methods specifically for the in situ measurement of the permeability of highway bases, subbases, and subgrades.

It was a recognition of the need for such a test method or methods that led to the award of Contract No. DOT-FH-11-9060 - "In Situ Determination of Permeability of Base and Subbase Courses". The overall objective of this research was to develop a test apparatus and procedure that could be used to determine the in situ permeability of highway base, subbase and subgrade materials. Phase I of the project involved the development and laboratory investigation of feasible measurement techniques, leading to the selection of one technique that was used as a basis for the Phase II construction and laboratory and field evaluation of a prototype field permeability test device (FPTD). These phases consisted of specific project tasks and subtasks which were outlined as follows:

Phase I

Task A: Literature Review and Evaluation of Existing or New Techniques

Subtask A-1: Literature Review and Survey of Existing Techniques

Subtask A-2: Development and Analysis of Existing or New Techniques

Task B: Design and Construction of Laboratory Test Cells

Subtask B-1: Design of Laboratory Test Cells

Subtask B-2: Construction and Evaluation of Laboratory Test Cells

Task C: Laboratory Investigation of Promising Techniques

Phase II

Task D: Design and Construction of Prototype Field Permeability Test Device (FPTD)

Task E: Laboratory Evaluation of FPTD

Task F: Field Evaluation of FPTD

Throughout the course of this work, several very important factors regarding the nature of the problem and the required operating characteristics of the prototype FPTD were given special consideration:

1. It was recognized that the flow or seepage domain involving the highway pavement structural system consists of layered, nonhomogeneous, anisotropic media; and that of primary concern in designing the drainage of these layers was a knowledge of coefficient of permeability (saturated hydraulic conductivity) in the transverse and/or longitudinal direction (while keeping in mind the influence of the vertical permeability on the possible amount of surface water that can infiltrate into and out of the pavement structural system). The overriding influence of the horizontal flow obviously limits the usefulness of those techniques which measure only vertical permeability.
2. It was considered desirable that the prototype FPTD be capable of measuring the coefficient of permeability of individual layers varying in thickness from 3 inches (76.2 mm)

to 18 inches (457.2 mm), with coefficients of permeability ranging from 10^{-4} cm/sec to 10 cm/sec, under a variety of boundary conditions. These boundary conditions included both initially saturated and unsaturated layers as well as underlying layers that were either more or less permeable than the layer being evaluated.

3. It was considered desirable that the measurement technique adopted be nondestructive or, at least, create minimum disturbance to the layer being evaluated.
4. It was required that the prototype FPTD be simple to operate and be rugged and durable for field use.
5. It was also desired that the device be capable of measuring the coefficient of permeability within a factor of two of the true permeability ninety percent of the time.

Phase I of the research was completed in December of 1977 and an Interim Report covering that portion of work has been published (91). Although, for completeness, this report deals with both Phase I and Phase II of the project, the coverage of the Phase I research is somewhat abbreviated. For greater detail with respect to Phase I, the reader is referred to the Interim Report (91).

Although it is obvious that the various phases and tasks of the research outlined above are interrelated, for the sake of clarity, each of these tasks and aspects has been discussed separately in this report, the results have then been summarized and some specific recommendations for further research and development of the FPTD have been presented.

PHASE I

LITERATURE REVIEW AND EVALUATION OF EXISTING OR NEW TECHNIQUES (TASK A)

Introduction

The overall objectives of Task A were: (a) to provide as much information as possible about existing or potential methods of determining the in situ permeability of base, subbase and subgrade materials, by means of a thorough literature search; (b) evaluate existing techniques and/or modifications to existing techniques that might reasonably be expected to be suitable for such permeability determinations; and, (c) if necessary, investigate and/or develop new techniques for in situ permeability measurement that might be suitable for field use on highway bases, subbases and subgrades.

Although it is obvious that the review of literature (Subtask A-1) and the evaluation of existing or new techniques (Subtask A-2) are interrelated, for the sake of clarity they will be discussed separately in the following sections of this report.

Literature Review (Subtask A-1)

The initial approach to the review of literature was to utilize some existing bibliographies (34,64,67,133) on permeability determination to identify appropriate references. Each of the pertinent references, identified in this manner, was obtained, reproduced, and placed in notebooks, in alphabetical order by author, for future reference. The reference lists contained in each of these newly obtained publications were then compiled and all pertinent references not previously identified were secured, reproduced, and placed in the literature review notebooks. This process was continued until no additional pertinent references or cross-references could be identified.

As an outgrowth of this rather comprehensive process, a large number of references were collected that relate to the more general subject of hydraulic conductivity (i.e., permeability) under consideration here. In addition, a number of references were collected that pertain to the use of electric analogs for modeling flows associated with in situ permeability determination. Since most of these references did not deal specifically with methods of determining the in situ saturated permeability, they are not listed in the Bibliography. However, they were included in the bibliography of the Interim Report (91), and the interested reader is referred to that publication.

Other sources of pertinent literature included the Highway Research Information Service (HRIS), National Technical Information Service (NTIS) and recent issues of the publications in sanitary engineering, agriculture, soil science, groundwater and seepage, geophysics, etc.

Since it was recognized that analogies exist between heat transfer, the flow of electricity, and the flow of fluids in porous media, some classical references in the area of heat transfer and electricity were studied. In particular, the works of Smythe[(1)] and Carslaw and Jaeger[(2)] were given detailed consideration. However, it was found that these references were of the same general type as the classical text on seepage in porous media by Muskat (92). Although the indicated references were helpful in defining general mathematical approaches to analytical solutions for the problem, they were of little use in suggesting specific methods that might be used for in situ permeability determination.

---

(1) Static and Dynamic Electricity, McGraw Hill, New York, 1939.

(2) Conduction of Heat in Solids, 2nd Edition, Oxford University Press, New York, 1959.

A detailed review of the papers that were found to deal specifically with existing methods of in situ permeability determination showed that the methods could be grouped into a relatively small number of categories as outlined in Table 1. It is clear, from the summary presented in Table 1, that most of the existing methods for in situ permeability determination do not satisfy one or more of the performance criteria outlined in the INTRODUCTION, and, therefore, are not directly applicable to the in situ determination of the permeability of highway bases and subbases. For this reason, and for the sake of brevity, no attempt has been made to present details of the various test methods, including analytical considerations, equipment, procedures, etc. Copies of most of the papers cited in Table 1 are contained in the alphabetized literature review notebooks maintained in the Department of Civil Engineering at West Virginia University. In addition, many of the primary references (see footnote e in Table 1) have been summarized, and these summaries, which contain detail on the test methods, derivations of the governing equations, schematic diagrams, etc., are also contained in the project files at West Virginia University.

A careful evaluation of the information summarized in Table 1, and the criteria contained in the INTRODUCTION, indicated that only the two and four well systems (see References 38, 39, 70 and 118) would be worthy of further consideration relative to the in situ determination of the permeability of highway bases and subbases. In addition, it was also found that the concept embodied in the shoulder permeability test method, suggested by Maytin (86), had some promise. However, at the present time, the use of changing conductivity of the soil as an indicator of the movement of water in a transient (time dependent) unconfined flow problem is lacking an adequate mathematical explanation in terms of an appropriate theoretical solution. This concept did suggest that the change in soil conductivity associated with the flow of pore water with a salt

Table 1. Summary of Literature Review - In Situ Determination of Permeability

Test Method	Applicab. w/Respect to GWT	Direction of Measured Perm.	Relative Disturbance	Major Limitations on Applicability of Method	Applicability to Base and Subbase	References [e]
1. Individual Boreholes and wells						
(a) Uncased						
(1) Packer Tests	Below GWT	Horizontal	High	Requires Rock or Cemented Soil	Poor	1,88,127
(2) Pumping Tests	Below GWT	Primarily Horizontal	High	Below GWT, costly	Poor	10,11,90
(3) Auger Hole Method	Below GWT	Combined-Horiz. & Vert.	High	Requires Unstrat. Soil, Below GWT	Poor	12,13,68,70,71,82,88, 104,112,113,121,126,136
(4) Shallow Well Pump in (well piezometer, dry auger hole)	Above GWT	Primarily Horizontal	High	Water Quant., Equipment, Time	Poor	14,70,109,121,126,138
(b) Partially Cased						
(1) Piezometer Method	Below GWT	Varies-Depends on L/D	High	N.G. in Rocky Soils, Below GWT	Poor	13,63,68,70,80,88,89, 103,104,112,113,121,136
(2) Well Point Method	Below GWT	Varies-Depends on L/D	High	N.G. in Rocky Soils, Below GWT	Poor	47,57,63,88
(c)Pully Cased	Below GWT	Combined-Horiz. & Vert.	High	N.G. in Rocky Soils, Below GWT	Poor	52,53,54,57,63,69,70,88, 104,112(f),113(f), 127
2. Multiple Well Systems						
(a) Pumping Tests w/ Observation Wells	Below GWT	Primarily Horizontal	High	Below Groundwater Table	Poor	11,57,76,77,83,84,88, 115,133
(b) Two Well System w/one pumped into the Other	Below GWT	Primarily Horizontal	Low to High [d]	Equipment, Time, Hole Clogging	Fair to Poor [d]	38,39,70,133
(c) Four Well System	Below GWT	Primarily Horizontal	Low to High [d]	Equipment, Time	Fair to Poor [d]	70,118
3. Infiltrometers						
(a) Single Tube (Ring)	Above GWT	Combined-Vert. & Horiz.	Medium	Req. Unstrat. Soil, N.G. in C. Grav.	Poor	5,16,22,30,65,74,89,113
(b) Cylinder Permeameter	Above GWT	Vertical	High	Time, Equip., N.G. In C. Grav.	Poor	16,136
(c) Double Tube	Above GWT	Vert. w/Isotropic Soil [b]	High	Time, Equip., N.G. in C. Grav.	Poor	16,17,19,20,21,23,30, 66,98,113
(d) Gradient Intake	Above GWT	Vertical	High	Install., Equip., N.G. in C. Grav.	Poor	23
(e) Seepage Meter	Below GWT	Vertical (Indirect)	High	Exist. of External Flow Cond.	Poor	23,102,103,109
4. Air Entry Permeameter	Above GWT	Vertical	Medium	Lim. to Rel. Dry Soils, Installation	Fair	3,22,23,58
5. Spherically Symmetric Flow To/ From Spherical Cavity	(a)	Combined-Horiz. & Vert.	High	Install., N.G. In C. Grain Soils	Poor	46,63,99
6. Short Cell Apparatus	Below GWT	Combined-Horiz. & Vert.	High	Reg. Adit or Tunnel for Install.	Poor	57,88
7. Measurement of Seepage From Test Pools	Above GWT	Primarily Vertical	Very High	Disturbance, Equip., Time	Poor	85
8. Shoulder Perm. Test w/Elec. Probes	Above or Below GWT	Primarily Horizontal [c]	Low to Medium [d]	Lack of Applicable Theory	Presently Fair-Good to Excellent in Future	86

(a) Above GWT, see Ref. 46; Below GWT, see Refs. 63 and 99. (b) Combined Vert. & Horiz. w/Anisotropic Soil. (c) Actual Coeff. of Permeability not determined - Method gives relative measure of permeability. (d) Depends upon hole diameter and spacing. (e) Primary references, i.e., those that contain the most complete description of the test method and its background, are underlined. (f) Also developed for use above GWT.

concentration different than that of the natural pore water might be an effective means of measuring the seepage velocity between two points and, thus, lead to a direct application of Darcy's law for determination of permeability. Indeed, it was found that this principle had been used by Szily (120) in the study of the permeability of undisturbed sand samples and by Bouwer and Rice (26) and by Denisov (44) in the determination of the velocity of flow between two points in a natural soil deposit. Wenzel (133) even referred to the development of this method by Slitchter[1] as described in a paper published as early as 1902. This approach will be given more detailed attention in subsequent sections of this report.

Development and Analysis of Existing or New Techniques (Subtask A-2)

Introduction

The first step initiated during work on this Subtask was to consider existing techniques for in situ permeability determination that might have some promise for direct application, or might be modified for use with bases and subbases. As implied in the previous section of this report (see Table 1 and the accompanying discussion), none of existing methods satisfied all of the required criteria for use in determining the permeability of bases and subbases for the specified boundary conditions. However, further consideration of the two well (38,39,70) and four well methods (70,118) suggested that some use of the concepts embodied in these methods might be useful in developing a modified or new technique. Thus, considerable effort was devoted to the development and analysis of a possible technique that would involve the flow between two vertical wells or horizontal slots, with water being pumped from one into the other.

---

[1] Slitchter, C.S., 1902, The Motion of Groundwater, U.S. Geological Survey Water-Supply Paper No. 67, pp. 48.

For convenience, this general method will hereafter be referred to as the "circulation technique".

As noted in the preceding section of this report, the works of Maytin (86), Szily (120), Bouwer and Rice (26), and Denisov (44) suggested that it might be possible to use measured changes in electrical conductivity to determine the seepage velocity between two points in the flow domain. It was felt that if a reliable technique could be developed for measuring the velocity between the two points in this manner and the head loss between the two points could be measured or determined analytically, then Darcy's law could be used to compute the coefficient of permeability. Thus, this "velocity technique" was studied extensively.

Circulation Technique

Although it was recognized from the outset that the circulation technique was only applicable once saturated steady state flow was established between the vertical wells or horizontal slots, this restriction was temporarily set aside, and the primary effort was directed at overcoming the other limitations of the two well (38, 39,70) and four well (70,118) methods; i.e., that flow must take place in a homogeneous, isotropic porous medium with an impervious lower boundary located at a finite depth. It was found that these limitations could be overcome and, at least in principle, a solution could be obtained for the circulation of flow between vertical wells in a stratified anisotropic medium. However, this approach was abandoned as being impractical as soon as it was recognized that the solution for the permeability of any one layer was dependent upon a knowledge of the permeability of the other layers.

In order to study a system that could possibly minimize the effects of stratification, a mathematical solution was developed for the circulation of flow between a horizontal line hemi-source of finite length and a horizontal line hemi-sink of equal length and

strength located at the same depth in the flow domain beneath a horizontal impervious boundary. Using this solution, it was found analytically (and verified by electric analog) that, by properly controlling the system parameters[1], essentially horizontal flow could be maintained within relatively narrow limits. Thus, for practical purposes, the flow could be limited to a single layer of base or subbase and the effects of stratification and anisotropy could be minimized. It was envisioned that, in field use, the test setup would be essentially as shown schematically in Figure 1.

Theoretically, this system would work if initial saturation existed, or could be established, and steady state flow could be maintained for a sufficient period of time to obtain reliable measurements of flow rate and head loss between the rectangular injection and ejection tubes. However, further evaluation of the method revealed the following disadvantages:

1. The problems associated with establishing saturated steady state circulation of flow in initially unsaturated base or subbase layers appeared to be insurmountable;
2. The theoretical solution would have to be corrected to take into consideration the head losses associated with flow through the injection and ejection orifices, as well as any head losses associated with clogging of the pores near the injection tube[2];

---

[1] These include: (a) the length and width of the slots in the injection and ejection tubes, (b) the spacing between tubes, (c) the depth of the slots beneath the impervious surface, and (d) the lateral extent of the impervious surface covering.

[2] These problems could be eliminated or, at least, minimized by determining the head loss between two intermediate wells, as in the four well method (118).

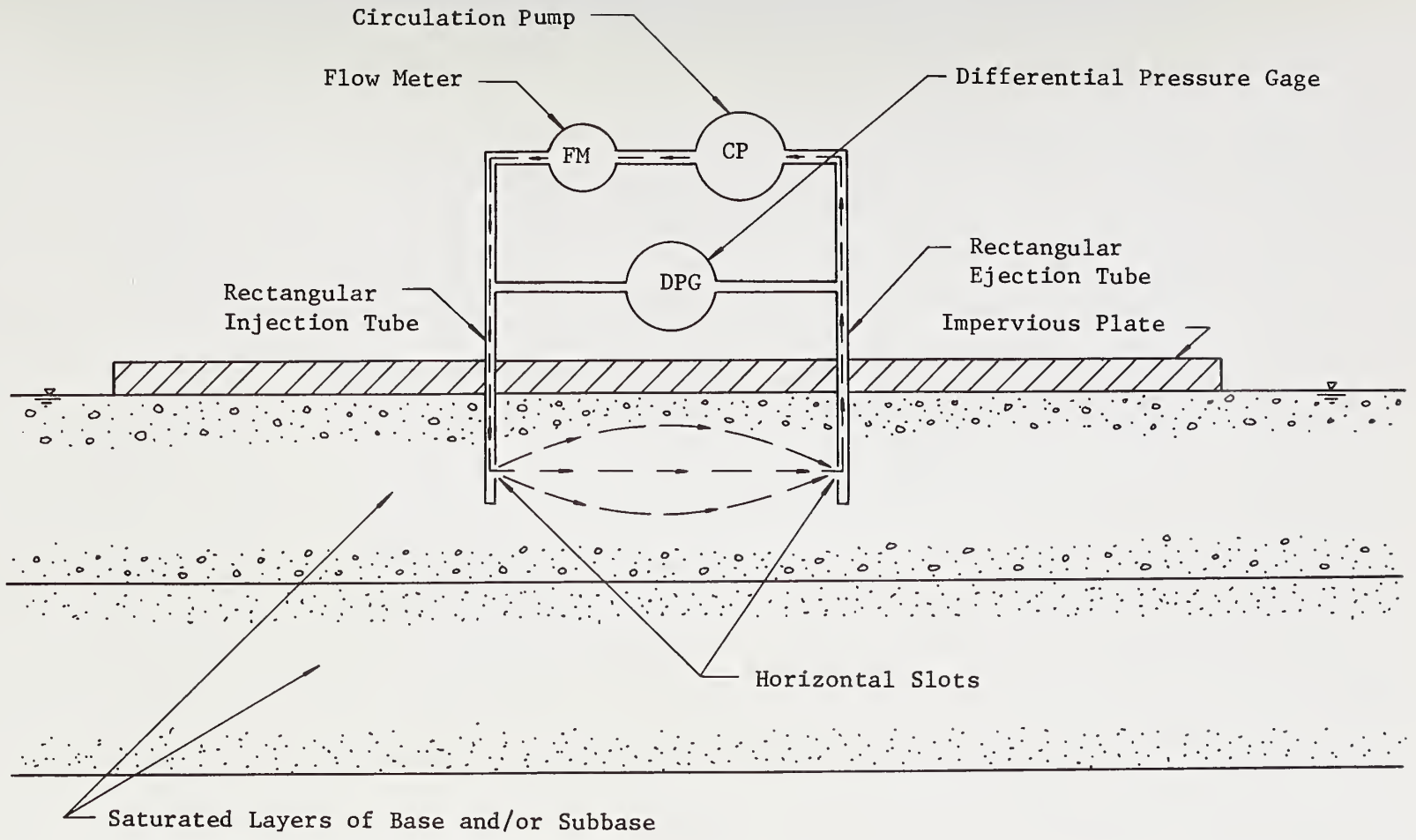

Figure 1. Schematic Diagram Showing Proposed Circulation Method of In Situ Permeability Determination

3. A small additional correction would have to be established experimentally, or by electric analog, to account for the effects of severe stratification; i.e., the effects of adjacent layers of substantially lower or higher permeability; and
4. It would be extremely difficult to establish (in advance) and maintain pumping rates that would insure that laminar flow would exist. Since the theoretical solution is based on the validity of Darcy's law, such a condition would have to be satisfied.

For the sake of brevity and clarity, no attempt has been made here to reproduce the mathematical derivations and analyses associated with the development and evaluation of the circulation technique. However, these mathematical developments are contained in the project files at West Virginia University.

Velocity Technique

As noted above, the velocity technique involves the direct application of Darcy's law, which can be stated as

$$v = ki,$$

where v is the discharge velocity, k is the coefficient of permeability (in units of velocity), and i is the dimensionless hydraulic gradient. The hydraulic gradient, i, can be expressed in finite difference form as

$$i = \frac{\Delta h}{L},$$

where Δh is the loss in total head between two points on a flow path (streamline) in the flow domain and L is the distance measured along the flow path between these two points. Furthermore, the discharge velocity, v, can be expressed as

$$v = n \cdot v_p,$$

where v_p is the seepage velocity (i.e., the actual average velocity of flow within the pores of the soil) and n is the porosity of the soil. Thus, Darcy's law can be rewritten and solved for the permeability, k, to give:

$$k = \frac{n \cdot v_p}{\Delta h/L} \quad .$$

Having arrived at this stage, the further development of the velocity technique required: (a) a method for the establishment of saturated steady state flow within the layer of base or subbase to be evaluated; (b) a method for measuring the average seepage velocity, v_p, along a flow path between two points, a known distance, L, apart; (c) a method for determining the head loss, Δh, between these two points; and (d) a method for determining the in situ porosity, n, of the base or subbase being evaluated.

Establishment of saturated steady state flow. Although several possible schemes were studied, it was ultimately concluded that the simplest method of establishing saturated steady state flow was by injecting water under constant head through a perforated injection tube located in the center of a circular plate as shown in Figure 2. Flow net studies, conducted using electric analogs, showed that the flow pattern and, thus, the configuration of streamlines and equipotential lines could be controlled by regulating the plate diameter and injection depth relative to the existing boundary conditions; i.e., the base and subbase layer thicknesses and their relative permeabilities. Ideally, it was desired to create a flow pattern such that the streamlines, within a certain zone in the top layer (i.e., the one being evaluated), would be essentially parallel to the surface. The flow net presented in Figure 2 shows that this condition can best be achieved by injection of water over the full

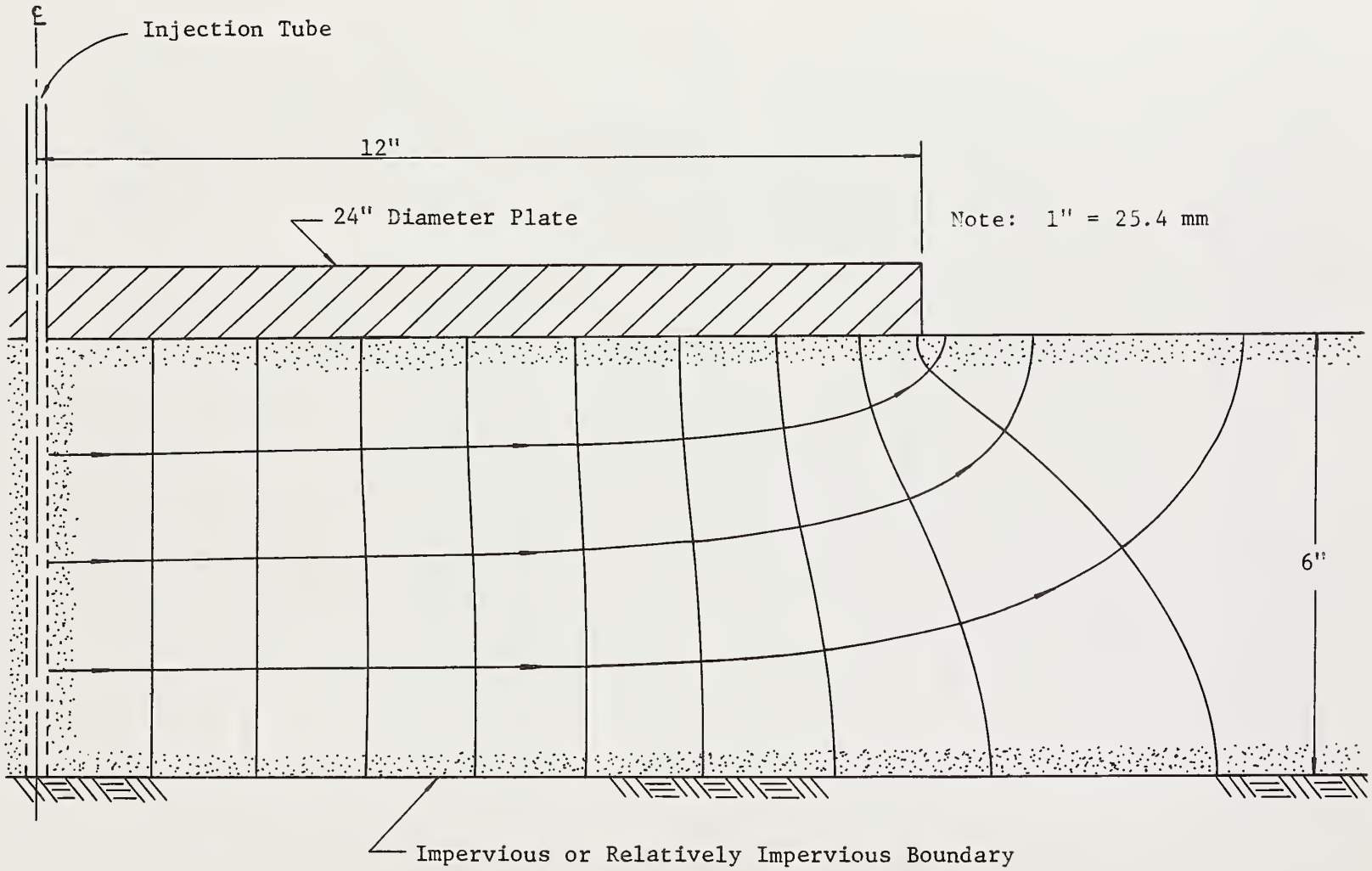

Figure 2. Flow Net for Full Depth Fluid Injection in 6" Layer Over Impervious Boundary

depth of the layer when it is underlain by an impervious stratum or one of much lower permeability. However, the flow net presented in Figure 3 shows that full depth injection is not absolutely necessary under these boundary conditions in order to establish a sizeable zone of essentially horizontal flow. When the layer under investigation is underlain by one of higher permeability, the plate diameter and injection depth become more critical, as illustrated in Figure 4. However, studies indicated that this problem was not serious and could be overcome by optimizing the combinations of plate size and injection depth for actual field use under the specified range of boundary conditions.

Measurement of seepage velocity. Initially, several techniques for the measurement of the average seepage velocity, v_p, between two points on a streamline were investigated. However, all of these techniques involved the introduction into the flow domain of a tracer of some kind and the use of a pair of sensor probes to determine the time required for the tracer to flow between them. The average seepage velocity could then be expressed as

$$v_p = \frac{L}{t},$$

where L is the distance between the sensor probes and t is the measured time required for the water containing the tracer to move between the two probes.

Although some consideration was given to the use of nuclear tracers and detectors, the potential complexity of the system and its attendant instrumentation led to the abandonment of this method in favor of the much simpler electric conductivity probes (26,44,86, 120). In this scheme, once saturated steady state flow has been established, a quantity of electrolyte solution is introduced through the injection tube and electric conductivity probes are used to time the rate of flow between two selected points on a streamline.

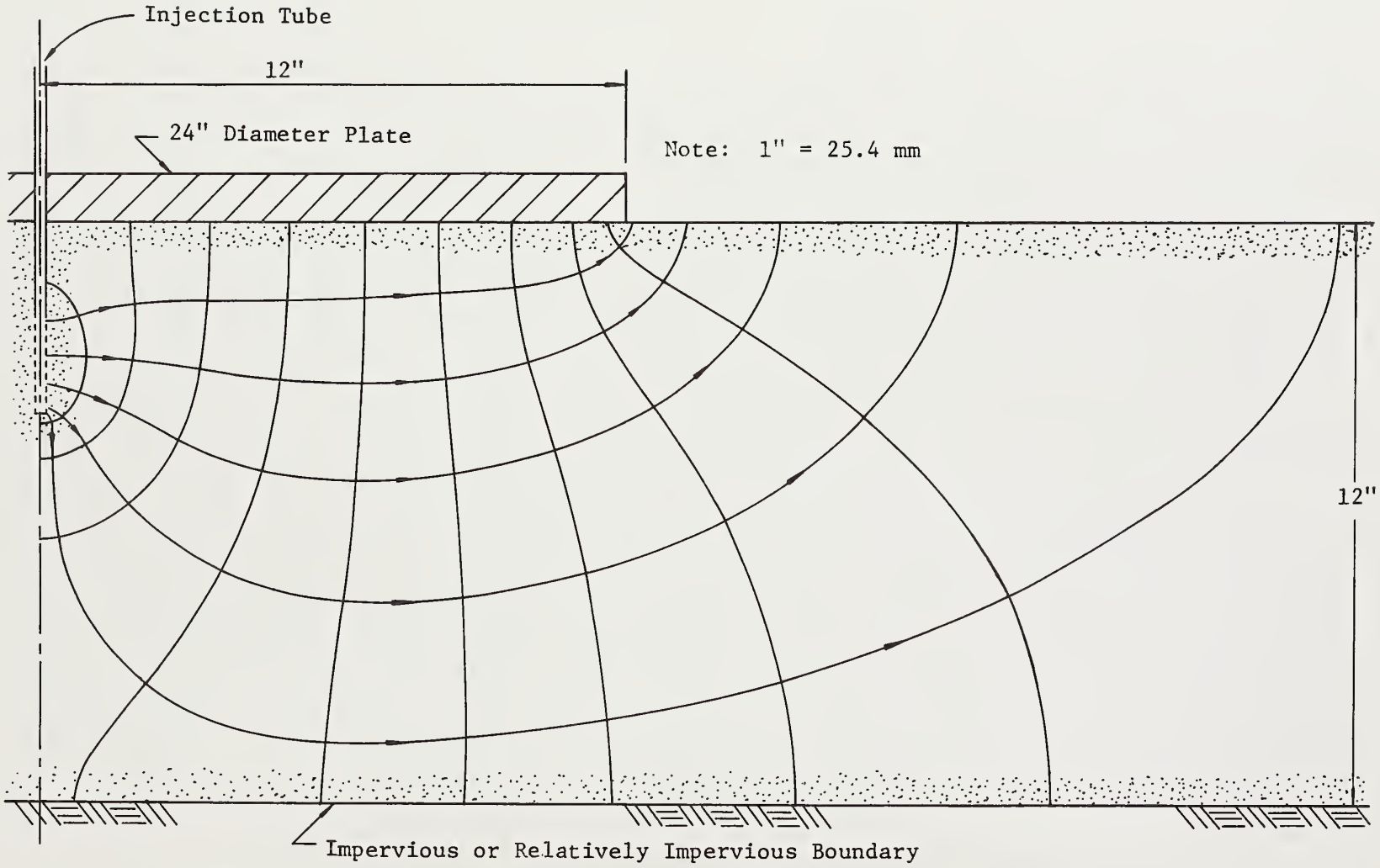

Figure 3. Flow Net for Limited Depth Fluid Injection in 12" Layer Over Impervious Boundary

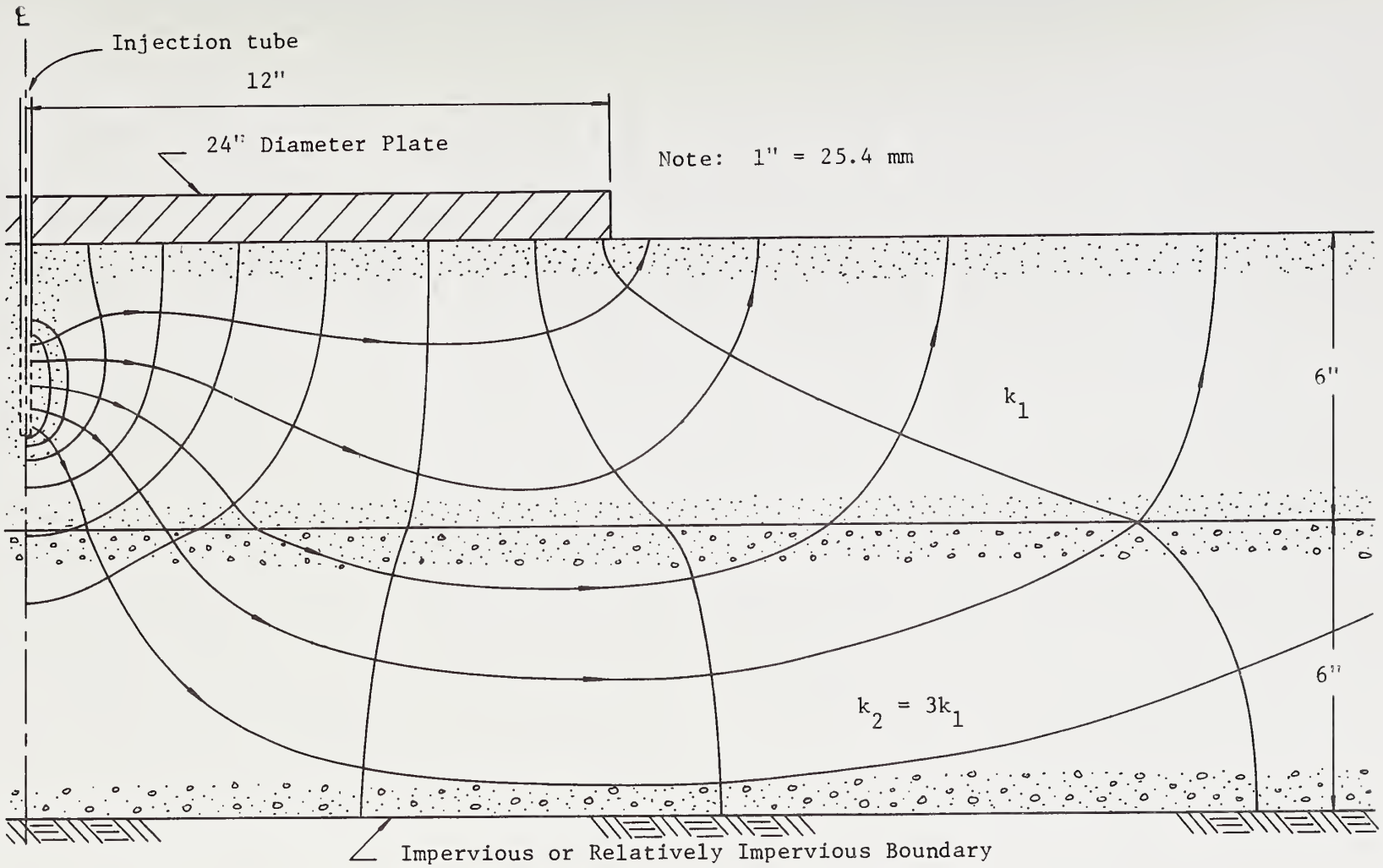

Figure 4. Flow Net for Limited Depth Fluid Injection in 6" Layer Underlain by Layer of Higher Permeability

Three different combinations of conductivity probes and detector devices were considered. At first, a three wire probe was used, and the change in conductivity in the flow media was indicated by a change in recorded potential within the circuit (see Figure 5a). A simpler and more sensitive two wire probe with a recorder indication was also investigated (see Figure 5b). Typical recorder traces produced by the three wire and two wire probes are shown in Figures 6a and 6b, respectively. Unfortunately, the recorder response for both of these systems is dependent upon a great many factors including the initial conductivity of the flow medium, the chemical composition and concentration of the electrolyte solution, the rate at which dispersion and diffusion of the electrolyte take place, the recorder sensitivity setting, the recorder chart speed, etc. Furthermore, the anticipated use of a relatively complex recorder system under field conditions raised considerable doubt with respect to the reliability, economy and overall efficacy of these techniques. Therefore, the direct indication of conductivity, using a two wire probe and a microammeter, was investigated. After some experimentation, this technique was judged to be the simplest, most effective, and most economical for both laboratory and field use.

Determination of head loss. Two possible methods were considered for determining the head loss, Δh, between the velocity measuring probes in the flow domain: (a) the analytical (mathematical) evaluation of the head loss between the two points as a function of the measured flow rate and total head loss through the system, and (b) the direct measurement of the head loss between the two points.

Although it was found that, in principle, a solution to the general class of radial flow problems under consideration (see Figures 2, 3, and 4) could be obtained, it was concluded that the rather complex solution that resulted would be of little practical value, since the calculation of the head loss was dependent upon a knowledge of the ratio of the permeabilities of the various layers

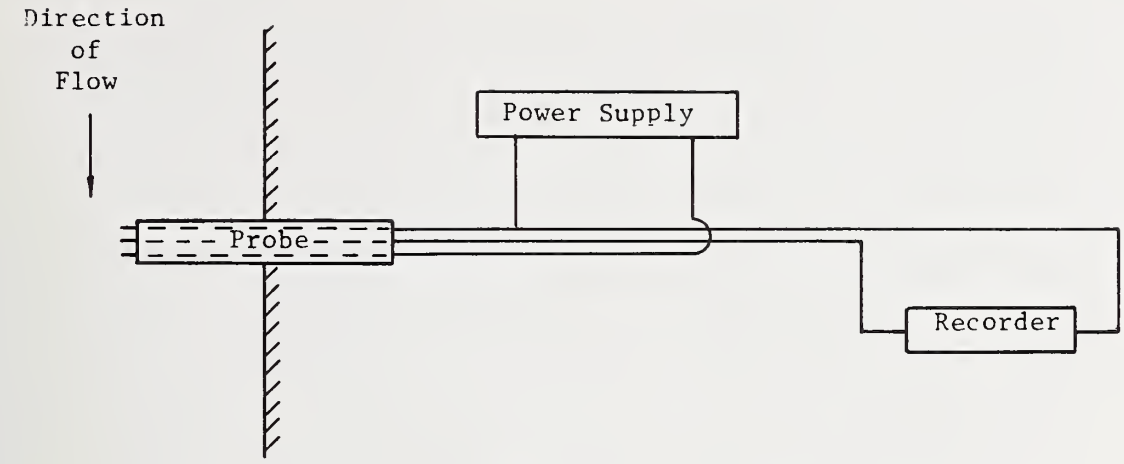

(a) Three-Wire Probe System

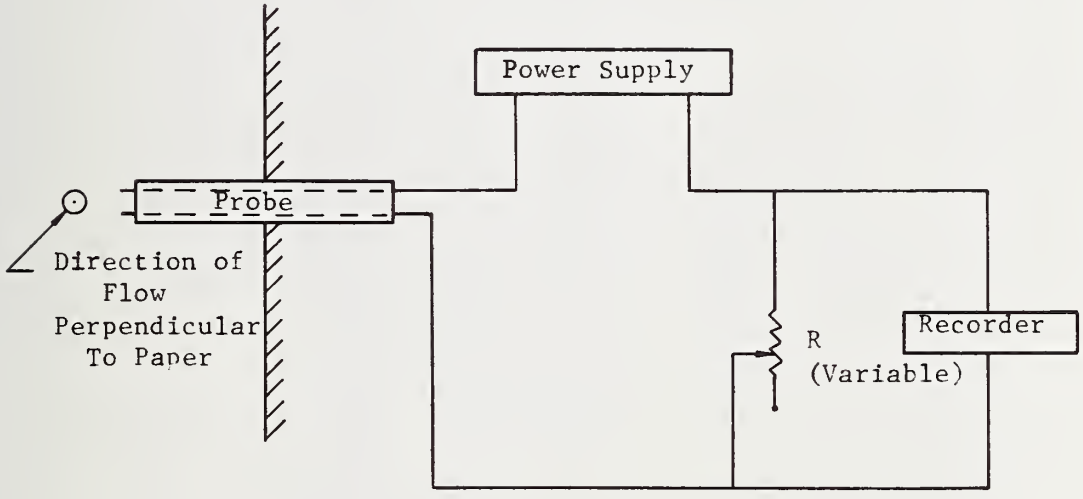

(b) Two-Wire Probe System

Figure 5. Schematic Diagrams Showing Comparison of Two and Three Wire Probe Systems for Sensing Changes in Electrical Conductivity of Flow Medium

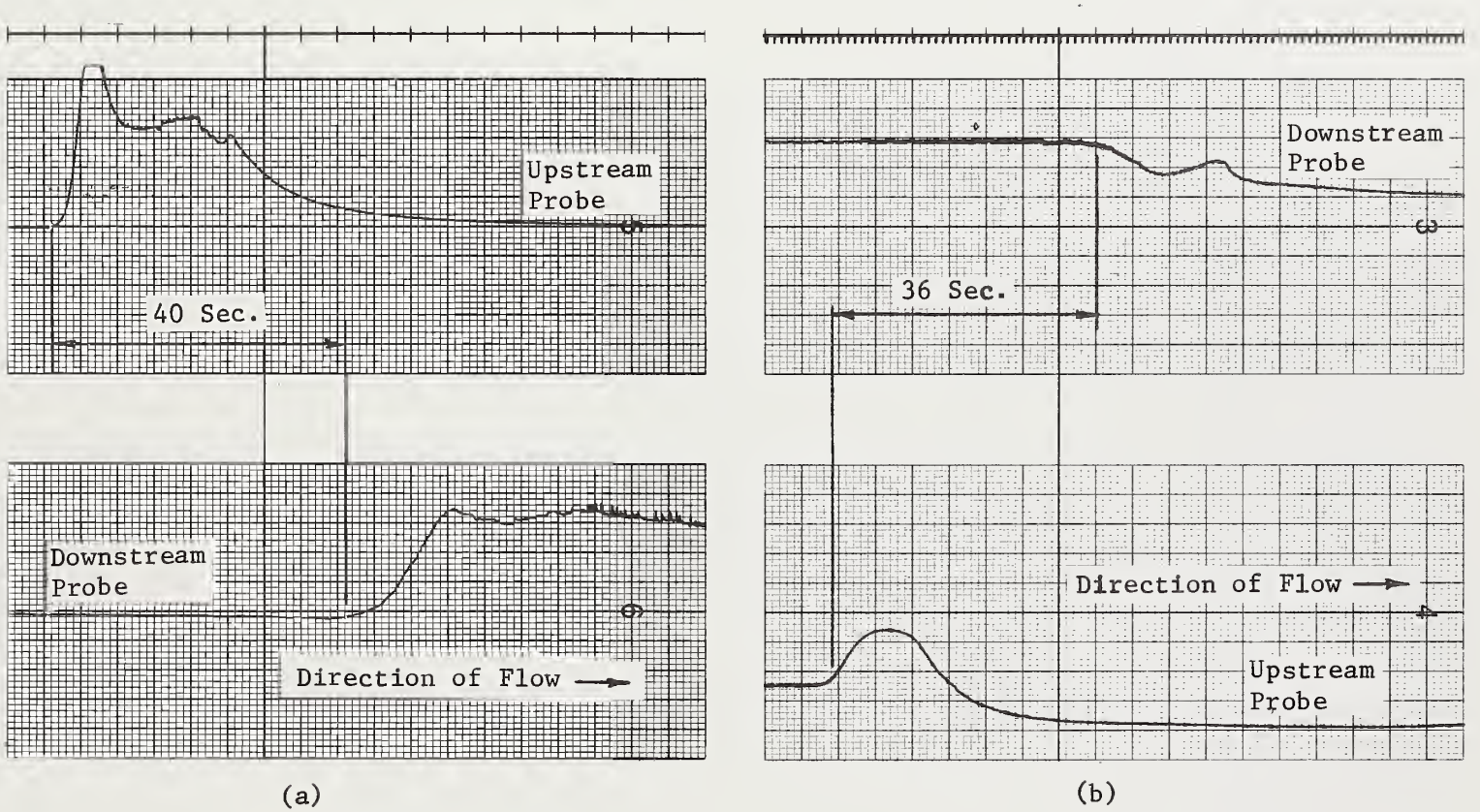

Figure 6. Typical Recorder Traces Produced by (a) Three Wire and (b) Two Wire Electrical Probes During Saturated Flow in Ottawa Sand - Probes Spaced 5 Inches (127 mm) on Centers - Chart Speed = 1 mm/sec.

in the flow domain. Therefore, it was decided that the head loss, Δh, would be determined by direct measurement of the fluid pressures at the ends of the electric conductivity probes. After some experimentation, it was found that this could be accomplished very simply by the use of a manometer or differential pressure gage (DPG) connected to pressure taps incorporated into the electric conductivity probes, as illustrated in Figure 7. The configuration of the electric conductivity probe was subsequently modified based on the experience gained in Tasks C and D.

Determination of porosity. The porosity, n, of the layer under consideration can be determined from the well known relationship

$$n = 1 - \frac{\gamma_d}{G_s \gamma_w}$$

where γ_d is the dry density of the soil, G_s is the specific gravity of the soil solids, and γ_w is the unit weight of water. In general, all of the quantities on the right hand side of this equation are either specified or known within reasonable limits for the base and subbase materials being used on highway construction in any particular area. If necessary, the dry density can be measured with little or no disturbance using well known techniques employing a nuclear moisture-density gage.

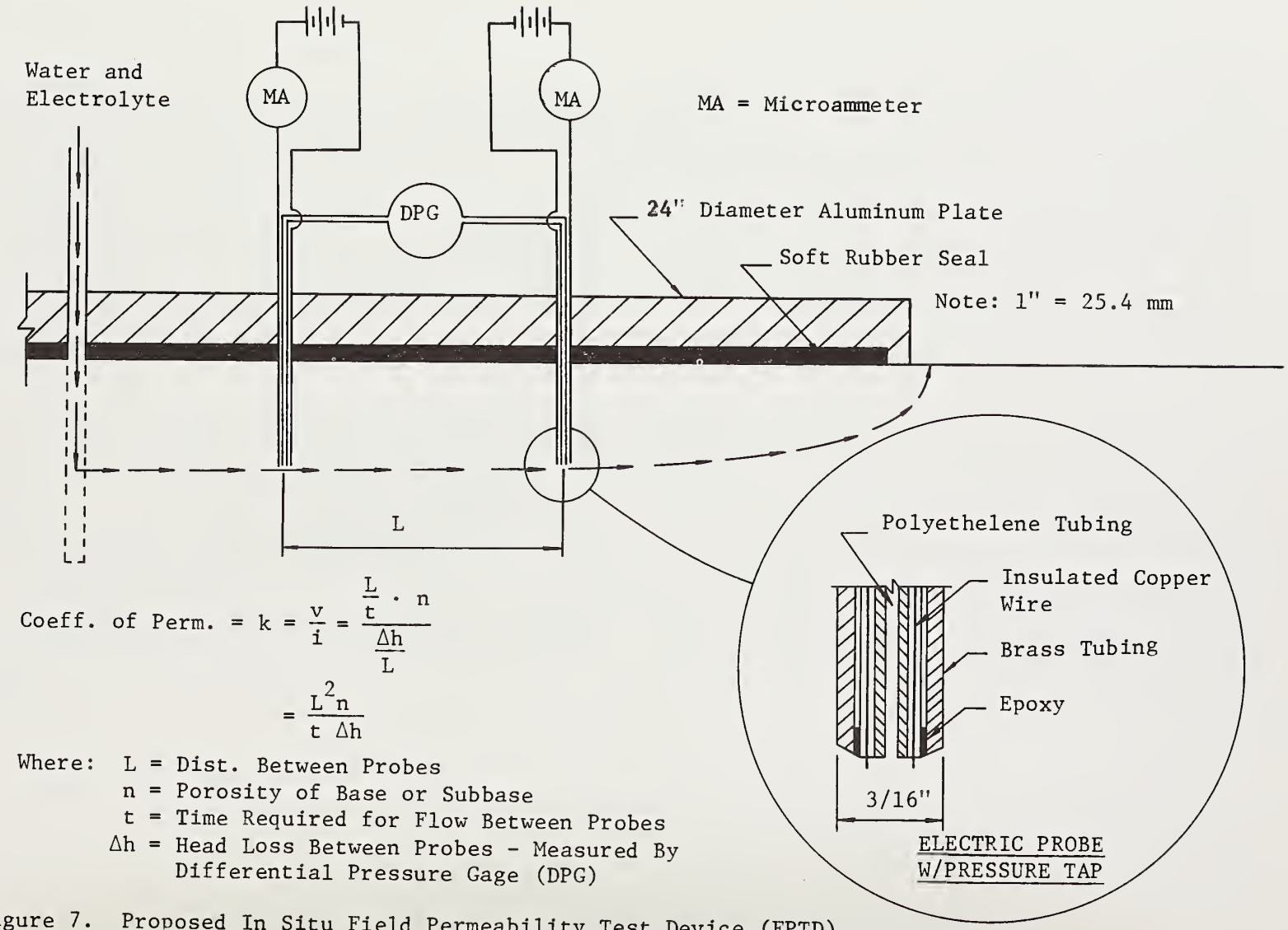

$$\text{Coeff. of Perm.} = k = \frac{v}{i} = \frac{\frac{L}{t} \cdot n}{\frac{\Delta h}{L}}$$

$$= \frac{L^2 n}{t\ \Delta h}$$

Where: L = Dist. Between Probes
n = Porosity of Base or Subbase
t = Time Required for Flow Between Probes
Δh = Head Loss Between Probes - Measured By Differential Pressure Gage (DPG)

Figure 7. Proposed In Situ Field Permeability Test Device (FPTD)

DESIGN AND CONSTRUCTION OF LABORATORY TEST AREAS (TASK B)

Introduction

The laboratory permeability test areas were designed and constructed to permit testing and evaluation of the proposed field permeability testing device (FPTD). Based on certain performance and construction requirements as well as physical limitations, two separate test cell systems were selected to comprise the test area. One of the systems was designed for use with low permeability base and subbase materials whereas the other was designated for use with high permeability base and subbase materials. However, the general performance requirements and operational features of both systems were essentially the same. Each test cell system consists principally of three subsystems:

1. The individual cell subsystem: their size, configuration, structural components, and support.
2. The hydraulic circulation subsystem: components, sizes, and configuration.
3. The saturation/underdrainage subsystem: size, components, and configuration.

This portion of the report contains an outline of the general design and operational requirements for the laboratory permeability test cell systems and a brief description of the physical and operational features of the systems. The details of the design, construction and operation of the systems are presented in Appendix A.

Design, Construction and Operational Requirements

The following requirements were established for the laboratory test cells. The criteria are organized as they relate to the three subsystems.

Individual Cell Subsystems

The physical features of the individual cells were based on the following considerations:

1. It should permit the simulation of a full scale pavement section.[1]
2. Its boundaries should not influence the flow condition introduced by the FPTD and, hence, the permeability of any or all of the soil layers adversely.
3. It should permit the establishment of steady sheet flow through the pavement section to facilitate the evaluation of the permeability of the simulated pavement layers.
4. The water head should be able to be controlled across the simulated pavement section.
5. It should permit ease of measurement of flow through the simulated pavement section.
6. It should permit slow and uniform saturation of soil from the bottom.
7. It should be constructed with relative ease and should be light enough to be handled by the overhead crane in the laboratory.
8. A sufficient number of cells should be provided to permit testing a variety of aggregate/soil layer combinations while minimizing time and material handling requirements.

Hydraulic Circulation Subsystem

The following operational criteria were considered in the design of the hydraulic circulation system:

---

[1] Conventional highway standards and practice indicate that the cross slopes of the highway pavement would not be more than 10 percent.

1. The hydraulic circulation system should be capable of supplying the test cells continuously with a sufficient quantity of water.
2. It should provide for accurate measurement of the flow.
3. It should be economical in its use of water.
4. It should be easy to work with.
5. It should be fail-safe.

Saturation/Underdrainage Subsystem

The design of the saturation/underdrainage subsystem was governed by the following criteria:

1. It should saturate the soil slowly and uniformly without disturbing it.
2. It should be controlled so that a constant level of saturation could be maintained.
3. It should be able to act as a subsurface drainage system.

Physical and Operational Features

Based on the criteria summarized in the previous sections as well as certain physical and equipment limitations, a laboratory permeability testing system was designed that consisted of two independent sets of three concrete test cells and their associated hydraulic circulation and saturation/underdrainage subsystems. As noted earlier, one of the systems was designed for use with low permeability base and subbase materials and the other was designed for use with high permeability bases and subbases. The physical features of the individual test cells comprising these systems are illustrated in Figure 8. An overall view of the high permeability cell system, showing the individual cells and hydraulic circulation system, is shown in Figure 9.

Figure 10 illustrates schematically the basic cell and hydraulic configuration that is common to both high permeability and low permeability systems. Operationally, the system functions as follows: Water from the sump tank (B) is pumped (A) to the upstream constant

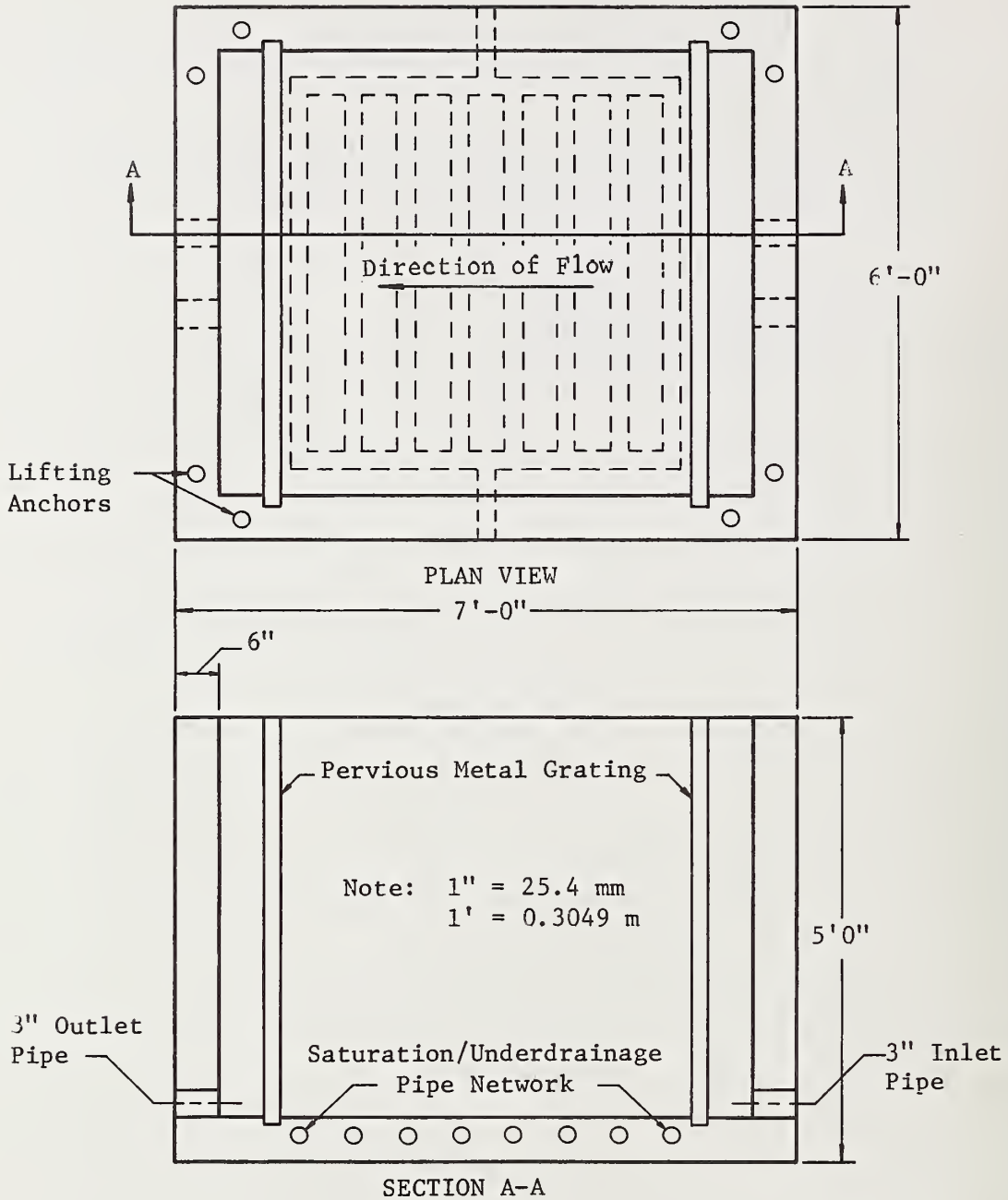

Figure 8. Basic Physical Features of Individual Test Cells

Figure 9. Overall View of High Permeability Cell System Showing Cells and Hydraulic Circulation System

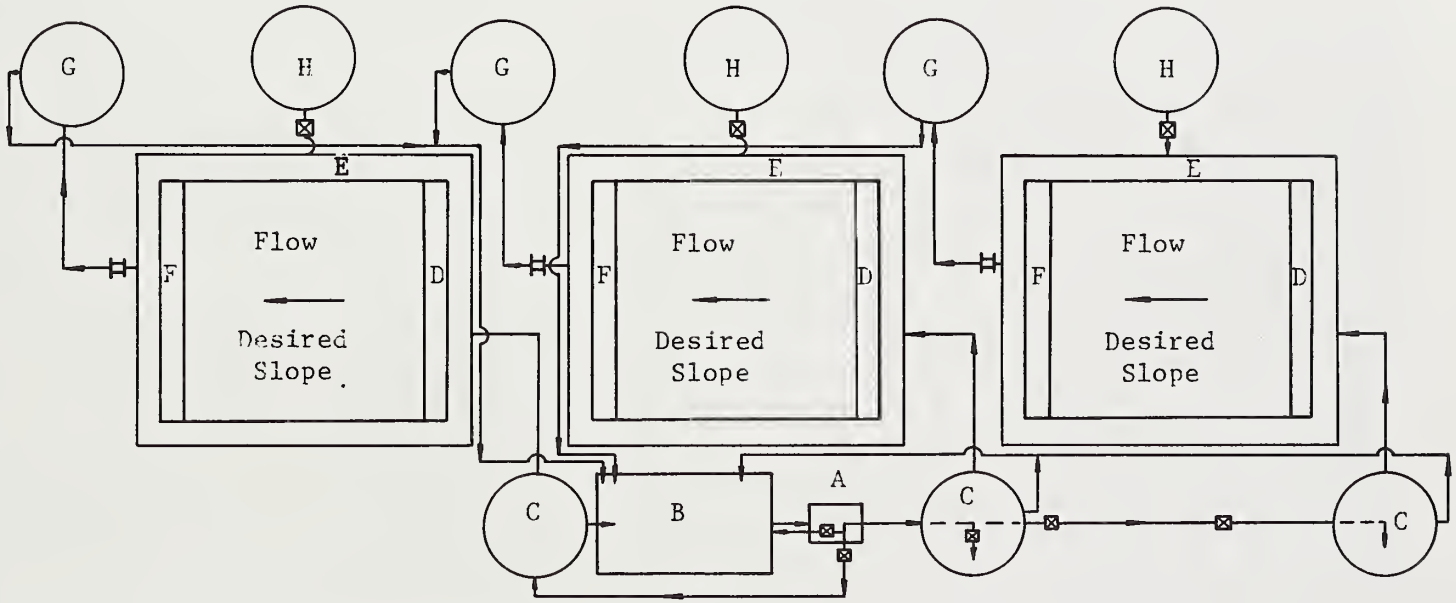

⊠ Indicates valve locations

⊟ Flow meter locations (for High Permeability Cell System only).

Figure 10. Basic Cell and Hydraulic Configuration

head tank (C) which in turn delivers it to the upstream water pool (D) of the cell (E). The water level in the downstream water pool (F) is maintained by the downstream constant head tank (G). Overflow from both the upstream and downstream constant head tanks (C and G) is returned by gravity to the sump tank (B). Uniform sheet flow through the simulated pavement layer is produced by tilting the tank to a slope consistent with the gradient established by the differential levels in the upstream and downstream constant head tanks. To permit a gravity return of water from the overflow pipes, the system of three cells was placed on wide-flanged steel beams. Valves were placed in appropriate locations to permit any combination of independent or coupled-cell operation. In addition, a direct valved return line from the pump permits a coarse flow adjustment, thus minimizing the amount of required overflow. The tank (H) connected to the pipe network in the base of the cells supplies the necessary amount and level of water for saturation purposes.

LABORATORY INVESTIGATION OF PROMISING TECHNIQUES (TASK C)

Introduction

The work on this task was conducted, in part, simultaneously with the work on Subtask A-2 (The Development and Analysis of Existing or New Techniques). As the work on these tasks progressed, it became evident that only the velocity method, previously described in the discussion of Subtask A-2, and illustrated in Figure 7, was worthy of further laboratory investigation. This investigation was conducted in two phases. First the components of the system (i.e., the electric conductivity probes, for use in determining the velocity of flow, and the pressure taps, for determining the head loss between probes) were evaluated in an extensive series of permeameter tests. Then, a preliminary prototype FPTD was fabricated, and its use was evaluated under simulated field conditions in the test cells designed and constructed during the performance of Task B.

Permeameter Test Series

The initial experimentation in this test series was directed at the development of a suitable conductivity probe for use in determining the velocity of flow. The early tests were conducted in a simple constant head permeameter constructed from plastic pipe. The conductivity probes were fabricated and inserted through the side of the permeameter so that their tips would be located in the soil along the axis of the permeameter. Epoxy putty was used to affix the probes to the permeameter and prevent leakage. The soil samples were saturated from the bottom up by gradually raising the level of the water in the sample. Once the samples were saturated, a constant differential head was applied to the specimen, reversing the flow direction, and observations of the flow rate were made to assure that steady state flow conditions were achieved. A quantity of salt solution was then introduced into the flow while maintaining the

head constant. A special effort was made to introduce the salt solution abruptly, but without interrupting the flow or creating local changes in hydraulic gradient. The time required for flow between the two probes was taken as the time which elapsed between the first indication of conductivity change in upstream and downstream probes (see Figure 6). It was recognized immediately that this procedure introduced some error into the velocity determination, because of the effects of hydrodynamic dispersion and diffusion of the salt solution. Thus, the apparent velocity of flow between the two probes, as measured by the initiation of conductivity change, was slightly higher than the actual average velocity of flow as determined in the constant head permeameter. Although this error might have been minimized or eliminated by measuring the elapsed time between peak conductivity changes (26), in many cases the response curves were so flat that it was difficult to determine, with reasonable accuracy, where the peak conductivity change had actually occurred. It was found, however, that the magnitude of this error was time dependent and could be minimized by using a combination of probe spacing and hydraulic gradient that permitted the test to be run in the shortest possible time. It was also found that, of all the electrolyte solutions tested, the best results were achieved using an ammonium chloride (NH_4Cl) solution consisting of 25 milligrams of ammonium chloride in 100 milliliters of water.

As noted earlier, in the discussion of Subtask A-2, three different combinations of conductivity probes and indicator systems were investigated. In all cases, the probes consisted of insulated copper wires encased in 3/16 inch (4.8 mm) diameter brass tubing for protection and for ease of insertion into the soil. Initially, the three wire probe system (Figure 5a) was used, with the change in conductivity being indicated by a change in electric potential measured on a chart recorder (Figure 6a). However, the sensitivity of this system was found to be dependent, in part, upon the rate of flow between the

individual wires constituting the probe. Although these wires were spaced very close together, less than 1/16 inch (1.6 mm) on centers, for low permeability soils tested at relatively low hydraulic gradients, the time response and, thus, the sensitivity of this system became unacceptable. This sensitivity was greatly improved by using a two wire probe (Figure 5b) with the change in conductivity also being indicated by a change in electric potential displayed on a chart recorder (Figure 6b). However, as indicated earlier, both of these probe systems were eventually abandoned in favor of a simpler, more reliable, and more economical two wire probe system, using a microammeter to indicate the change in conductivity (see Figure 7) and a stopwatch to determine the time required for flow between probes.

During the course of the investigations described above, it was found that the range of soils that could be studied was limited by the maximum differential head that could be maintained practically in a conventional constant head permeameter. Consequently, a modified constant head permeameter was assembled that would permit the use of the higher hydraulic gradients required for the evaluation of the permeability of relatively fine grained and well graded soils (i.e., those with permeabilities approaching 10^{-4} cm/sec). In this device, the differential head was maintained essentially constant by means of a large water supply reservoir. The pressure in the electrolyte supply reservoir was also controlled by this system, so that the flow of electrolyte could be initiated without changing the flow rate or introducing any local changes in the hydraulic gradient within the system.

As soon as it became evident that the change in head, Δh, between probes could not be determined analytically, the conductivity probes were redesigned to include pressure taps, as illustrated schematically in Figure 7. The head loss between the two probes was determined using a mercury manometer. Although this system proved

to be satisfactory for the permeameter test series and for use in the preliminary prototype FPTD, it was found that greater sensitivity could be obtained by the use of Capsuhelic Differential Pressure Gages, manufactured by Dwyer Instruments, Inc. Several of these gages of different sensitivities were purchased, and it was anticipated that they would be substituted for the manometer system in the prototype FPTD.

In an effort to investigate the effect of gravity on the flow system during the movement of the higher specific gravity salt solution, a series of horizontal permeameter tests were conducted using the equipment described above. However, no significant differences were observed between the results of these tests and those in which the flow was vertical.

As a result of the investigations described above, a large number of tests of the velocity technique were performed in the modified constant head permeameter, resulting in a substantial amount of data. The two wire electrical probe with pressure tap, used for most of these tests, is shown in Figure 11 and an overall view of the permeameter test setup is shown in Figure 12. The resulting data are summarized in graphical form in Figure 13, which shows the comparison between the coefficient of permeability (k_{ch}) measured with the modified constant head device, and that determined with the velocity technique (k_p) using the two wire electrical probe system. These data were analyzed statistically using the Statistical Analysis System (SAS Package) developed by A. T. Barr and J. H. Goodnight. The linear regression equation established by this analysis (shown as the solid line in Figure 13) can be expressed as

$$k_{ch} = 0.64\ k_p^{0.958}$$

This equation represents a very good fit to the experimental data, as evidenced by a coefficient of determination (r^2) of 0.991 and a

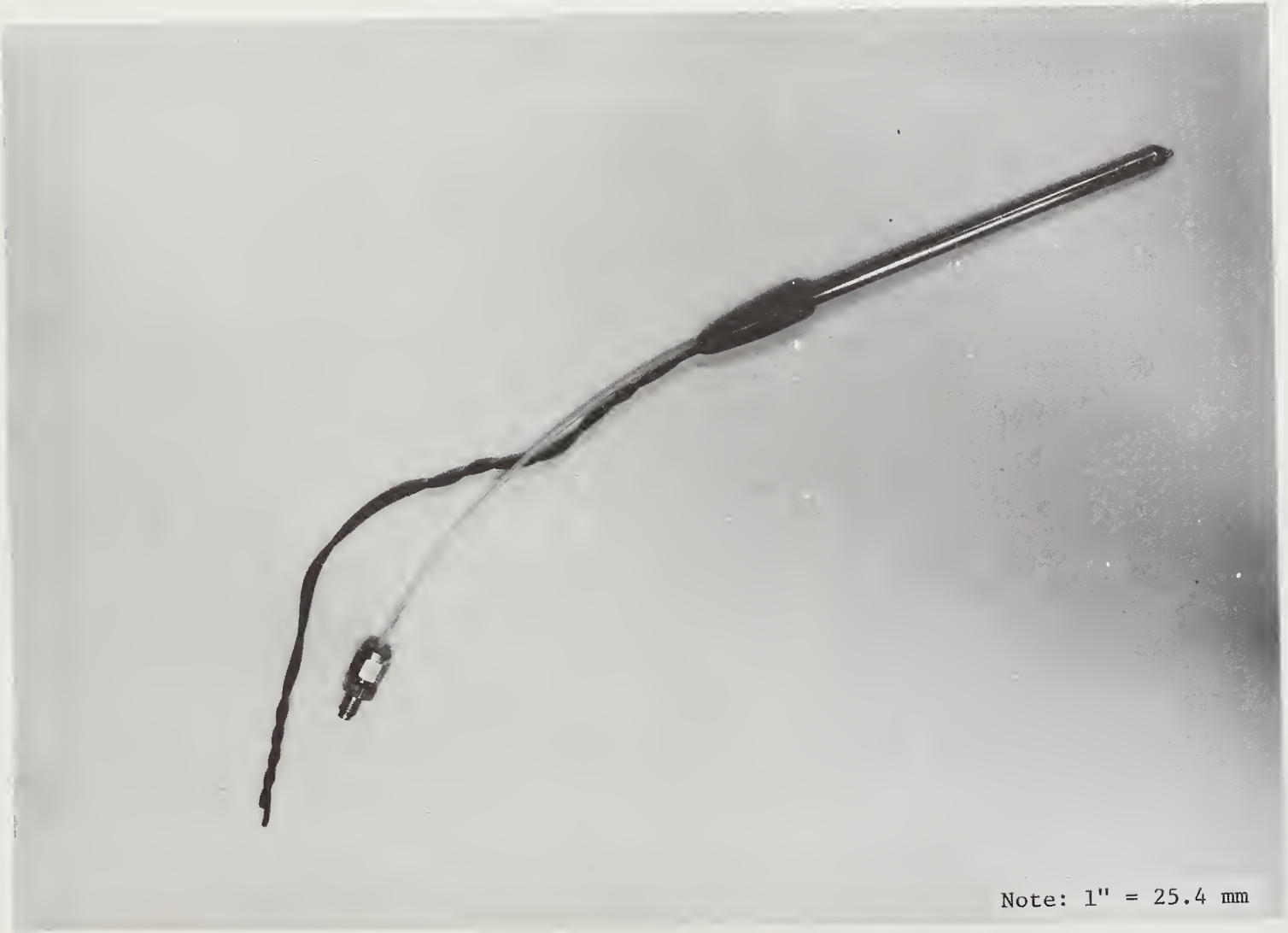

Figure 11. Electric Conductivity Probe With 1/16" Diameter Polyethelene Pressure Tap

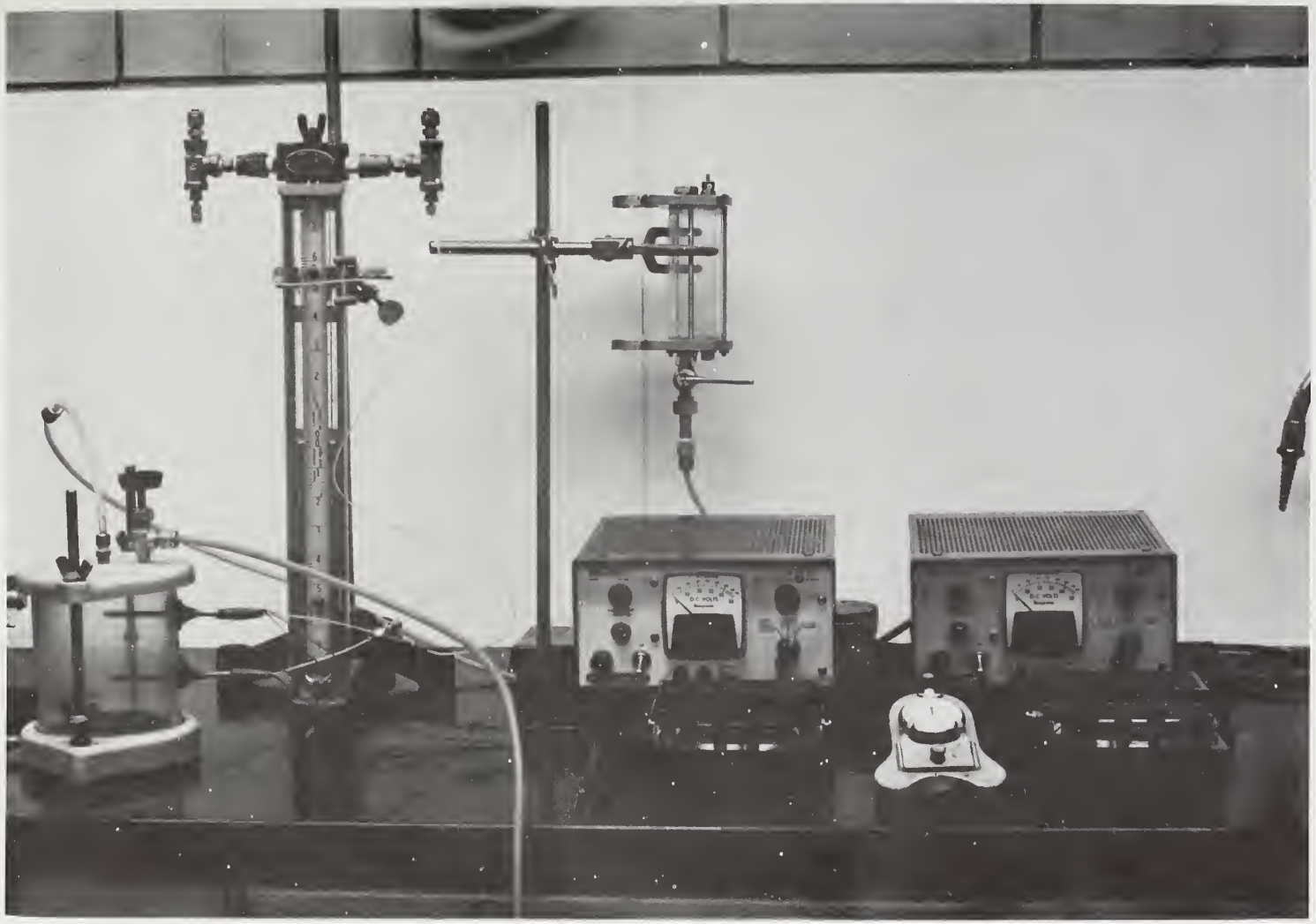

Figure 12. Permeameter Test Setup With Electric Conductivity Probes And Pressure Taps In Position For Testing

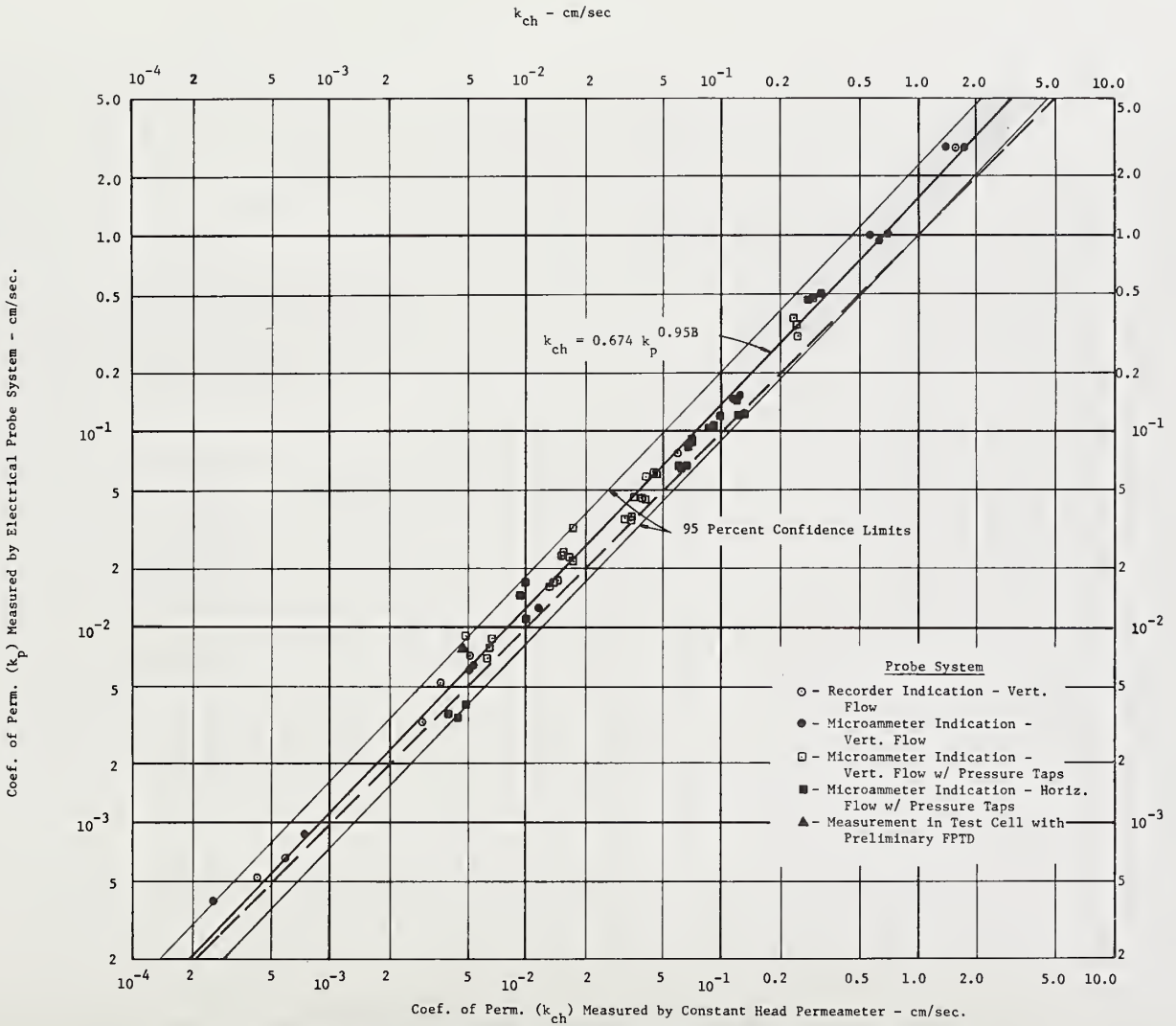

Figure 13. Comparison Between Coefficients of Permeability Measured With Modified Constant Head Device and Two-Wire Electrical Probe System.

coefficient of variation (CV) of 5.08 percent. However, a comparison of the regression line for the data (shown solid) and the 45° line (shown dashed) clearly indicates that the velocity method, using the electrical conductivity probe system, produced a slight over prediction of the coefficient of permeability. As noted earlier, this effect is produced as a result of dispersion and diffusion phenomena associated with the movement of the electrolyte through the soil. In an effort to provide a reliable means of correcting for this effect, both theoretical and experimental studies were undertaken. However, it was found that there were so many factors that exerted an influence on dispersion and diffusion that a simple, practical correction for the effect of these phenomena could not be obtained theoretically. Thus, it was concluded that ultimately it might be necessary to resort to the use of a simple empirical correlation, such as that embodied in the regression equation presented above, as a means for correcting the observed values. In any event, judging from the 95 percent confidence band shown in Figure 13, it was judged that the proposed measurement system showed great promise in terms of being able to satisfy specified performance criteria.

Simulated Field Condition Tests

Prior to the evaluation of the preliminary version of the FPTD using the low permeability test cell system, a series of cell tests were conducted on three different materials. Although the primary purpose for undertaking these tests was to evaluate the FPTD, it also offered an opportunity to check the operation of the low permeability laboratory test cell system. Because of a trucking strike during the period of these tests, only a limited number of materials were available: a washed river gravel, a "crusher-run" limestone aggregate, and a silica mortar sand. On the basis of the test cell results, the silica mortar sand was selected for evaluation of the FPTD. The following discussion will first summarize the series of

cell tests and, secondly, describe the results of the tests using the FPTD.

Laboratory Test Cell Test Series

Since the high permeability test cell system was not completed at the time of this test series, the low permeability cell system had to be utilized. It was subsequently determined that this circumstance limited the testing that could be accomplished.

Initially, the river gravel was placed in the LPCS cell having the independent return pipe. Laboratory permeability measurements on this material, run for comparison purposes using the time-lag permeameter (7), indicated a coefficient of permeability in the range of 4.5 to 5.0 cm/sec. It should be noted, however, that during this test the timing period was less than that recommended for accurate measurement (7). The gravel was placed in two, approximately 6 inch (152.4 mm) thick lifts and compacted with multiple passes of the hand-operated vibratory plate compactor to an average total thickness of 1.12 feet (341.4 mm). Because of the uniform gradation characteristics and rounded particles of the material, effective compaction was difficult. Based on the results of rodded laboratory compaction tests, it was estimated that the in place dry density and porosity were approximately 97 pcf (1553.8 kg/m^3) and 40 percent, respectively. Following saturation of the layer, the upstream end of the tank was raised and chocked to produce a slope of 7 percent. In addition, the overflow levels in the upstream and downstream CHT's were adjusted to produce a hydraulic gradient compatible with the slope of the tank (i.e.,0.07). For the measured flow rate of 12 gpm (7.571×10^{-4} m^3/s) and the assumption of steady state sheet flow, the calculated coefficient of permeability was 2.07 cm/sec. Since this value was not too different from the value determined on the basis of the time-lag permeameter, it was felt that the operation and accuracy of the cell system was adequate.

Although the coefficient of permeability of the river gravel fell within the limits specified by the project, it was not utilized for the FPTD evaluation test series for the following reasons: (a) the small head loss could not be measured accurately with the mercury manometer system and (b) the sensing probes had not yet been developed to the point that they could be inserted into the coarse aggregate without being damaged. Thus, a silica mortar sand and crushed limestone aggregate were obtained for consideration and use for the evaluation tests. Preliminary measurements with the test cell indicated the limestone aggregate to be unsatisfactory for the same reasons cited previously for the river gravel, hence the mortar sand was selected for the FPTD evaluation tests.

The mortar sand was placed in the cell in three loose lifts and compacted with the hand-operated plate vibrator to an average total thickness of 1.23 feet (374.9 mm). Following saturation of the layer, the average wet density and moisture content were found to be 118.5 pcf (1898.2 kg/m^3) and 26.9 percent, respectively, using a Troxler 2400 Series nuclear moisture-density gage. The porosity of the mortar sand was determined to be 43.5 percent.

For the initial cell permeability tests on the mortar sand, the cell was tilted and the CHT overflow pipes adjusted to develop steady state sheet flow at a hydraulic gradient of 0.05. Subsequent to the establishment of steady state flow conditions, flow measurements (using the manual method) yielded a flow rate of 0.167 gpm (1.054×10^{-5} m^3/s) for a depth of flow of 1.00 feet (304.8 mm). Using Darcy's law, the coefficient of permeability was determined to be 0.0451 cm/sec. A subsequent series of four tests conducted at a hydraulic gradient of 0.058 and a flow depth of 0.96 feet (292.6 mm) yielded flow rates ranging from 0.192 to 0.197 gpm (1.211 to 1.243×10^{-5} m^3/s) for an average of 0.195 gpm (1.230×10^{-5} m^3/s). The corresponding coefficient of permeability values ranged from 0.0468 to 0.0481 cm/sec for an average value of 0.0474 cm/sec.

The same mortar sand was also tested using the laboratory modified constant head permeameter and the electric conductivity probe system with pressure taps and manometer. The coefficient of permeability values from the constant head test ranged from 0.0092 to 0.0102 cm/sec for an average value of 0.0095 cm/sec. The probe system gave values, uncorrected for dispersion and diffusion, ranging from 0.0082 to 0.0108 cm/sec for an average value of 0.0098 cm/sec. The porosity of the sand was 37.5 percent.

Prototype FPTD Test Series

Subsequent to the tests previously described, the preliminary prototype FPTD was utilized to determine the coefficient of permeability of the mortar sand layer located in the test cell. Figure 14 is a photograph of the preliminary FPTD positioned on top of the layer of mortar sand for the velocity (coefficient of permeability) determination tests. Labels on the photograph indicate the detailed components of the FPTD. Also noted in the photograph is the filter fabric[1] that was utilized on the upstream and downstream faces of the sand layer to prevent possible erosion and piping losses.

Five separate velocity measurements were made, two of which were at the same hydraulic gradient while the other three were at different gradients. Based on the data collected for the five trials, coefficient of permeability values ranging from 0.0556 to 0.101 cm/sec were calculated. The average value for the five trials was 0.077 cm/sec. Thus, the average value of the coefficient of permeability determined using the FPTD (i.e., 0.077 cm/sec) can be compared to the average coefficient of permeability value determined using the cell system (i.e., 0.0474 cm/sec). However, the results of the tests utilizing the laboratory constant head permeameter demonstrated a similar correlation between the constant head and probe system values. As indicated

[1] Mirafi(TM) 140 Fabric, Celanese Fibers Marketing Company, New York.

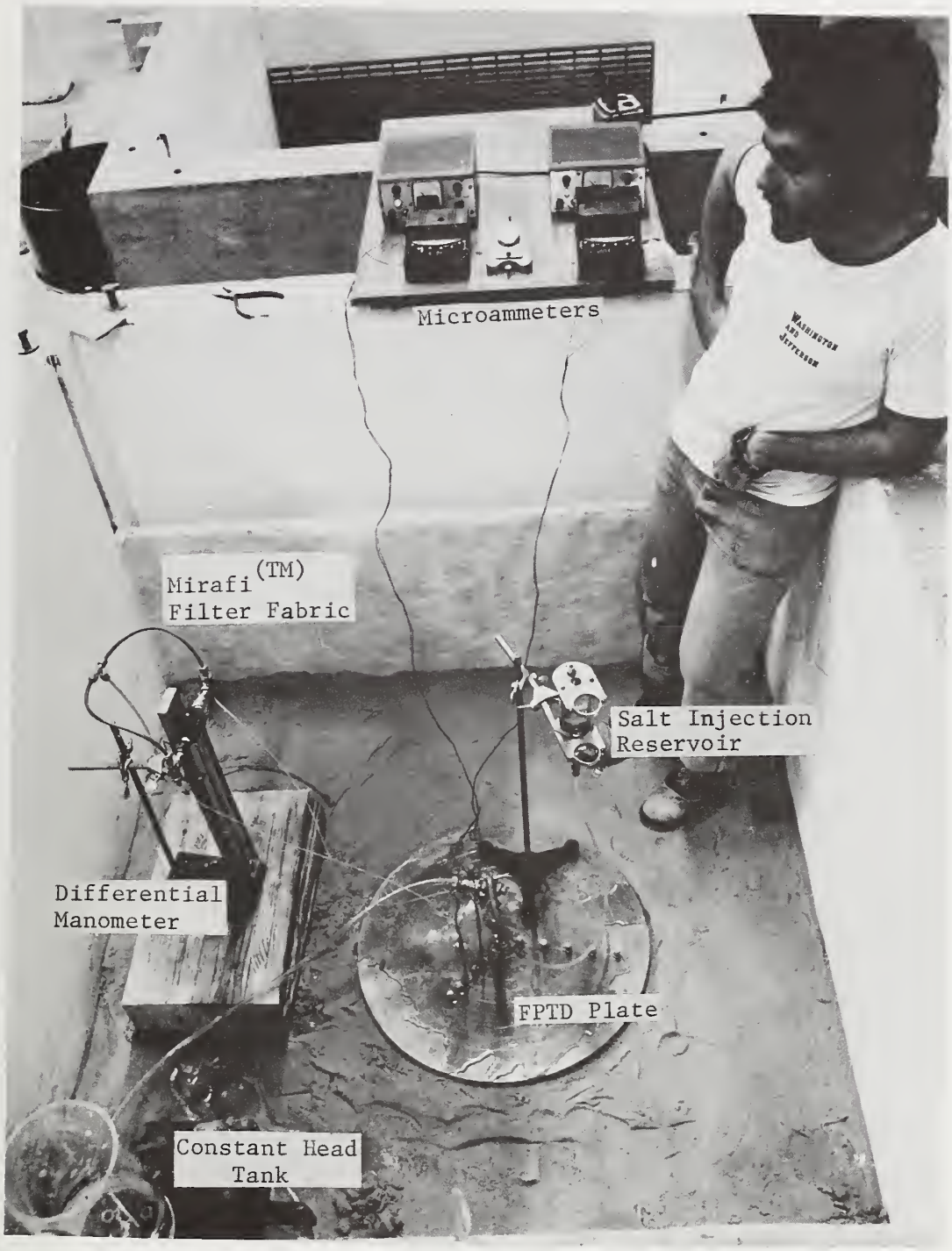

Figure 14. Preliminary FPTD Positioned on Layer of Mortar Sand for Permeability Determination

earlier, based on the results of these tests, which are plotted in Figure 13, an empirical correlation equation (see Figure 13) was developed. Utilizing this equation and the FPTD results to predict the corresponding constant head coefficient of permeability values yields a range of values from 0.047 to 0.0725 cm/sec and an average value of 0.0556 cm/sec. It is observed that these predicted values compare quite favorably with the range of measured values, 0.0468 - 0.0481 cm/sec, and the average measured value, 0.0474 cm/sec. It was anticipated that the planned replacement of the differential manometer with a precise differential pressure gage would produce more accurate and reliable results.

Conclusions and Recommendations

Based on the results of the studies described above, it was concluded that the velocity method of in situ permeability determination, using electric conductivity probes, represented a very promising technique that could be further developed to produce a rugged, reliable field permeability test device (FPTD). It was recognized that the electric conductivity and pressure sensing probes used in the preliminary prototype of the FPTD would have to be modified to permit them to be driven into base and subbase materials without risk of damage to the conductivity and pressure sensing system. In addition, it was felt that a variety of plate sizes, fluid injection tubes and probe spacings might have to be made available to adequately cover the range of boundary conditions anticipated during field use. However, based on the results of the studies reported herein, it was felt that all of these modifications could be readily implemented during the performance of Phase II of the project. It was therefore recommended that Phase II of the research be initiated immediately.

PHASE II

DESIGN AND CONSTRUCTION OF PROTOTYPE FIELD PERMEABILITY TEST DEVICE (TASK D)

Introduction

The objective of Task D was to design and construct a working model (prototype) of the FPTD. This device was to embody the velocity technique measurement principle, developed during Subtask A-2 and Task C (see Figures 7 and 14), in a rugged, portable device that is simple to operate and as trouble free as possible. The prospective operational features and performance requirements for the device were those outlined in the INTRODUCTION.

The device as designed and constructed consists of three major subsystems: (a) the reservoir and pressure subsystem, (b) the control and measurement subsystem, and (c) the plate and probe subsystem; as illustrated schematically in Figures 15 and 16. This portion of the report contains a general description of these subsystems and explains the operation of the prototype FPTD. The design and construction details for the device are presented in Appendix B.

Some modifications were made in the basic design of the apparatus as a result of experience gained during laboratory (Task E) and field (Task F) testing. However, for the sake of brevity, the details of the developmental aspects of the work are omitted for the most part, and only the final version of the prototype FPTD is discussed.

Reservoir and Pressure Subsystem

The reservoir and pressure subsystem consists of the fresh water supply tanks, a salt water supply tank and a pressure source (Figure 15).

The fresh water supply tanks provide the source of water for

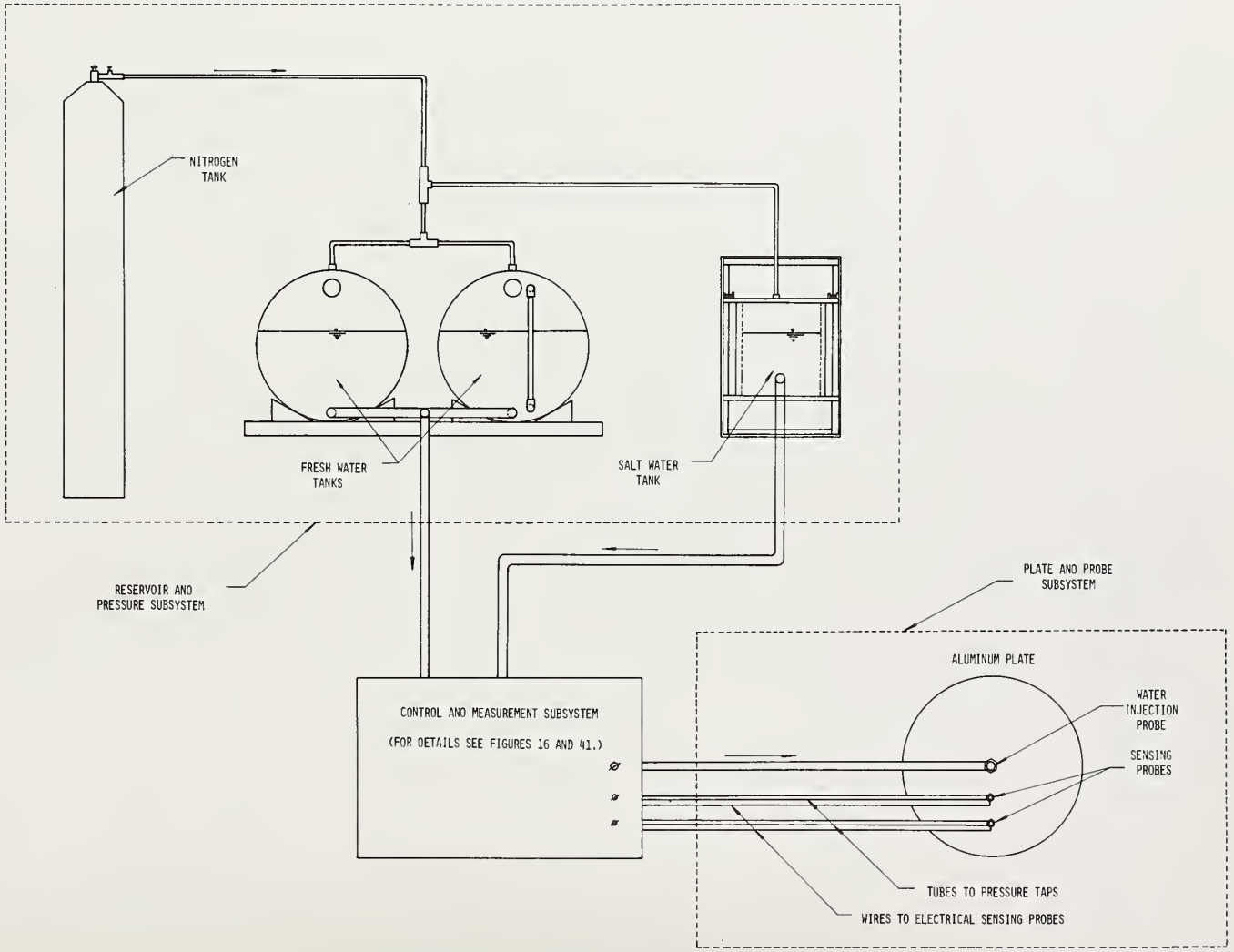

Figure 15. Schematic Diagram of FPTD and Its Subsystems

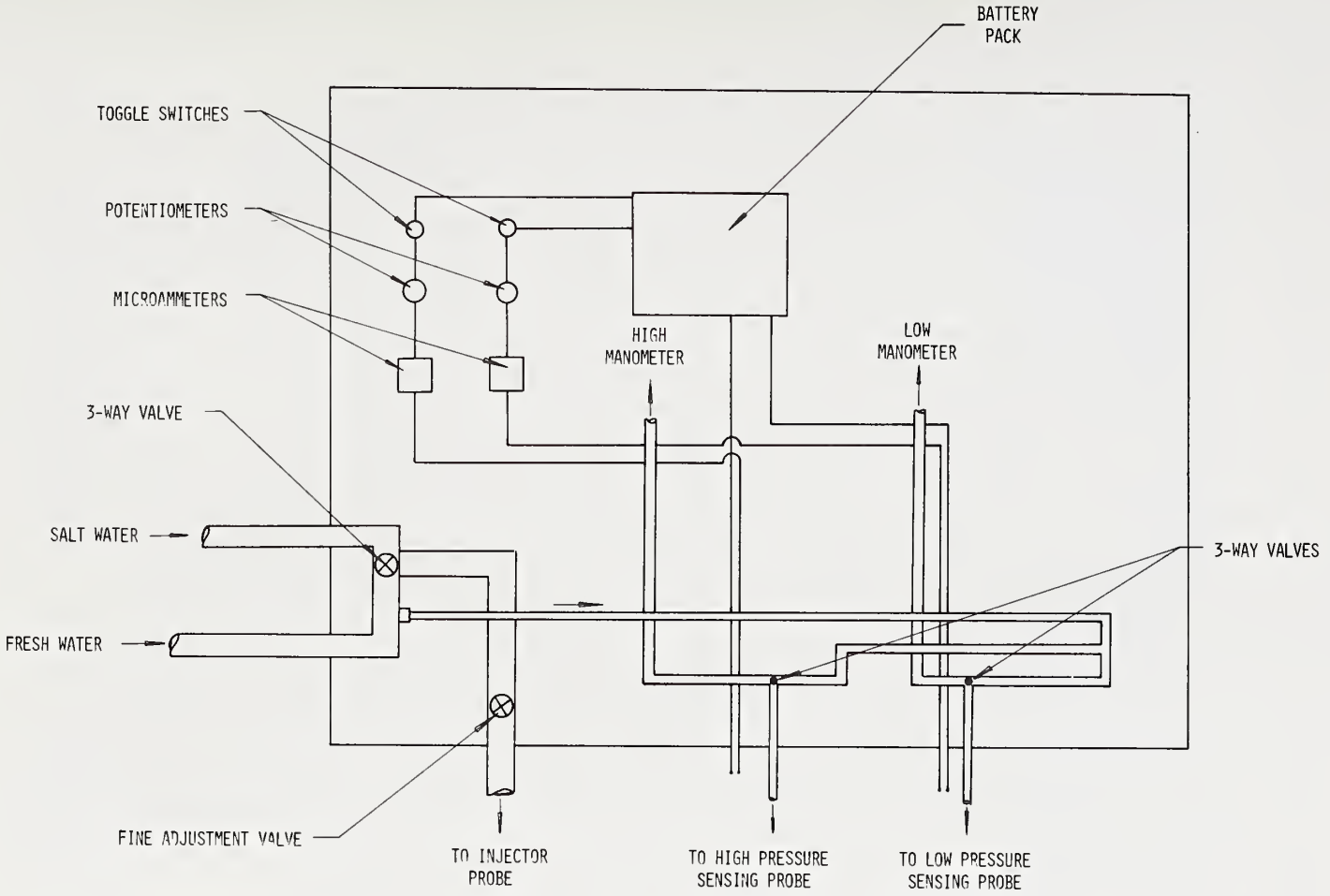

Figure 16. Schematic Diagram of FPTD Control and Measurement Subsystem

saturating the base or subbase and establishing steady state flow during permeability testing.

The salt water (electrolyte) supply tank is mounted on an adjustable frame which permits the tank to be raised or lowered so the salt water level is the same as the fresh water level during testing.

The pressure source consists of a cylinder of nitrogen equipped with a coarse adjustment pressure regulator. Fine pressure control is provided by an additional pressure regulator in the plastic line between the nitrogen tank and the water supply tanks.

For field use, the reservoir and pressure subsystem was mounted in the rear of the West Virginia University mobile research unit (International Van) shown in Figure 17. The reservoir and pressure subsystem is shown in position in the rear of the van in Figure 18. The fine adjustment pressure regulator is shown in the bottom left hand corner of Figure 18.

Control and Measurement Subsystem

The control and measurement subsystem, which is shown schematically in Figure 16, consists of the hydraulic controls, the electrical sensing system, and the pressure sensing system. A photograph of the unit is shown in Figure 19. The hydraulic controls provide for shut-off of the water supply or precisely regulated control of the flow of either fresh water or salt water (electrolyte) to the water injection probe. The two electrical sensing circuits are designed to provide for an adjustable response to the conductivity change that occurs as the electrolyte solution passes the electrodes in the sensing probes during permeability testing. The pressure sensing system consists of a differential manometer that is used to determine the head difference between the pressure taps, contained in the sensing probes, during testing.

Figure 17. West Virginia University Mobile Research Unit

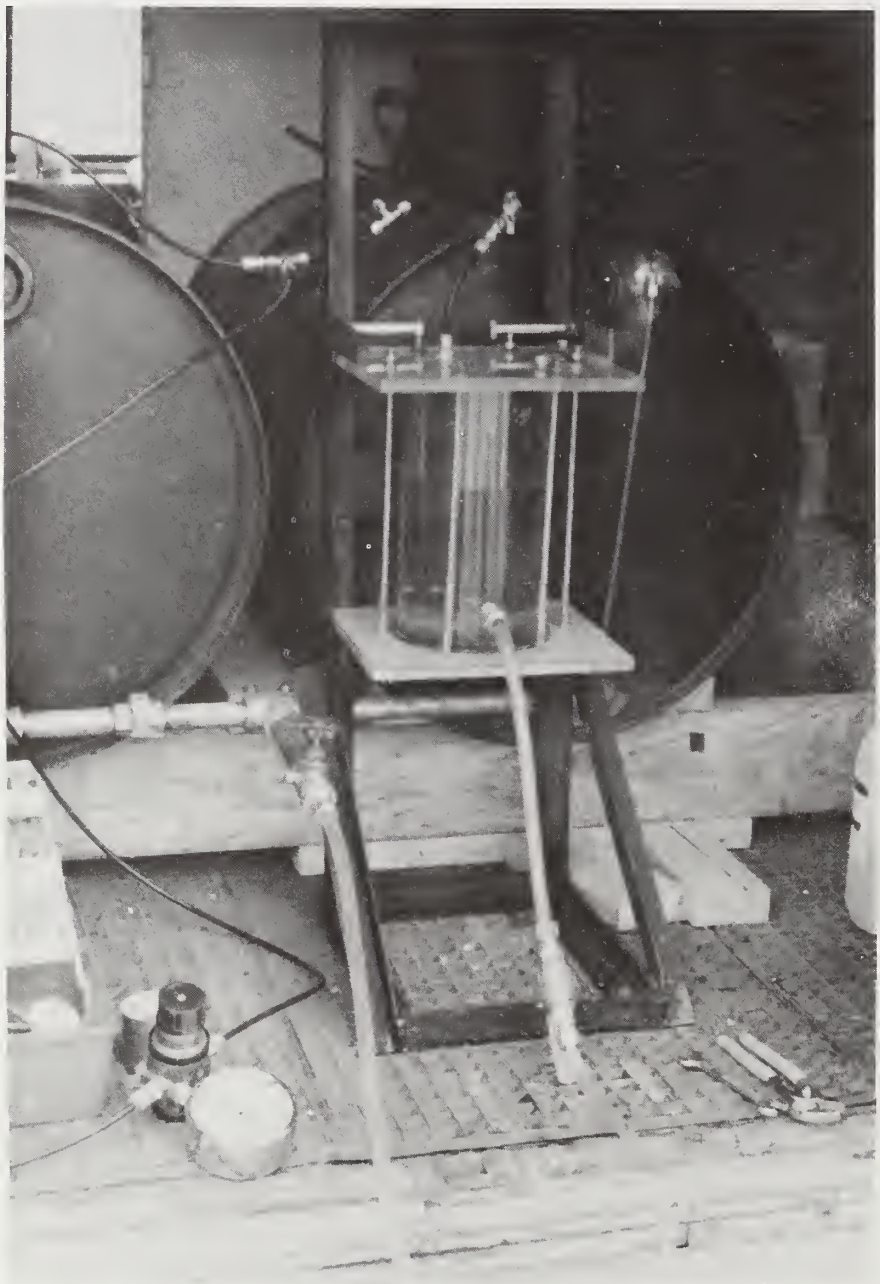

Figure 18. Reservoir and Pressure Subsystem Mounted in the Rear of the Van

Figure 19. Closeup View of Control and Measurement Subsystem

Plate and Probe Subsystem

The plate and probe subsystem consists of the horizontal plate, the water injection probe, and the sensing probes.

Two versions of the 18 inch (457.2 mm) aluminum plate were developed. Both versions are equipped with a central port through which the water injection probe is inserted and radially located ports through which the sensing probes can be inserted. The original plate was recessed on the bottom to permit the placement of a soft rubber seal between the surface of the plate and the base or subbase. However, during field evaluation of the FPTD, some difficulty was encountered occasionally with the development of piping at the interface between the plate and the base or subbase. In an effort to avoid or minimize this difficulty, a revised plate was prepared with annular projections as shown in Figure 20. This piping problem is discussed further in the section of this report entitled FIELD TESTING OF PROTOTYPE FPTD (TASK F).

The water injection probe simply consists of closed-end tubing equipped with holes distributed at regular intervals along its length. During testing, the probe is oriented so that these holes point in the direction of the row of plate ports; i.e., in the direction of testing. Water injection probes were made in several different lengths to suit the geometry of the test situation. The influence of the depth of the water injection probe is discussed in the section of this report entitled LABORATORY EVALUATION OF THE PROTOTYPE FPTD (TASK E).

The sensing probes were constructed from stainless steel tubing with a brass tip. The tip contains four ports to permit the access of water to the manometer for head measurement. A two-wire electrode is brought down through the sensing probe and secured in the tip. The sensing probes were made in various lengths to suit the geometry of the test situation. The influence of depth of sensing probe is

Figure 20. Revised Plate and Its Impression On a Subbase Surface

also discussed in the section of this report entitled LABORATORY EVALUATION OF THE PROTOTYPE FPTD (TASK E).

A closeup view of the plate and probe subsystem in position for testing is shown in Figure 21.

Auxiliary Equipment

In addition to the van, which is used to carry the reservoir and pressure subsystem and other equipment for field testing, auxiliary equipment includes an outrigger and jacking assembly, predrive rods, a stopwatch, a nuclear moisture-density gage, and a tool box equipped with a supply of spare pipe and tube fittings and miscellaneous small tools.

The outrigger and jacking assembly, shown in Figure 22, is required to hold the plate firmly against the base or subbase during testing.

The predrive rods include a 1/2 inch (12.7 mm) rod and a 1/4 inch (6.35 mm) rod used for making holes for the water injection probe and sensing probes, respectively, prior to their final insertion and seating before testing.

The stopwatch is used during testing to determine the time required for flow between the sensing probes.

The nuclear moisture-density gage is used to determine the dry density of the base or subbase. This information is used to calculate the porosity of the base or subbase as described earlier.

The tool box, equipped with spare pipe and tubing fittings and small tools, proved to be an invaluable aid during the setting up for testing and in the occasional replacement of any of the small components or fittings that might leak or otherwise become troublesome during field testing.

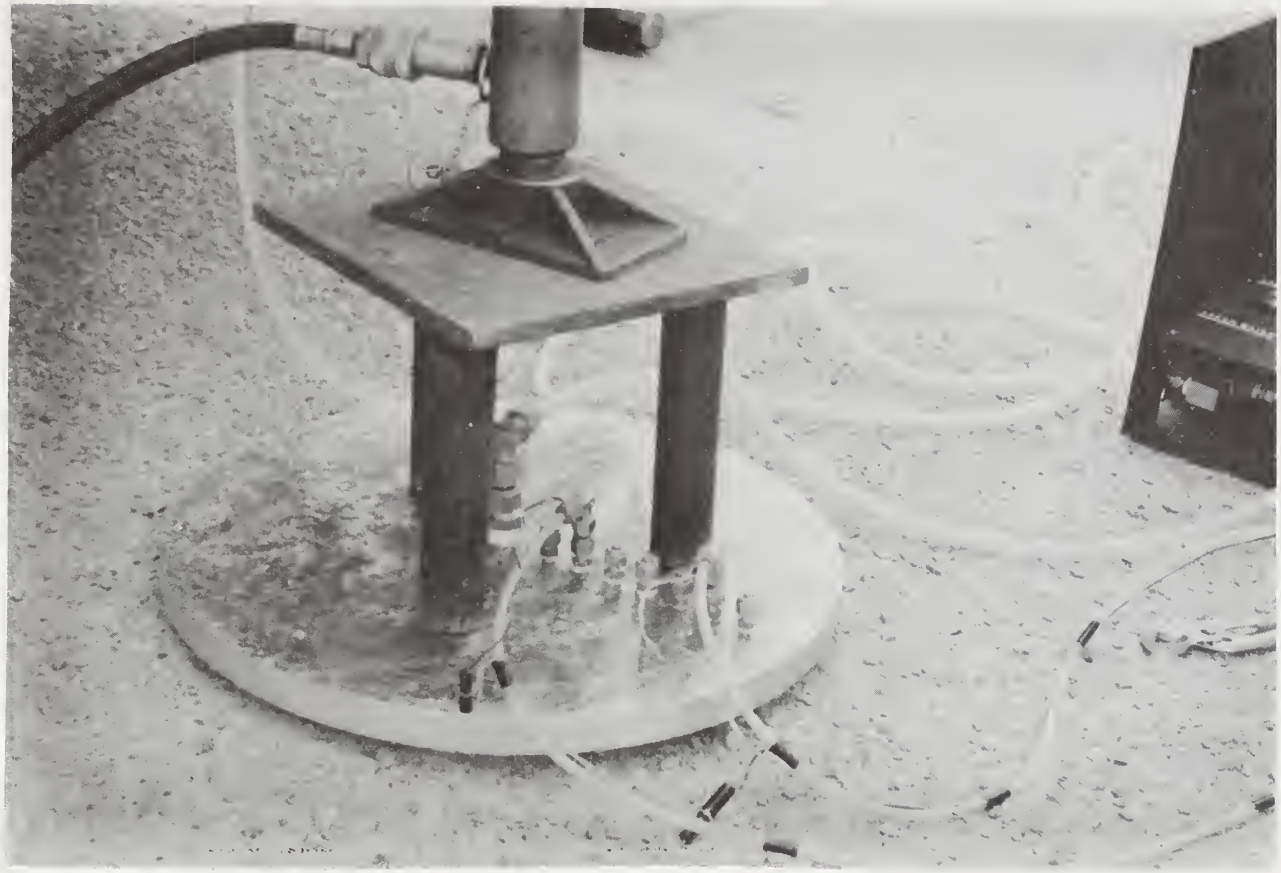

Figure 21. Closeup of Plate and Probe Subsystem in Position for Testing

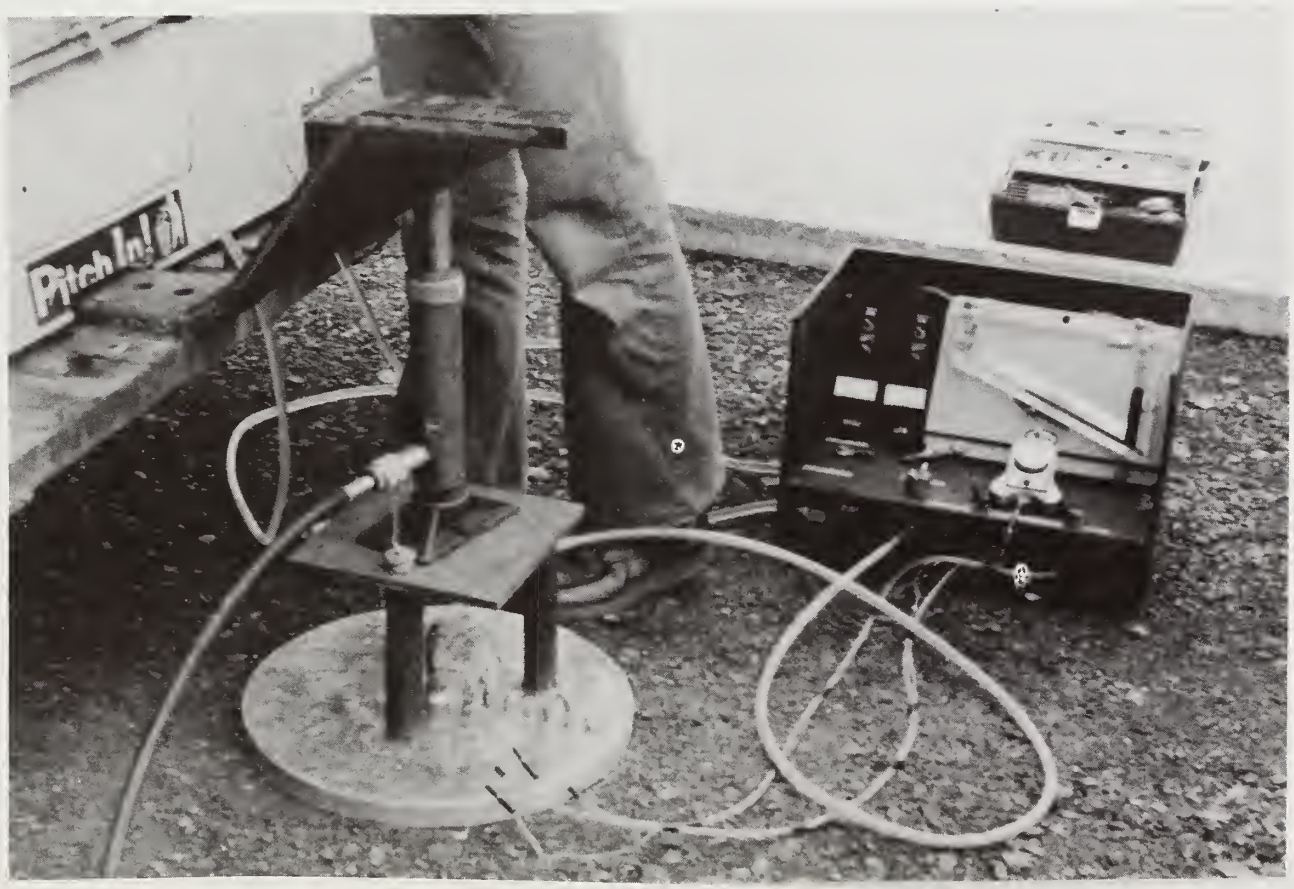

Figure 22. Overall View of Test Setup Prior to Initiation of the Flow of Water.

Operation of the FPTD

The operation of the FPTD during field testing involves the following general procedure:

1. Locate a suitably level area on the surface of layer to be tested and position rear of van adjacent to test area.
2. Insert jacking flange into the rear bumper and temporarily locate the plate beneath the anticipated position of the jack. If interfacial sealing materials are to be placed between the plate and the layer, the position of the plate can be scribed on the ground for assisting in placing sealing materials and repositioning the plate.
3. Once the plate is repositioned, remove jacking frame to permit easy insertion of the water injection and the sensing probes.
4. Use the predrive rods to make holes for the water injection and sensing probes.
5. Insert the probes to the preselected depth and orient to produce a consistent flow/measurement direction. The sensitivity and stability of the sensing probes should be verified by connection to the microammeter system.
6. Connect fresh and salt water reservoir inflow lines to the control/measurement system (C/M S) and the inflow line from C/M S to the water injection probe. Connect piezometer lines from the sensing probes to the differential manometer of the C/M S.
7. Reinsert the jacking frame and position the jacking stand and jack along the centroidal axis of the plate. Jack against frame until maximum safe working force is achieved. Figure 22 shows the test setup at this stage.
8. Initiate flow from the fresh water reservoir through the three-way flow adjustment valve of C/M S to the water

injection probe. Visually monitor the development of seepage adjacent to the edge of the plate. If difficulty is encountered in producing visible flow, utilize the NO_2 pressure system to increase the available head. Figure 23 shows the development of flow around the plate.

9. After visually stable flow conditions are achieved, as shown in Figure 24, monitor development of differential pressure head between the two sensing probes. It may be necessary to back-flush the probes to eliminate entrapped air in the lines. The presence of significant entrapped air is usually indicated by a differential head outside the range of the manometer. The satisfactory hydraulic operation of the equipment is usually signified when the indicated differential head is responsive to adjustments of the flow regulation valve.
10. Prior to introducing a "slug" of salt solution into the flow stream, the electrical system should again be checked for stability and responsiveness. Such a condition is usually verified if the microammeter indicator needles are stable and at their full undeflected position. In addition, the potentiometers should be set for maximum sensitivity.
11. Subsequent to verification of the satisfactory operation of the electrical and hydraulic systems, the level of the salt water reservoir is adjusted to correspond to the fresh water reservoir level (similarly, any applied pressures are equalized). Using the three-way flow adjustment valve, a "slug" of salt solution is introduced into the flow stream. Timing is begun when the microammeter for the upstream probe deflects and is stopped when a deflection is seen on the microammeter for the downstream probe. It should be noted that the salt slug is followed by a continuous flow from the fresh water reservoir. Thus, after the initial test, the

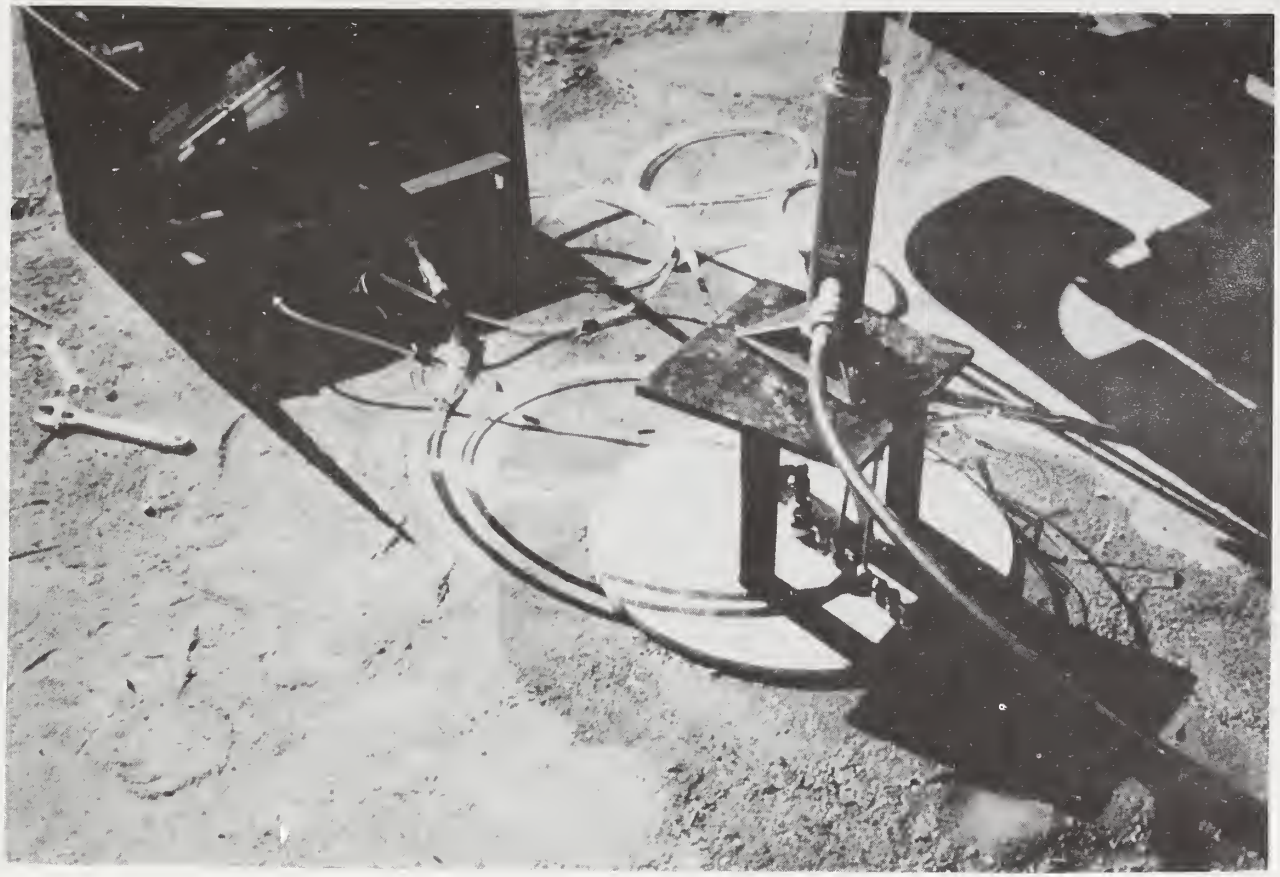

Figure 23. Test Setup Showing Development of Flow Around the Plate

Figure 24. Test Setup After Stable Flow Conditions Have Been Established

fresh water is allowed to "flush" the salt solution from the flow domain, thus causing the microammeter needles to return to their original undeflected positions.

12. The data that are recorded and utilized for calculation of the coefficient of permeability are:
    (a) the travel time, t (in secs);
    (b) the differential head, Δh (in cm); and
    (c) the travel distance, L (in cm).
    A typical data sheet, used for recording the data and calculating the coefficient of permeability, is shown, filled out with typical test data, in Table 2.
13. Once the system returns to its original condition prior to the injection of the salt slug, the flow (and, thus, the differential head) are adjusted and another test can be conducted.

Table 2. Typical FPTD Field Test Data Sheet

Date 8-25-78

Location GREENE COUNTY, TENNESSEE, ROUTE 11E, PROJECT No. F-62-2, STATION 416+65 E.B., 70' RT ℄

Material/Pavement Section 303.01 BASE*, TYPE "A", GRADING "D"

Probe Lengths 2.5" Layer Tested BASE

Layer Thickness 5.0" Central Probe Type D *

Constant Head Permeability(s) 7.23×10^{-1} cm/sec @ γ_d = 128.0 pcf.

γ_{dry} 136.4 pcf. n 0.224

* WITH 5% CALCIUM CHLORIDE

Water Level from Ground Surface NONE VISIBLE

Test No.	Probe Location**	D	L	Δh	t	$k = \frac{L^2}{t \times n} \frac{}{\Delta h}$ (cm/sec)
1	2-4	18"	5.08	1.88	17.8	1.73×10^{-1}
2	2-4	"	5.08	1.83	12.8	2.47×10^{-1}
3	2-4	"	5.08	2.24	22.0	1.17×10^{-1}
4	2-4	"	5.08	3.91	10.2	1.45×10^{-1}
5	2-4	"	5.08	1.32	28.2	1.55×10^{-1}
					AVE.	$= 1.67 \times 10^{-1}$

D = Plate Diameter (in), L = Probe Spacing (cm), Δh = Head Loss (cm), t = Time of Flow Between Probes (sec), and n = Porosity = $1 - \frac{\gamma_d}{G_s \gamma_w}$

(A value of n = 0.24 can be used with little loss of accuracy if γ_d is unknown.)

* - Given in Length and D - Directional or G - General

** - Relative to Central Saturation Probe Being Position Zero

LABORATORY EVALUATION OF THE PROTOTYPE FPTD (TASK E)

Introduction

Proposed Objectives and Scope of Task

The overall objective of Task E was to completely evaluate the limitations of the FPTD and the reproducibility of the results achieved. In keeping with the requirements outlined in the INTRODUCTION, it was proposed to test the prototype FPTD on different layer thicknesses between 3 inches (76.2 mm) and 18 inches (457.2 mm) and for materials having permeabilities at each order of magnitude between 10^{-4} cm/sec and 10 cm/sec. Originally, it was anticipated that the following boundary conditions would be investigated:

1. Tests on a non-stratified (homogeneous) material.
   a. Free water surface outside the layer being tested.
   b. Free water surface within the layer being tested.
2. Tests on the top layer of a layered system.
   a. Impermeable material below the layer being tested; free water surface below the layer being tested.
   b. Moderately permeable material below the layer being tested.
      (i) Free water surface outside the influence of the layer being tested.
      (ii) Free water surface at the interface between the layer being tested and the one below it.
   c. Very permeable layer below the layer being tested.
      (i) Free water surface outside the influence of the layer being tested.
      (ii) Free water surface at the interface between the layer being tested and the one below it.
3. Tests on the individual layers within a layered system.

a. Free water surface below the layer being tested.
b. Free water surface within the layer being tested.
c. Free water above the layer being tested.

Further, it was anticipated that, for each of the materials to be tested, the investigation of each of the listed boundary conditions would require a separate test setup.

Actual Scope of Work Accomplished in Task E

As soon as the Phase I research had progressed to the point that the nature of the test device and test method had been established and subjected to preliminary evaluation in the laboratory test cells, it became clear that the program of testing implied by the above listing of boundary conditions was not entirely appropriate. It was found that, except for the testing of an individual layer within a layered system, two basic types of test cell setups were all that were required to satisfy all of the boundary conditions listed. A single layer of aggregate with a varying free water surface can be made to satisfy boundary conditions 1a and 1b. It also can be considered to satisfy boundary conditions 2a since the impervious bottom of the test cell can be considered to be the ultimate in an underlying impervious layer in a layered system. It was also found that evaluation of the FPTD for boundary condition 2b was unnecessary, because the nature of the equipment and test procedure is such that boundary condition 2c is the most critical, and if it can be satisfied, then there is no question that the device will perform satisfactorily for boundary condition 2b.

Based on this analysis of testing requirements, the FPTD was evaluated in the test cells loaded either with a single layer of the various materials or with two layers of materials with the underlying layer consisting of very high permeability material. Time did not permit the laboratory testing of an individual layer within a layered

system. However, testing of this type was performed in the field, as part of Task F, at the Detroit, Michigan, test site with very satisfactory results. Consequently, this omission was not considered to be serious.

During the progress of the testing, considerable time and effort was devoted to consideration of the influence of several of the FPTD test parameters on the test results. These included the direction of testing, the plate size and depth of the water injection probe and the location, depth and spacing of the sensing probes. Particular attention during testing was devoted to the latter set of parameters.

During the course of this task, a great deal of data was generated. In fact, more than 400 individual tests were performed that were considered valid. In the following portions of this section of the report, all of these data are presented in one form or another. However, for the sake of brevity and clarity, only selected portions of the data are presented to illustrate the influence of the various boundary conditions and test parameters on the test results. The complete test results are available in tabular form in the files of the Civil Engineering Department of West Virginia University.

Testing of the FPTD

Materials

Initially, it was intended to test the FPTD on typical highway base and subbase materials, and, to this end, the local aggregate supplier was contacted and asked if he could prepare aggregate mixtures meeting the base and subbase requirements of the State of West Virginia and some other states. Although there was some reluctance on the part of the supplier to alter his production to produce these gradations in small batches, some batches of aggregates were obtained and subjected to permeability testing in the laboratory with constant head and/or time lag (7) permeameters. The permeability of these

materials was also determined in the laboratory test cells using steady sheet flow as described in Appendix A. Very quickly, it became evident that the materials obtained and tested would not be entirely satisfactory for two reasons: (1) the aggregate supplier was not always able to meet specified gradation requirements for small batches of aggregates, and (2) the permeabilities of the typical bases and subbases tested fell within a relatively narrow range and did not come close to encompassing the full range of permeabilities for which the FPTD was to be evaluated.[1] Consequently, it was decided to base the material selection process more on the permeability of the material rather than on its suitability as base or subbase. On this basis, six different materials were selected or blended to produce permeabilities between 10^{-4} and 10 cm per sec. These materials were, in order of decreasing permeability: (1) a crushed limestone aggregate, satisfying WVDOH 307-1 base course requirements; (2) a crushed limestone aggregate meeting the AASHTO No. 9 gradation requirements (washed); (3) a limestone sand meeting the WVDOH requirements for fine aggregate in asphaltic concrete; (4) an Ohio River sand meeting the WVDOH requirements for fine aggregate in Portland cement concrete; (5) a silica mortar sand supplied by the WVU Physical Plant; and (6) a blend of 60 percent asphalt sand, 30 percent Ohio River sand, and 10 percent fly ash. The grain size distribution curves for these materials are shown in Figures 25 and 26, and the measured values of laboratory (k_l) and test cell (k_{tc}) permeabilities are given in Table 3.

---

[1] Subsequently, during the Task F field testing of the FPTD, this relatively narrow range of permeabilities of conventional bases and subbases was verified.

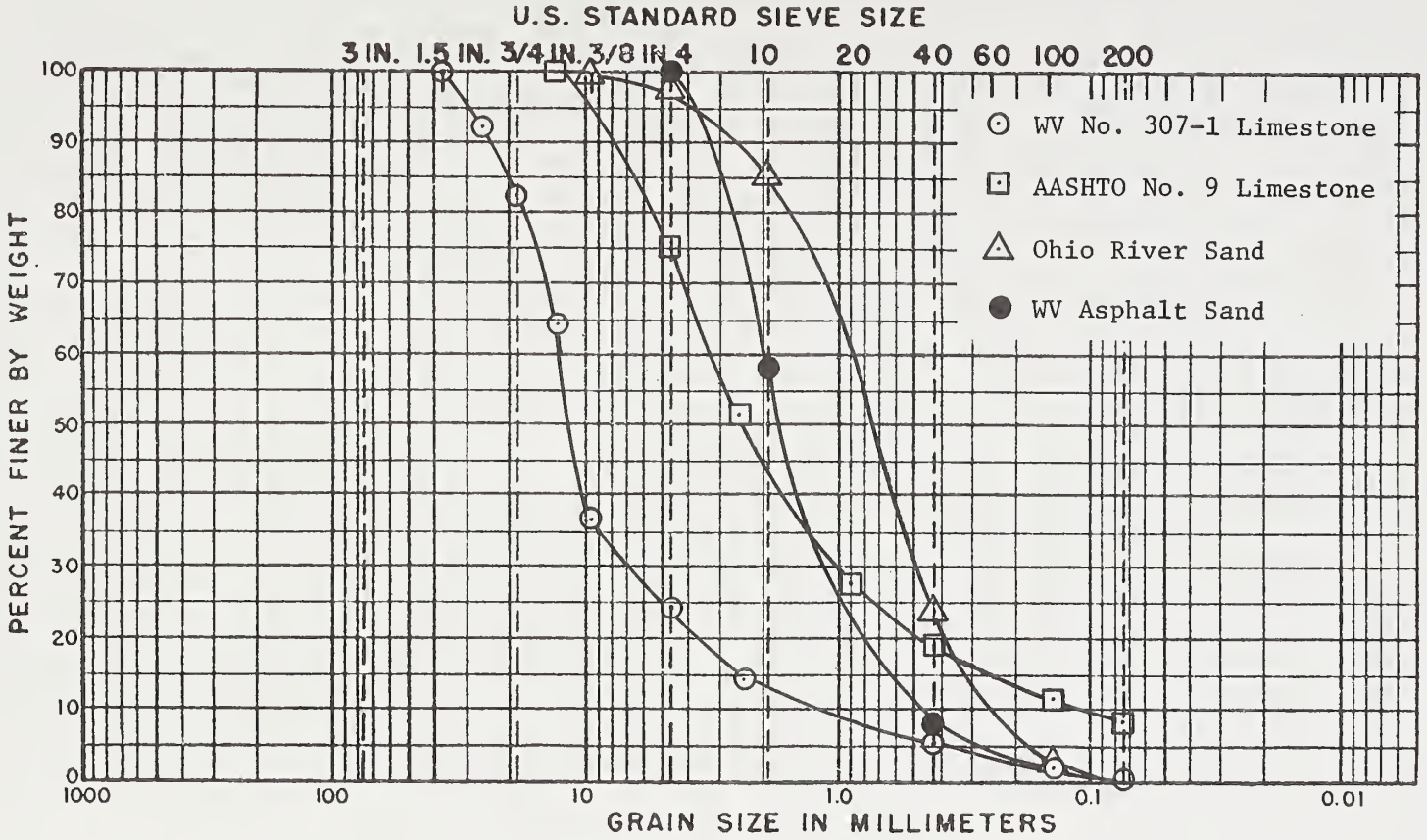

Figure 25. Grain Size Distribution Curves for Four of the Materials Used in the Test Cells to Evaluate the FPTD.

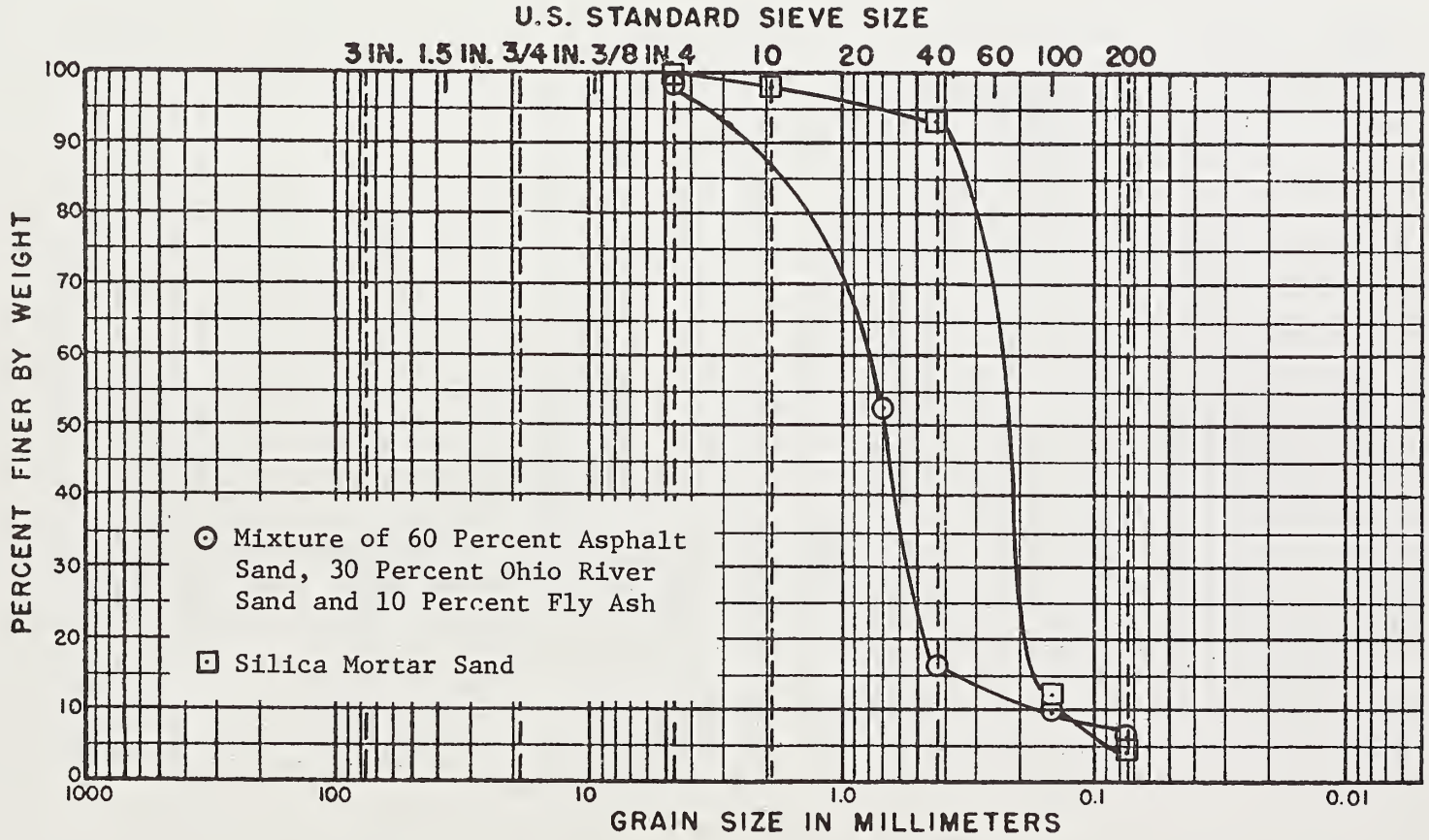

Figure 26. Grain Size Distribution Curves for Two of the Materials Used in the Test Cells to Evaluate the FPTD.

Table 3. Laboratory and Test Cell Permeability Values for Materials Used to Evaluate the FPTD

Material	Specific Gravity	Laboratory Values Dry Density pcf	Laboratory Values Permeability[1] cm/sec	Test Cell Values Dry Density pcf	Test Cell Values Permeability cm/sec
WV No. 307-1 Limestone	2.72	121.2	2.00	117.6	3.56
AASHTO No. 9 Limestone	2.71	92.2	2.53	115.6	3.70×10^{-1}
WV Asphalt Sand	2.72	101.0	1.81×10^{-1}	109.8	1.10×10^{-1}
Ohio River Sand	2.71	99.2	5.10×10^{-2}	101.6	5.90×10^{-2}
		104.7	2.44×10^{-2}	95.6	3.75×10^{-2}
		104.4	1.91×10^{-2}	99.1	3.51×10^{-2}
Silica Mortar Sand	2.65	90.8	2.35×10^{-2}	98.8	1.80×10^{-2}
		96.1	0.90×10^{-2}		
Mixture of 60% Asphalt Sand, 30% Ohio River Sand, and 10% Fly ash	2.68	109.0	3.10×10^{-3}	106.9	3.75×10^{-3}

[1] Given values represent the average of several test runs.

Influence of Layer Thickness

The influence of layer thickness on the ability of the FPTD to measure coefficient of permeability was determined by performing tests with the FPTD on layers of materials varying from 3 inches (76.2 mm) to 18 inches (457.2 mm) in thickness. Since the full range of layer thicknesses was not used for all materials, and because the measured coefficients of permeability for the various materials cover such a large range (3.75×10^{-3} to 3.56 cm/sec), the influence of layer thickness can best be illustrated by using normalized permeability data obtained by dividing the average permeabilities measured by the FPTD (k_d) by the corresponding values measured in the test cells (k_{tc}) using steady sheet flow. Normalized permeability data of this type are shown plotted against the corresponding layer depths in Figure 27. Examination of this figure shows that there is no consistent tendency for the permeability to vary with the depth of layer thickness. Thus, it can be concluded that, as long as steady state flow can be established, the thickness of layer being tested has little or no influence on the value of permeability measured by the FPTD.

Influence of Watertable Depth

The influence of the watertable depth on the ability of the FPTD to measure permeability was evaluated by performing tests with the watertable at various depths within the materials being tested. Since the watertable depths were not varied uniformly over the full layer depth of all materials, and because the coefficients of permeability of the various materials vary over such a wide range, it is considered desirable to illustrate the influence of watertable depth on measured permeability by comparing selected normalized permeability values, k_d/k_{tc}, with the watertable depth, expressed as a percentage of the total material depth. A comparison of this type is given in Figure 28 for three of the materials tested. Examination of

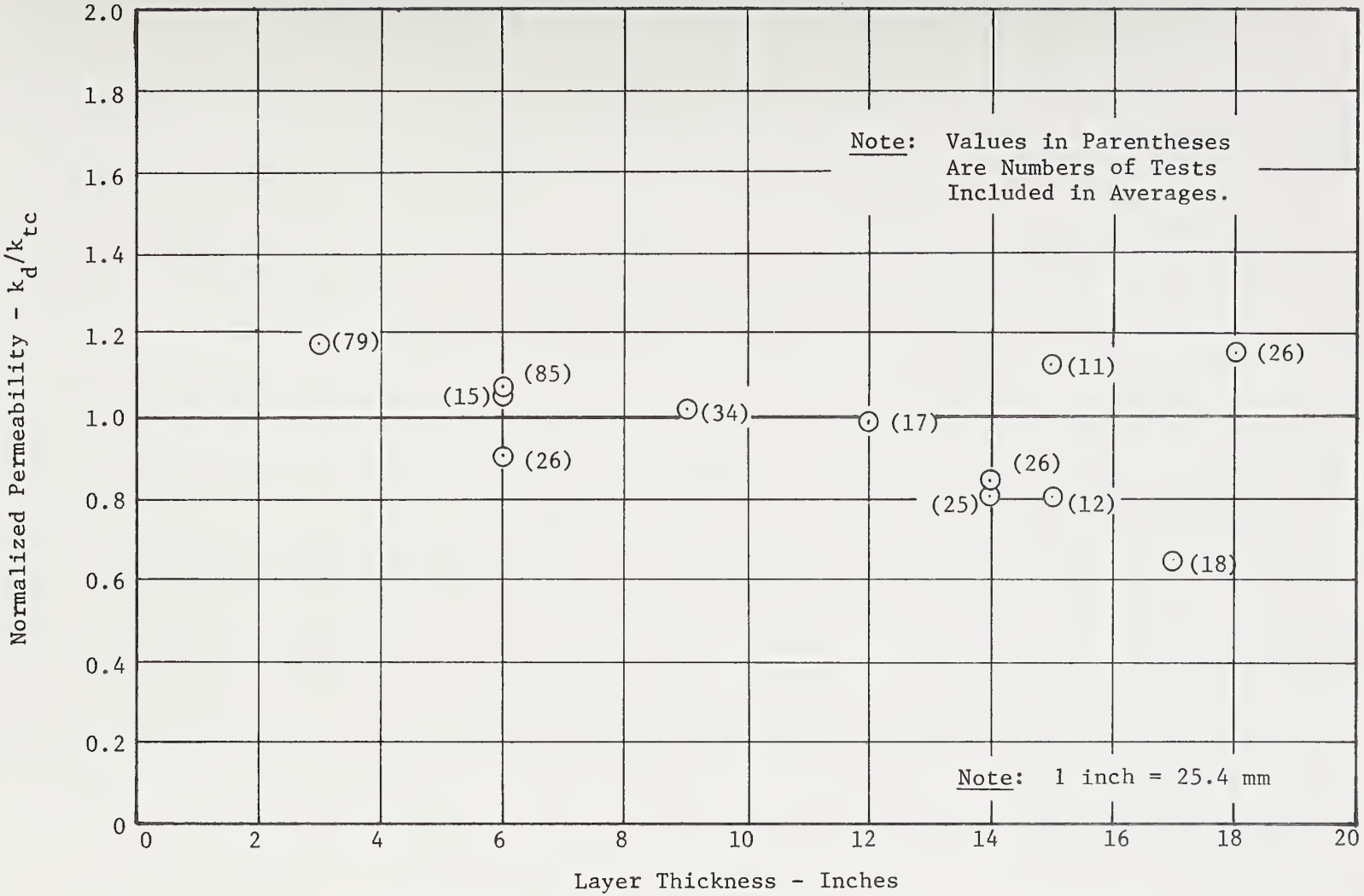

Figure 27. Influence of Layer Thickness on Normalized Permeability, k_d/k_{tc}

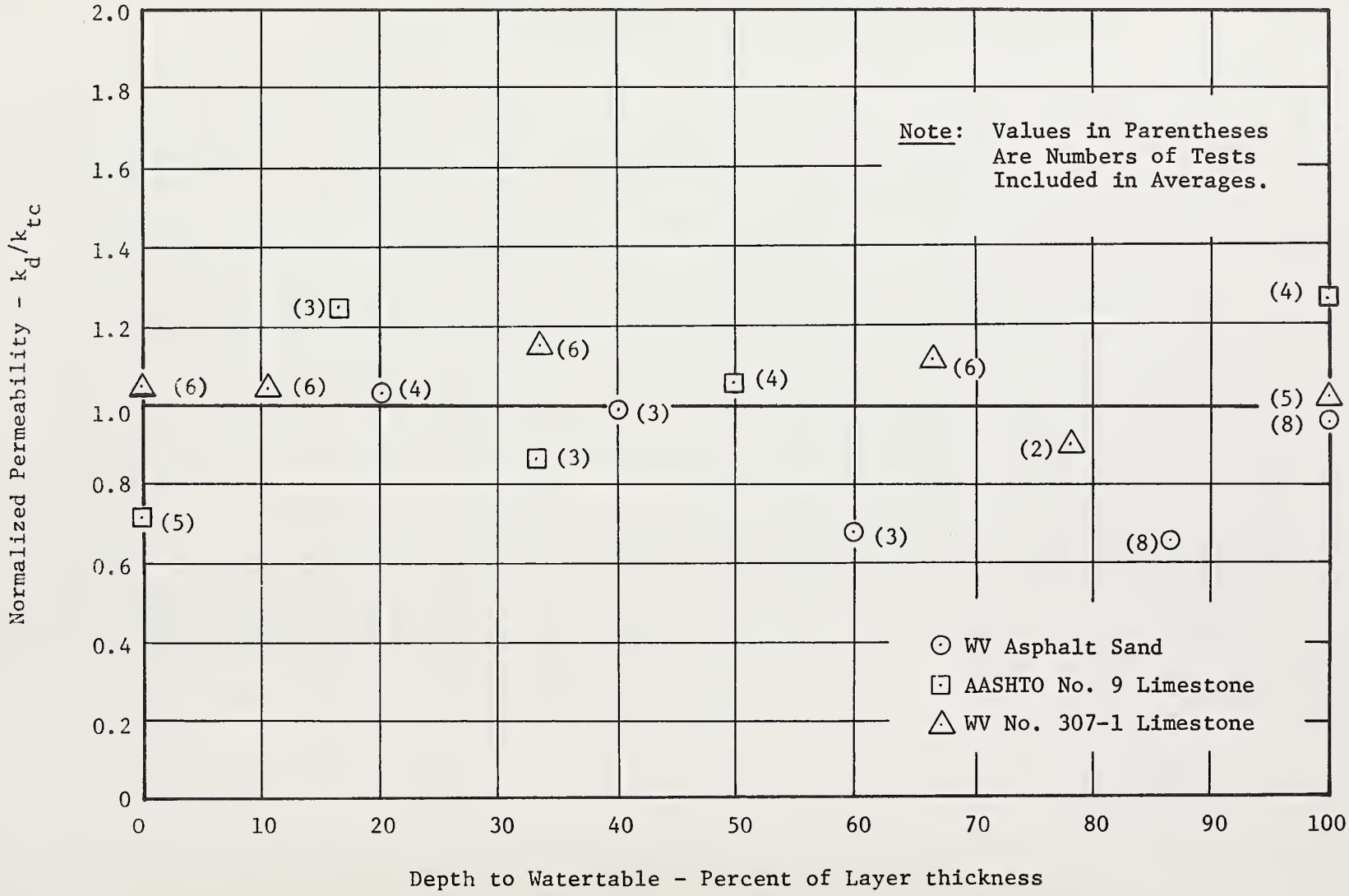

Figure 28. Influence of Watertable Depth on Normalized Permeability, k_d/k_{tc}

Figure 28 shows very clearly that there are no general trends that would indicate that the depth of watertable has any significant influence on measured coefficient of permeability, as long as a zone of saturated steady state flow is established during testing.

Influence of Underlying Layer of High Permeability

The ability of the FPTD to measure the permeability of a layer of material underlain by a material of very high permeability was evaluated by testing 3 inch (76.2 mm) and 6 inch (152.4 mm) layers of Ohio River sand over a 12 inch (304.8 mm) layer of WVDOH No. 307-1 crushed limestone. The 3 inch (76.2 mm) and 6 inch (152.4 mm) thick layers of Ohio River sand had coefficients of permeability of 3.75×10^{-2} and 3.51×10^{-2} cm/sec, respectively, as determined in the test cells using steady sheet flow. The test cell determined coefficient of permeability for the No. 307-1 limestone was 3.56 cm/sec. Thus, the permeability of the underlying layer was over 100 times that of the layer being tested.

Initially, some difficulty was encountered in making the measurements, because the water injection probe was only placed to a depth equal to the depth of the layer being tested. This led to a situation somewhat like that illustrated in Figure 4. In general, the differential head readings were either unobtainable or so high that they indicated that the bulk of the flow was moving abruptly downward and then horizontally through the more permeable layer, thus effectively bypassing the layer being tested. In an effort to overcome this difficulty, another series of tests was conducted holding all test conditions the same, except for the depth of the water injection probe, which was lowered to a depth of 12 inches (304.8 mm) below the surface of the layer being tested. This resulted in a more nearly horizontal flow pattern in both layers, and a series of measurements were obtained that were judged to be reliable. For example, for the 3 inch (76.2 mm) layer using the No. 2 and No. 4

sensing probes (50.8 mm probe spacing), the nine measured values ranged from 2.38×10^{-2} to 4.11×10^{-2} cm/sec, with an average of 3.33×10^{-2} cm/sec, compared to the test cell measured permeability of 3.75×10^{-2} cm/sec. For the 6 inch (152.4 mm) layer, using the same probes and probe spacing, the nine measured values ranged from 2.40×10^{-2} to 3.68×10^{-2} cm/sec, with an average of 2.75×10^{-2} cm/sec, compared to the test cell measured permeability of 3.51×10^{-2} cm/sec. Thus, it can be concluded that the FPTD is capable of producing reasonably reliable measurements of the permeability of a layer of base or subbase that is underlain by a much more permeable layer, as long as a condition of steady state saturated flow is introduced into both layers.

Influence of FPTD Test Parameters

Direction of Testing. The influence of the direction of testing was evaluated by performing a series of tests at the same location on a layer but varying the direction of the sensing probes so that the permeability was evaluated in two or more directions. As might have been expected, considerable variation occurred in the test results. In some instances, a change in testing direction produced no significant difference in test results, while in other cases the differences were more pronounced. For example, in one series of tests on the WVDOH asphalt sand, testing in the direction of test cell flow produced an average coefficient of permeability of 1.103×10^{-1} cm/sec (the test cell measured value was 1.10×10^{-1} cm/sec), while testing at right angles to the direction of test cell flow produced an average coefficient of permeability of 0.950×10^{-1} cm/sec. In contrast, in a series of tests on the AASHTO No. 9 limestone, testing in the direction of test cell flow produced an average coefficient of permeability of 3.85×10^{-1} cm/sec (the test cell measured value was 3.70×10^{-1} cm/sec), while testing at right angles to the direction of test cell flow produced an average coefficient of permeability of

5.89×10^{-1} cm/sec.

These results suggest that considerable anisotropy might exist, particularly under field conditions, where placement and compaction of bases and subbases might not be as uniform as in the laboratory test cells. Consequently, in actual practice it would probably be desirable to perform tests in orthogonal directions at a given test location and then take the permeability as the geometric mean of the results.

Plate size, probe location and spacing. The influence of the plate size, depth of water injection probe, and the depth, location and spacing of the sensing probes is governed by the interrelationship between these parameters. Ideally, these parameters should be controlled in such a way that a zone of essentially horizontal flow is produced so that the tips of the sensing probes can be located on a single streamline.

In an effort to optimize the relationship between parameters, both flow net studies and experimental measurements in the laboratory test cells were conducted. Although plates of three different sizes, 24 inch (609.6 mm), 18 inch (452.2 mm), and 12 inch (304.8 mm), were manufactured, flow net studies and tests performed with the 24 inch (609.6 mm) and 18 inch (457.2 mm) plates showed that there was no real advantage to varying the plate size for different layer thicknesses, as long as the depth of the water injection probe and the depth and location of the sensing probes were properly controlled. Therefore, the 12 inch (304.8 mm) and 24 inch (609.6 mm) plates were abandoned and the 18 inch (457.2 mm) plate was used for the remainder of the tests.

Both flow net studies and laboratory experimentation showed that a depth of water injection probe equal to the thickness of the layer being tested produced the pattern of flow that was desired. However, as mentioned earlier, this criterion did not prove to be valid when the layer being tested was underlain by a layer of higher

permeability, and it was necessary to lower the depth of the water injection probe to produce saturated flow in both layers in order for the FPTD to yield satisfactory results.

For layers thicker than 12 inches (304.8 mm), satisfactory results were produced with the 12 inch (304.8 mm) long water injection probe, even though it did not penetrate all the way to the bottom of the layer.

For layers up to 14 inches (355.6 mm) in thickness, sensing probe depths as deep as the center of the layer, i.e., up to 7 inches (177.8 mm) deep, proved to be satisfactory during laboratory experimentation. However, for layers in excess of 12 inches (304.8 mm) thick, flow net analysis would suggest that the sensing probe depth should not exceed 6 inches (152.4 mm). Thus, for these thicker layers, greater than 12 inches (304.8 mm) thick, if measurements are to be made at a single depth, then they should be made somewhere in the upper half of the layer rather than being at the center of the layer as recommended for layers less than 12 inches (304.8 mm) thick. However, because the FPTD measures the coefficient of permeability within a relatively thin zone vertically, it would probably be desirable to make measurements at several depths throughout the layer of interest and average the results.

The influence of the location and spacing of the sensing probes was investigated by varying these parameters throughout the testing program. During the early part of the investigation, while using the 24 inch (609.6 mm) diameter plate, probe spacings varying from 2 inches (50.8 mm) to 6 inches (152.4 mm) were used with good results. In most of these tests, the interior (high head) probe was located within the inner third of the plate, i.e., from 2 inches (50.8 mm) to 4 inches (101.6 mm) from the center. These early data led to the conclusion that measurements made with the FPTD were not particularly sensitive to the location and spacing of the sensing probes. Later, however, a more comprehensive series of tests were

performed with the 18 inch (457.2 mm) diameter plate, both for single layers of material and for the two layer system. In these tests, it was decided to cycle through all possible combinations of location and spacing in order to get as comprehensive a view of the influence of these parameters as possible.

Although there was considerable scatter in the test results, in general, the data tended to show that the best results were produced with 2 inch (50.8 mm) and 3 inch (76.2 mm) probe spacings, with the interior probe within the center third of the plate, i.e., within 3 inches (76.2 mm) of the center. This was particularly true for the case where the layer being tested was underlain by a layer of high permeability material.

Accuracy and Reproducibility of Results

The overall accuracy of the FPTD and the reproducibility of the results achieved were evaluated by comparing coefficients of permeability measured by the FPTD (k_d) with the coefficients of permeability for the same materials measured in the test cells (k_{tc}) using steady sheet flow. A graphical comparison of these data is shown in Figure 29. These data were analyzed statistically using the Statistical Analysis System (SAS Package) developed by A. T. Barr and J. H. Goodnight. The linear regression equation established by this analysis (shown as the solid line in Figure 29) can be expressed as

$$k_d = 1.023\ k_{tc}^{1.023}$$

This equation represents a very good fit to the experimental data as evidenced by a coefficient of determination (r^2) of 0.959. In addition, a comparison of the regression line for the data (shown solid) and the 45° line (shown dashed) shows that, on the average, the FPTD

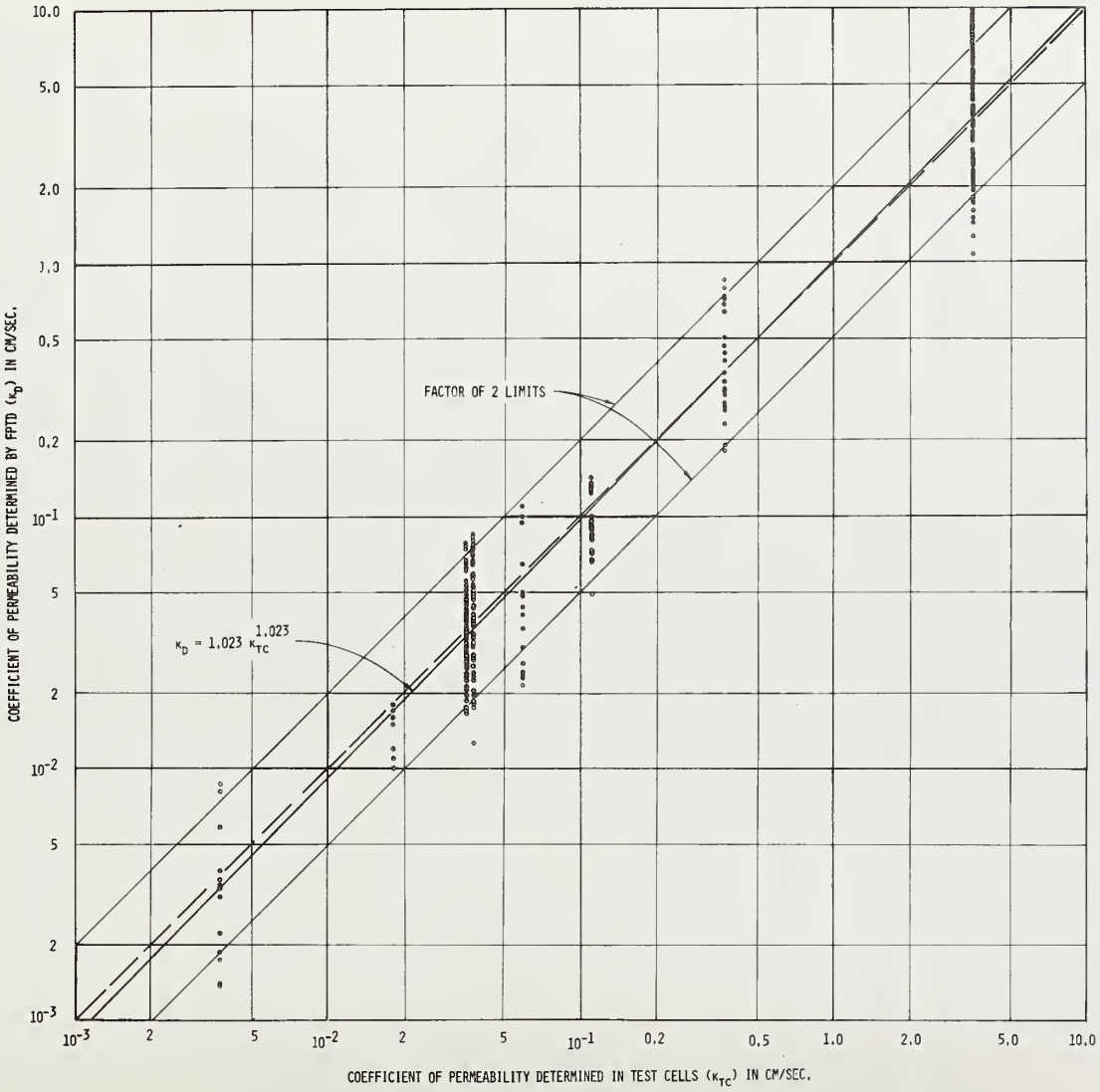

FIGURE 29. COMPARISON BETWEEN PERMEABILITY DETERMINED IN TEST CELLS AND PERMEABILITY MEASURED BY FPTD.

tended to produce values very close to those measured by the test cell technique, with only a slight tendency for under prediction in the low permeability range and a very slight tendency for over prediction in the high range. The rather obvious manifestation of over prediction of coefficient of permeability, which showed up during Task C as a result of dispersion and diffusion phenomena, did not show up here.

Figure 29 was prepared and the statistical analysis was performed using all 410 test results that were obtained during Task E. Although the accuracy of certain of these data was open to serious question for one reason or another, they were deliberately included in Figure 29 and the analysis so that the resulting comparison between k_d and k_{tc} would represent the "worst condition" and thus could be thought of as representing the lower limit of the accuracy and reproducibility of the values obtained with the FPTD.

The shaded area on Figure 29 represents the zone in which the data would fall, if the FPTD measured the coefficient of permeability within a factor of two of the true value. When all of the test results are considered, 336 of the 410 test values (82.0 percent) fall within the shaded zone. However, as noted earlier, certain of the test data are open to serious question. Included in this category are some of the data obtained with what proved to be unsatisfactory locations and spacings of the sensing probes. If these 44 pieces of data are excluded from the total, then 336 of the remaining 366 test values (91.8 percent) fall within the shaded zone. On this basis, it would appear that the prototype FPTD would satisfy the requirement that it measure the coefficient of permeability within a factor of two of the true value ninety percent of the time.

FIELD TESTING OF PROTOTYPE FPTD (TASK F)

Introduction

Proposed Scope and Objectives of Task

The work undertaken in this Task was concerned with field testing the prototype FPTD to determine its performance characteristics under actual field operating conditions. It was originally proposed that ten different field sites would be visited and that at least three test sections would be evaluated per site. Permeability tests were to be conducted on the subgrade, subbase, and base layers at each test section. One of the objectives of the field testing program was to select sites that contained boundary conditions similar to those outlined for the LABORATORY EVALUATION OF THE PROTOTYPE FPTD (TASK E). Initially, it was anticipated that the sites would be distributed among a number of states in the eastern portion of the United States based on a selection process accomplished in cooperation with the Federal Highway Administration and the various state highway (transportation) departments. Samples were to be collected at each test site and returned to the laboratory for physical properties and permeability testing. Results of the field and laboratory permeability tests could then be compared and, possibly, correlated.

Secondary objectives of this Task included an observational evaluation of: the ruggedness and reliability of the equipment; the ease of operation; time requirements for setup and testing; and other related factors. In addition, careful consideration was to be given to the need for subjective and objective judgments required in setting up the equipment and conducting a test.

Actual Scope of Work Accomplished in Task F

The actual scope of work accomplished in Task F differed from that proposed in two major respects: (a) the number of test sites and sections investigated and (b) the range of materials and

conditions encountered. The principal reasons for these differences were: (a) the limited amount of construction underway during the field testing time period; (b) the similar nature of subbase and base course materials within a state and between states; (c) the use of relatively consistent layer thicknesses and pavement sections from state to state; and (d) the absence of any permanent groundwater table within the pavement section. In reality, the limited number of sites, associated with the limited amount of construction, dictated that any or all possible sites be evaluated irrespective of whether they met any preconceived boundary conditions and material type requirements.

Task F consisted of four basic components: (a) identification of potential test sites; (b) modification and adaptation of the laboratory version of the FPTD for field use; (c) field testing; and (d) laboratory evaluation of the physical properties and permeability of representative samples collected during the field testing program. The scope of the field testing program consisted of investigations at 18 test sections in 13 different locations in 8 different states. In almost all instances, the test section consisted of a single base or subbase layer overlying an impervious subgrade. In addition, at no test section was there evidence of the presence of a groundwater table within or immediately below the pavement section.

As originally proposed, samples were collected at each permeability test location and returned to the West Virginia University laboratories for physical properties and permeability testing. In addition, field nuclear moisture-density determinations were made at each permeability test location. These tests were conducted in order to calculate the in situ porosity of the layer as well as to provide the target dry density values for the laboratory permeability tests. The porosity values were generally calculated using the average in situ dry density value and an assumed average specific gravity of solids value.

Prior to and during the field testing program the laboratory version of the FPTD was adapted, modified, and improved for field use. The performance of the unit under field conditions provided a continuing basis for evaluation and upgrading of the equipment. A description of the prototype FPTD was presented in the section of this report dealing with DESIGN AND CONSTRUCTION OF PROTOTYPE FIELD PERMEABILITY TEST DEVICE (TASK D), and the details of its construction are presented in Appendix B. As pointed out in those sections of the report, modifications were made to the equipment as dictated by experience accumulated during the field testing program.

Field Testing Program

The general scope and objectives of the field testing program (Task F), both as originally proposed and as actually conducted, were summarized above. Within this section of the report, a detailed description of the field test sections and associated materials will be given. In addition, the field and companion laboratory test results will be presented and discussed along with more general observations related to the equipment and its operation.

Test Sections - Selection and Description

As stated in the earlier Report (91), highway departments in fifteen states in the eastern United States were contacted with assistance from the FHWA Regional Offices. The contacted states were:[1] Alabama, Florida, Georgia, Indiana, Kentucky*, Maryland*, Michigan*, Mississippi, New Jersey, North Carolina*, Ohio*, Pennsylvania*, Tennessee*, Virginia, and West Virginia*. Only one of the departments (Florida) was eliminated from further consideration

[1] The states actually visited are marked by an asterisk.

because of technical limitations. Specifically, it was found that the base courses in general use in Florida have a coefficient of permeability less than the lowest practical operating limit of the prototype FPTD (also lower than the specified minimum limit of 10^{-4} cm/sec). Definitive plans had been made to visit New Jersey and Virginia during the early Fall of 1978, but the anticipated test sections did not develop because of construction delays and the onset of the end of the construction season. Thus, a total of eight of the original fifteen states contacted were visited. As stated earlier, within these eight states, there were eighteen test sections at thirteen different locations. A descriptive summary of the test locations and sections is given in Table 4.

A review of Table 4 reveals several important observations relative to the various test sections. These observations can be summarized as follows:

1. The base and/or subbase layers ranged in thickness from a minimum of 4 inches (101.6 mm) to a maximum of 14 inches (355.6 mm).
2. With perhaps one exception, the subgrade was essentially impervious (i.e., a coefficient of permeability less than 10^{-4} cm/sec).
3. With few exceptions, a single layer crushed aggregate base or subbase was utilized.
4. The only state utilizing open graded aggregates specifically for the purpose of subsurface drainage was Kentucky, and their sections were experimental.
5. No evidence was observed to indicate the presence of a groundwater level in or near the base of a subbase or base layer.

Table 4. Summary of Task F Field Testing Program

Description of Site			Test	Description of Test
State	Location(s)	Project No./Station	Section No.	Section(s)
KY	Campbellsville, Taylor County	DP55-1(9)/342 + 50	1	11 inches (279.4 mm) Dense Graded Aggregate Base Over Impervious Subgrade
		DP55-1(9)/341 + 00	2	2 inches (50.8 mm) Black Base Over 5 inches (127.0 mm) No. 57 Limestone Drainage Layer Over 4 inches (101.6 mm) DGA Over Impervious Subgrade
MD	Rising Sun	Route 274/346 + 50	1	12 inches (304.8 mm) "Select Borrow" (Sand and Gravel of Glacial Origin) Subbase Over Impervious Subgrade
		Route 274/343 + 50	2	As Above
MI	Detroit	U.S. 24 (Telegraph Road)/364 + 40	1	5 inches (127.0 mm) 22A Gravel Base Over 10 inches (254.0 mm) Class 2 Granular Material (Blend of MI 2NS Sand and Fine Sand)

Table 4. Summary of Task F Field Testing Program (cont.)

State	Description of Site: Location(s)	Description of Site: Project No./Station	Test Section No.	Description of Test Section(s)
NC	Murphy	NC Route 19/23 - 8.3019119/179 + 50	1	12 inches (304.8 mm) Crushed Granite Base Meeting Table 908-1 Specifications Over Impervious Subgrade
OH	Athens	Route 50/614 + 00	1	6 inches (152.4 mm) OH 310-A Limestone and Sand Base Mixture Over Impervious Subgrade
	Neff	Route 149/183 + 50	2	4 inches (101.6 mm) OH 304 Basic Oxygen Furnace Steel Slag Base Over Impervious Subgrade
PA	North of Bedford, Bedford County	U.S. 220, LR 1061-Sect. 4APD55(8)/750 + 05 749 + 85	1A 1B	10 inches (254.0 mm) PA No. 2 Crushed Limestone Subbase Over Impervious Subgrade
	North of Harrisburg	U.S. 322/22, LR 1089-3A/ 194 + 55	2	12-14 inches (304.8-355.6 mm) PA No. 2A Crushed Limestone Subbase Over Impervious Subgrade

Table 4. Summary of Task F Field Testing Program (cont.)

State	Description of Site: Location(s)	Description of Site: Project No./Station	Test Section No.	Description of Test Section(s)
PA	Northeast of Reading	LR 783 - A03/145 + 50	3	12 inches (304.8 mm) PA No. 2A Crushed Limestone Subbase Over Impervious Subgrade
TN	Near Greenville, Greene County	Route 11E, F-62-2/ 416 + 65	1	5 inches (127.0 mm) TN No. 303.01 Type A Crushed Limestone (Grading D) Subbase, with 5 Percent Calcium Chloride, Over Impervious Subgrade
WV	South of Beckley, Mercer/Raleigh County	I-77-2(55)201/1150 + 00	1	6 inches (152.4 mm) WV No. 307-2 Crushed Sandstone Over Impervious Subgrade
	North of Princeton	I-77-2(54)9/435 + 00	2	5 inches (127.0 mm) WV No. 307-1 Crushed Limestone Over 6 inches (152.4 mm) WV No. 307-2 Crushed Limestone Over Impervious Subgrade
	Princeton	APD-200(36), C-1/251 + 00	3	6 inches (152.4 mm) WV No. 307-2 Crushed Limestone Over Impervious Subgrade

Performance of Field Tests

The prototype FPTD utilized for conducting the field permeability tests was described in an earlier section of this report, which included a discussion of the experimental procedure and associated data collection and reduction methods. As stated earlier, the FPTD measures, at a constant value of hydraulic gradient, the average seepage velocity, v_p, from which the average discharge velocity, v, can be calculated if the porosity, n, of the layer is known. Correspondingly, the value of porosity can be determined if the values of specific gravity of solids and dry density are known or can be measured. During the field testing program the dry density values were obtained with the use of TROXLER Model 3411 Nuclear Moisture-Density Meter using the direct transmission measurement configuration. The dry density value used for calculation purposes was the average of the direct transmission values at two to four 2 inch (50.8 mm) intervals within the layer being tested. For field calculations, the specific gravity of solids value was generally assumed to be 2.7. In some instances, assisting state highway department personnel supplied a value based on previous test results.

For the purposes of this Project, field bag samples were taken at each test section and returned to the laboratory for bulk specific gravity, specific gravity of solids, gradation, and permeability tests.

The experimentally determined specific gravity of solids values were then utilized to calculate "corrected" field coefficient of permeability values. In actual practice, it is anticipated that the specific gravities of the aggregates would be known within reasonable limits and, thus, no significant error would be expected from this source.

The gradation characteristics of the materials served to provide a basis for comparison or reference as well as to give a

qualitative indication of the probable permeability characteristics of the material, and the laboratory determined coefficient of permeability values permitted a direct comparison to be made between these values and the field values.

Companion Laboratory Testing Program

As indicated above, bag samples were taken at each test location. When possible, the material directly under the plate was excavated, subsequent to the test, and utilized for the field sample. The desirability of this approach became apparent after the Pennsylvania test series when the properties of three samples, one taken directly beneath the plate and two taken approximately 10 feet away, were compared and indicated significant differences.

Bulk specific gravity and specific gravity of solids tests were conducted in accordance with appropriate AASHTO Test Methods on the plus No. 4 and minus No. 4 fractions, respectively. The particle size analysis tests were conducted using standard methods and a sieve nest appropriate for the particular material being tested. That is, the composition of the sieve nest was adjusted to be compatible with the specified material gradation requirements of a given material in a given state.

The permeability tests were conducted using a time-lag permeameter described by Barber and Sawyer (7). The specimens were compacted in 6 inch (152.4 mm) diameter CBR molds using a minus 3/4 fraction having the same coarse-to-fine fraction, i.e., plus No. 4 to minus 3/4 inch (19.1 mm), present in the original sample. The recommended AASHTO replacement technique was utilized for this purpose. The specimen was compacted in layers using a standard Proctor drop hammer. An effort was made to obtain a dry density approximately equal to the dry density measured at the corresponding test location. As will be noted later, this effort met with only limited success.

Results of the Field and Laboratory Tests

Table 5 summarizes the average field test results and the corresponding laboratory results. The measured specific gravity of solids (G_s) values and calculated porosity (n) values are included since both values are used in the data reduction process. The in situ dry density values and laboratory dry density values are given to provide a satisfactory basis for comparing the field and laboratory coefficient of permeability values. Reference to Table 5 shows that significant difficulty was encountered in attempting to fabricate laboratory specimens having dry densities approximately equal to those for the corresponding field test.

No field test results are given for the two test locations in Kentucky and the one test location in North Carolina because of the inability of the equipment to measure the permeability at these test locations. At the high permeability sites (i.e., North Carolina and one of the Kentucky locations), stable steady state flow could not be maintained for a sufficient period of time to make a satisfactory measurement. Attempts to increase the flow rate to develop and maintain a steady state condition generally led to the development of piping at the interface between the plate and the base course materials. At the high permeability Kentucky locations the coefficient of permeability value approached the proposed upper limit of the operating range for the equipment (i.e., 10 cm/sec). Subsequent to the attempted test in North Carolina, annular serations were machined into the base of the plate in an attempt to develop a better interfacial seal and, therefore, minimize the piping potential.

Problems were also encountered in generating sufficient flow to develop saturated conditions in the dense graded aggregate (DGA) base at the remaining Kentucky test location. Again, as the pressure was increased to develop sufficient flow for saturation and measurement purposes, piping developed. The laboratory coefficient of permeability determined for this material (i.e., 2.73×10^{-3} cm/sec) was

Table 5. Summary of Field and Laboratory Permeability Results

State	Test Location	Test Section No.	G_s [a]	Field Results: Average [b][g] In Situ γ_d (pcf)	Field Results: Calculated Porosity (%)	Field Results: Avg k [c] (cm/sec)	Laboratory Results: γ_d (pcf) [g]	Laboratory Results: Avg k [c] (cm/sec)
KY	Campbellsville, Taylor Co.	1	2.73	--	--	(f)	139.0	2.73×10^{-3} (4)
		2	2.72	--	--	(f)	101.0	8.27 (6)
MD	Rising Sun	1	2.64	133.6 (3)	19	9.96×10^{-2} (4)	131.7	2.55×10^{-3} (5)
		2	2.67	130.5 (3)	22	2.88×10^{-2} (3)	131.2	3.18×10^{-3} (5)
MI	Detroit	1 [d]	2.73	132.5 (2)	22	2.17×10^{-2} (2)	135.0	1.90×10^{-2} (5)
		1 [e]	2.72	118.7 (5)	30	2.38×10^{-2} (4)	120.00	1.60×10^{-2} (6)
NC	Murphy	1	2.83	137.2 (3)	22	(f)	126.0	2.78 (6)
OH	Athens	1	2.70	127.7 (3)	24	1.01×10^{-2} (3)	134.0	2.19×10^{-2} (6)
	Neff	2	3.52	163.4 (3)	26	2.99×10^{-1} (5)	158.7	2.45×10^{-2} (5)
PA	North of Bedford, Bedford Co.	1A	2.72	126.7 (3)	25	1.43 (3)	128.0	1.60 (6)
		1B	2.77	124.0 (3)	28	5.80×10^{-1} (4)	128.0	1.66 (5)
	North of Harrisburg	2	2.81	130.2 (4)	26	1.00 (11)	125.0	1.66 (5)
	Northeast of Reading	3	2.79	133.1 (5)	24	2.18 (3)	130.0	2.90×10^{-1} (6)

[a] Based on laboratory determination of specific gravity of solids using ASTM Test Method D854 and the minus No. 4 fraction.
[b] Value in parentheses indicates number of individual direct transmission measurements.
[c] Value in parentheses indicates number of individual permeability measurements (made during one test setup).
[d] Values given are for the 5 inch (127.0 mm) layer of MI 22A Gravel Base.
[e] Values given are for the 10 inch (254.0 mm) layer of MI Class 2 Granular Material (Blend of MI 2NS Sand and Fine Sand).
[f] Beyond measurement capability of equipment.
[g] Note that 1 pcf = 16.03 kg/m^3.

Table 5. Summary of Field and Laboratory Permeability Test Results (cont.)

State	Test Location	Test Section No.	G_s [a]	Average In Situ [b][e] γ_d (pcf)	Calculated Porosity (%)	Avg k [c] (cm/sec)	γ_d (pcf) [e]	Avg k [c] (cm/sec)
TN	Near Greenville, Green Co.	1	2.82	136.4 (3)	23	1.52×10^{-1} (5)	128.0	7.23×10^{-1} (6)
WV	South of Beckley, Mercer/Raleigh Co.	1	2.62	120.6 (1)	26	3.02×10^{-1} (1)	134.0	7.38×10^{-3} (5)
	North of Princeton, Mercer Co.	2	2.72	132.8 (3)	22	5.60×10^{-1} (2)	134.7	2.15×10^{-2} (10)
	Princeton, Mercer Co.	3	2.70 [d]	125.2 (2)	26	6.45×10^{-1} (4)	126.8	4.46×10^{-1} (2)

(a) Based on laboratory determination of specific gravity of solids using ASTM Test Method D854 and the minus No. 4 fraction.
(b) Value in parentheses indicates number of individual direct transmission measurements.
(c) Value in parentheses indicates number of individual permeability measurements (made during one test setup).
(d) Assumed. Actual value not determined.
(e) Note that 1 pcf = 16.03 kg/m^3.

reasonably close to the proposed lower operating limit for the equipment (i.e., 10^{-4} cm/sec).

The Kentucky test series was the first attempt to utilize the prototype FPTD and revealed a number of equipment deficiencies. Of particular note was the poor design and operational characteristics of the salt injection and the electrical/hydraulic control and measurement system. Prior to any subsequent field testing, modified systems were fabricated using revised designs based on the Kentucky experience. Only minor equipment modifications were made subsequent to these initial efforts.

Comparison of Laboratory and Field Permeability Test Results

Although the laboratory permeability tests were conducted to provide a basis of comparison with the field test results, certain inherent problems exist in making a valid comparison irrespective of the accuracy of the field test results. Those factors felt to be of possible significance are: (a) differences in dry density (porosity); (b) difference in direction of fluid flow; and (c) difference in fabric (particle orientation). The numerical consequences of these possible differences are not known, but it is believed they can be very significant.

Based on the Kozeny-Carman equation, the relationship between the field measured coefficient of permeability, k_f, and the laboratory measured coefficient of permeability, k_l, for variable dry density can be shown to be

$$k_f \sim \beta \left[\frac{\gamma_{dl}}{\gamma_{df}}\right]^2 k_l ,$$

where $\beta = \left[\frac{G_s\gamma_w - \gamma_{df}}{G_s\gamma_w - \gamma_{dl}}\right]^3$, γ_{df} is the field dry density, and γ_{dl} is the laboratory dry density. Assuming $G_s = 2.70$, and using the actual values of γ_{df} and γ_{dl} from Table 5, yields values of β ranging from about 0.4 to 2.7, thus indicating that the field measured coefficient of permeability, k_f, could vary from 0.34 to 3.3 times the laboratory measured value, k_l, based on variation in dry density alone. However, examination of Table 5 shows that, in this case, the above relationship does not offer a consistent explanation for the differences between field and laboratory measured values of coefficient of permeability.

Table 6 was prepared in an attempt to obtain a better indication of the overall performance of the prototype FPTD over the range of material types and boundary conditions encountered during the field testing. The ranges of values given were obtained directly from Table 5. Similarly, the average values given are the averages of the values given in Table 5.

An examination of Table 6 leads to the following observations:

1. The range of specific gravity of solids values for naturally occurring materials fall within a reasonably narrow range (2.62 - 2.83 with an average of 2.72).
2. Similarly, the range of in situ dry density values for both natural and crushed aggregates is comparatively small, 118.7 - 137.2 pcf (1903.1 - 2199.7 kg/m^3) with an average of 129.2 pcf (2071.4 kg/m^3).
3. The consequence of the first two observations is that the in situ porosity values fall within narrow limits (19 to 30 percent with an average of 24 percent). The presumptive use of n = 24 percent for field calculations should not produce an error in the calculated coefficient of permeability of

Table 6. Summary of Range and Average of Field and Laboratory Test Values

Parameter	Range of Values[a]	Average Values[b,c]	
Field Dry Density (pcf)[g]	118.7 - 163.4	131.9	(14)
	(118.7 - 137.2)[d]	(129.2)[d]	(13)
Specific Gravity of Solids	2.63 - 3.52	2.76	(18)
	(2.62 - 2.83)[e]	(2.73)[e]	(14)
Field Porosity (%)	19 - 30	24	(14)
Field Coeff. of Perm. (cm/sec)	1.01×10^{-2} - 2.18	4.1×10^{-1}	(12)
Lab Coeff. of Perm. (cm/sec)	2.55×10^{-3} - 8.27	1.72	(18)
	(2.55×10^{-3} - 1.66)[f]	3.7×10^{-1} [f]	(13)

(a) Based on average values presented in Table 5.
(b) Based on average of the average values presented in Table 5.
(c) Numbers in parentheses indicate numbers of values included in ranges and averages.
(d) Excludes value for blast furnace slag.
(e) Excludes value for blast furnace slag, bulk specific gravity values, and the 2.7 value assumed for one of the WV test sections.
(f) Excludes all lab values not having corresponding field values.
(g) Note that 1 pcf = 16.03 Kg/m^3.

greater than $\pm$ 25 percent.

4. The range of field measured coefficient of permeability values is a subset of the corresponding laboratory values. Previously discussed experimental difficulties prevented measurement of coefficient of permeability values less than approximately 1×10^{-2} cm/sec. However, it is not suggested that these values necessarily represent the lower and upper operating limits of the prototype FPTD.
5. Excluding the Kentucky material (ASTM No. 57 crushed limestone) that was placed specifically for drainage purposes, the prototype FPTD was able to measure coefficient of permeability values corresponding to the upper limit exhibited by the conventionally used base and subbase materials encountered in this study.
6. Comparing the average field coefficient of permeability value with the average laboratory coefficient of permeability value, excluding those laboratory values which have no corresponding field values, yielded 4.1×10^{-1} cm/sec and 3.7×10^{-1} cm/sec for the field and laboratory, respectively.

It is difficult to make any definitive statements relative to the accuracy of the prototype FPTD based on a direct comparison between field and laboratory test results. There are insufficient data available to conduct a statistical analysis. However, the comparison shown in Table 7 is quite revealing. It shows that for 6 of the 14 measured coefficients of permeability (43 percent), the field values are very nearly within a factor of 2 of the laboratory values, and for 10 of the 14 measured coefficients of permeability (71 percent), the field values are within a factor of 10 of the laboratory values. Although this comparison is not good, it certainly is not bad, when the rather significant differences between field and laboratory test conditions are considered.

Table 7. Comparison Between Field and Laboratory Measured Values of Coefficient of Permeability

State	Test Location	Test Section No.	Measured Permeability (cm/sec.) Field Value (k_f)	Lab Value (k_l)	Ratio k_f/k_l
KY	Campbellsville, Taylor County	1	--	2.73×10^{-3}	--
		2	--	8.27	--
MD	Rising Sun	1	9.96×10^{-2}	2.55×10^{-3}	39.05
		2	2.88×10^{-2}	3.18×10^{-3}	9.05
MI	Detroit	1(a)	2.17×10^{-2}	1.90×10^{-2}	1.14
		2(b)	2.38×10^{-2}	1.60×10^{-2}	1.48
NC	Murphy	1	--	2.78	--
OH	Athens	1	1.01×10^{-2}	2.19×10^{-2}	0.46
	Neff	2	2.99×10^{-1}	2.45×10^{-2}	12.20
PA	North of Bedford,	1A	1.43	1.60	0.89
	Bedford County	1B	5.80×10^{-1}	1.66	0.35
	North of Harrisburg	2	1.00	1.66	0.60
	Northeast of Reading	3	2.18	2.90×10^{-1}	7.52
TN	Near Greenville	1	1.52×10^{-1}	7.23×10^{-3}	0.21
WV	South of Beckley	1	3.02×10^{-1}	7.38×10^{-3}	40.92
	North of Princeton	2	5.60×10^{-1}	2.15×10^{-2}	26.04
	Princeton	3	6.45×10^{-1}	4.46×10^{-1}	1.45

(a) Values are for 5" Layers of MI 22A Gravel Base

(b) Values are for 10" Layer of MI Class 2 Granular Material

Evaluation of the Field Performance of the Prototype FPTD

In evaluating the field performance of the FPTD, two factors should be kept in mind; viz, the Device continued to undergo modification during the testing program and any quantitative comparison of the field and laboratory coefficients of permeability is subject to question because of fundamental and experimental differences in the procedures.

Although data presented in the preceding sections of this report appear to indicate a rather erratic behavior by the prototype FPTD, the laboratory evaluation of the prototype (Task E) indicated that it was capable of producing consistent and accurate results over a range of material types and boundary conditions. The comparative permeability results for Task E were obtained under more nearly the same conditions of porosity, flow direction, and fabric. Thus, it is felt that the Task E results should be utilized to judge the ability of the equipment to accurately determine the coefficient of permeability of base and subbase layers. Therefore, on that basis, the performance of the prototype FPTD would be judged satisfactory in its ability to determine accurately and consistently the coefficient of permeability of aggregate base and subbase layers.

The field evaluation Task (Task F) did serve to identify potential problems with the equipment, to test its ruggedness and durability, and to assist in developing a systematic procedure for conducting the tests. The Task also identified possible refinements that could be made to the equipment for improving its portability and operation. These will be discussed in a later section along with other suggestions for the future implementation of the equipment.

The ruggedness and durability of the equipment proved to be excellent. The only components of the Device that gave problems from time to time were the sensing probes. However, these components

are inexpensive and easy to construct, thus a replacement probe can be inserted in place of the original probe should a problem occur. It is expected that a little refinement in the construction of and material for these probes would reduce the need for replacement to a minimum.

Because of the concentrated salt solution that is utilized in the test, corrosion of the fittings and framework is possible unless care is taken to reduce the amount of spillage and to flush all systems with fresh water at the end of the testing sequence. The only other components that are subject to any wear or mechanical damage are the predrive rods for the central water injection and sensing probes. Again, the items are inexpensive and easy to construct and thus do not pose a substantial problem. However, some improvement in these predrive rods could be made that would assist in minimizing potential piping adjacent to these probes. That is, the diameter of the predrive rods should be slightly smaller than the probes. In addition, the probe rods could be slightly tapered (smaller at the bottom and tapering to a slightly larger uniform diameter at the plate) so they would produce a slight wedging action as they are inserted. This would be another way to minimize potential piping.

Although the subbase layer encountered in Tennessee contained 5 percent calcium chloride for stabilization, no problem was encountered in achieving stable steady state conditions and obtaining a satisfactory permeability measurement. Although this represents only one case, it is felt that the concentration of the salt solution utilized for the test is so large that it will, in a sense, "overpower" the relatively small concentrations of salt used for conventional stabilization purposes.

Typical combined setup and testing times for a given layer ranged from a minimum of approximately 45 minutes to a maximum of approximately 1 1/2 hours. Setup time for all the conditions

encountered generally did not exceed 20 minutes with a three person crew. In reality, however, a two person crew would be quite satisfactory and could probably set up and conduct the tests with as great an efficiency as a three person crew. With the exception of slightly increasing the time requirements, the setup and testing could be accomplished by one person.

Occasionally, a test setup would result in an ammeter deflection of the downstream probe prior to that of the upstream probe. Although no physical verification was possible, it was believed that this situation was due to the interference of an aggregate particle immediately upstream of the electrical contact point of the upstream probe. Upon introduction of the salt solution, the solution was deflected and streamed around the upstream probe, thus producing a registration on the downstream probe before the upstream probe. When this occurred, the sensing probes were removed and then reinserted after the plate was rotated. However, other possible solutions to this situation could be effected by changing the position of the probes along the same line or inserting the probes along another line without removing the plate. In fact, it may be desirable to measure permeability along orthogonal directions for a given test setup and utilize the geometric mean of the resulting values.

The major problem identified in the operation of the prototype FPTD is piping at the plate-layer interface and, possibly, at all probe-layer interface boundaries. Of course, the piping at the plate-layer interface is observable, whereas it is not observable at the other boundaries. It is quite apparent that this piping has to be preceded by piping adjacent to the central water injection probe. Thus, the possibility exists that water could flow from the point of injection along the central probe and plate boundaries and, finally, along the sensing probe boundaries to the electrical contact point. Under those circumstances, an outwardly satisfactory test would produce erroneous results.

Before going further with this discussion, it should be pointed out that plate-layer interfacial piping is not, in itself, detrimental. Perfectly satisfactory measurements can be made if sufficient flow to maintain saturated, stable, steady state conditions can be established within the layer. The concern with significant observable piping is that it indicates a portion of the total flow is being short-circuited (thus limiting the quantity of water available to the layer) and may lead to conditions involving flow simply along the plate and probe boundaries. Thus, a number of steps have been taken in an attempt to minimize the observable piping problem. Various grades of rubber and sand were placed between the plate and the layer to provide a "seal". These approaches met with varying degrees of success and no given system emerged as the best system under all circumstances. The major piping problems were generally associated with layers that had been in place and under traffic for some time. Such a situation produced a hard (compact) and rough surface, making it difficult to achieve an effective uniform seal. It was found that effective seals (not necessarily perfect) could generally be achieved in freshly compacted layers.

The effectiveness of the seal is also a function of the downward force that can be applied to the plate as well as the bearing area of the plate. For the field testing program, the magnitude of the downward force was limited by the weight of the rear axle of the van. Since an 18 inch (457.2 mm) diameter plate has an area of approximately 250 square inches (0.161 square meters), 250 pounds (113.5 kilograms) of downward force is required to produce a 1 psi (703.7 kg/square meter) stress beneath the plate. However, the actual stress is probably not uniform because of the imperfections of the surface of the layer. To increase this confining stress and, hopefully, minimize the piping potential, annular teeth were machined into the base of the plate prior to the Maryland and Michigan test series. In Maryland, the "select borrow" (bank run glacial sands and gravels)

had been in place for some time under traffic. Although apparently satisfactory measurements were made at the two test locations, there was significant observable piping. However, the performance of the modified plate was judged to be better than the corresponding original plate. The Michigan tests were conducted on a freshly compacted granular base and subbase of gravelly sand and sand, respectively. No major observable piping occurred and excellent results were achieved.

Another approach that was given consideration in minimizing the piping problem was to utilize montmorillonite clay sprinkled on the circular area between the plate and the aggregate. The concept was that the clay would expand and effectively seal all possible piping channels as it absorbed water. Such an approach seems quite feasible and would simply require the fabrication of a jig for placing the dry clay mineral in the proper fashion. Although this method met with success during limited use in the laboratory, it was not tried in the field.

CONCLUSIONS

As a result of the laboratory and field studies described herein the following conclusions have been reached:

1. The prototype field permeability test device (FPTD) provides a convenient means for the determination of the in situ coefficient of permeability of highway bases and subbases with reasonable accuracy and reproducibility.
2. The "velocity technique" of permeability determination, embodied in the FPTD, is the simplest and most direct method presently available for measuring the coefficient of permeability of highway base and subbase courses.
3. The FPTD is capable of measuring the average horizontal coefficient of permeability of each layer in a multilayered system within a factor of two of the true permeability ninety percent of the time.
4. The FPTD is capable of measuring the coefficient of permeability of bases and subbases within a practical range. However, it was not possible, at the present stage of development, to measure very low permeabilities in the order of 10^{-4} cm/sec or very high permeabilities in the order of 10 cm/sec.
5. The coefficient of permeability of layers of base and subbase, ranging in thickness from 3 inches (76.2 mm) to 18 inches (457.2 mm), can be measured by the FPTD, as long as saturated steady state flow can be maintained during testing.
6. The location of the watertable relative to the layer being tested has no influence on the test results, as long as a zone of saturated steady state flow can be established and maintained during testing.
7. The permeability of layers adjacent to the layer being tested has no influence on the test results, as long as

essentially horizontal, saturated, steady state flow is established and maintained in both the layer being tested and the adjacent layer(s). This requires that water be injected over the full depth of the layer being tested and over the full depth of any adjacent layer that has a significantly higher permeability than the layer being tested.

8. Because of the anisotropy of compacted layers of base and subbase, the direction of flow during testing can influence the test results. Thus, it is desirable to perform tests in orthogonal directions at a given test location and then average the results.
9. The depth of the sensing probes and their location relative to the water injection probe does influence the test results. The best results were produced with 2 inch (50.8 mm) and 3 inch (76.2 mm) probe spacings, with the interior probe located within three inches (76.2 mm) of the water injection probe. For measurement at a single depth, the tip of the sensing probes should be located at the center of the layer being tested, for layers up to 12 inches (304.8 mm) thick. For layers in excess of 12 inches (304.8 mm) thick, the depth of the tip of the sensing probes should not exceed 6 inches (152.4 mm).
10. In some instances, the coefficients of permeability determined by the FPTD in the field did not compare favorably with the values obtained in the laboratory, because of the inherent difficulties associated with duplicating field conditions in laboratory permeameters.
11. The ruggedness and durability of the FPTD for field use proved to be excellent. The components of the Device are inexpensive and easy to construct.

RECOMMENDATIONS

Although the prototype FPTD developed through this research satisfies project objectives and is capable of measuring the coefficient of permeability of highway bases and subbases with reasonable accuracy and reliability, the following recommendations for improving the equipment and its operation are presented:

1. Fabricate a new control and measurement system with panel type, quick connect couplings. This unit should be provided with hinged sides, as appropriate, to allow direct access to batteries and valves.
2. Consider mounting the entire system, including the revised control and measurement system, on a trailer frame. A storage locker should also be included for associated equipment, tools, etc. Integral with the trailer assembly should be a revised arrangement for jacking against the plate that will permit the removal of all probes without removal of the downward force. This system should also provide for rapid and positive placement of the jacking force along the centroidal axis of the plate. In addition, a "locator jig" for defining the exact position of the plate beneath the jacking point should be developed. Consideration should also be given to the replacement of the nitrogen tank pressure source with a simple compressed air tank that could be filled conveniently at a gas station.
3. Consideration should be given to the placement of an additional set of sensing probes along an orthogonal axis and conducting a series of tests along that axis as well as along the original axis. The permeability could then be taken as the geometric mean of the two values thus determined. Two possibilities for accomplishing this could be considered: (1) run the tests in the two directions at the same time (this would require an additional bank of measurement units

and two operators), or (2) run the two tests consecutively.

4. Since piping at the interface between the plate and the base or subbase continues to present an occasional problem, additional study of methods to overcome this difficulty appears to be warranted. One method might be to redesign the predrive rods, water injection probes and sensing probes to minimize piping potential. Another method might be to consider better sealing methods. Both of these techniques were discussed under FIELD TESTING OF THE PROTOTYPE FPTD (TASK F).
5. Although some guidelines for selecting depth of water injection probe and location and depth and spacing of sensing probes were established during the LABORATORY EVALUATION OF THE PROTOTYPE FPTD (TASK E), it is felt that additional research is required to confirm and optimize the selection of these parameters.
6. Finally, in order to develop and demonstrate the full potential of the equipment, it is recommended that the FPTD be subjected to a broad program of field testing under the most diverse conditions that might be expected to be encountered in routine use.

BIBLIOGRAPHY

1. Ahrens, T. P. and Barlow, A. C., "Permeability Tests Using Drill Holes and Wells," Geology Report G-97, U. S. Bureau of Reclamation, 1951, 45 pages.

2. Ahuja, L. R., El-Swaify, S. A. and Rahman, A., "Measuring Hydraulic Properties of Soil with a Double Ring Infiltrometer and Multiple Depth Tensiometers," Journal, Soil Science Society of America, Vol. 40, 1976, pp. 494-499.

3. Aldabaugh, A. S. Y. and Beer, C. E., "Field Measurement of Hydraulic Conductivity Above a Water Table with Air-Entry Permeameter," Transactions, American Society of Agricultural Engineers, Vol. 14, No. 1, 1971, pp. 29-31.

4. Aravin, V. I. and Numerov, S., Theory of Fluid Flow in Undeformable Porous Media, Gosstrolizdat, Moscow, 1953.

5. Aronovici, W. S., "Model Study of Ring Infiltrometer Performance Under Low Initial Soil Moisture," Proceedings, Soil Science Society of America, Vol. 19, 1955, pp. 1-6.

6. "ASTM Standard Method of Test for Permeability of Granular Soils (Constant Head)," D2434-68 (1974), ASTM Standards, Part 19, April 1974, pp. 298-304.

7. Barber, W. S. and Sawyer, C. L., "Highway Subdrainage," Public Roads, Vol. 26, No. 12, February, 1952, pp. 251-267.

8. Barenberg, E. J. and Hazarika, B. P., "Correlation of Pavement Behavior and Performance Between the University of Illinois Test Track and the AASHO Road Test," Project IHR-84, Illinois Cooperative Highway Research Program, University of Illinois, July, 1973.

9. Baver, L. D., 1936, "Soil Characteristics Influencing the Movement and Balance of Soil Moisture," Proceedings, Soil Science Society of America, Vol. 1, pp. 431-437.

10. Bennette, G. D. and Patten, E. P., Jr., "Constant-Head Pumping Test of a Multi-Aquifer Well to Determine Characteristics of Individual Aquifers," Water Supply Paper 1536-G, U. S. Geological Survey, 1962, pp. 181-203.

11. Bentall, R., Compiler, "Methods of Determining Permeability, Transmissibility and Drawdown," Water Supply Paper 1536-I, U.S. Geological Survey, 1963, pp. 243-341.

12. Boast, C. W. and Kirkham, D., "Auger Hole Seepage Theory," Proceedings, Soil Science Society of America, Vol. 35, 1971, pp. 365-374.

13. Boersma, L., "Field Measurement of Hydraulic Conductivity Below a Water Table," Monograph 9, Methods of Soil Analysis, American Society of Agronomy, Part 1, 1965, pp. 222-223.

14. Boersma, L., "Field Measurement of Hydraulic Conductivity Above a Water Table," Monograph 9, Methods of Soil Analysis, American Society of Agronomy, Part 1, 1965, pp. 234-252.

15. Bouwer, H. and Little, W. C., "A Unifying Numerical Solution for Two-Dimensional Steady Flow Problems in Porous Media With an Electrical Resistance Network," Proceedings, Soil Science Society of America, Vol. 23, 1959, pp. 91-96.

16. Bouwer, H., "A Study of Final Infiltration Rates from Cylinder Infiltrometers and Irrigation Furrows with an Electrical Resistance Network," Transactions, International Society of Soil Science, 7th Congress, Madison, 1960.

17. Bouwer, H., "A Double Tube Method for Measuring Hydraulic Conductivity of Soil in Sites Above a Water Table," Proceedings, Soil Science Society of America, Vol. 25, 1961, pp. 334-342.

18. Bouwer, H., "A Variable Head Technique for Seepage Meters," Journal, Irrigation and Drainage Division, American Society of Civil Engineers, Vol. 87, 1961, pp. 31-44.

19. Bouwer, H., "Field Determination of Hydraulic Conductivity Above a Water Table with the Double-Tube Method," Proceedings, Soil Science Society of America, Vol. 26, 1962, pp. 330-335.

20. Bouwer, H., "Measuring Horizontal and Vertical Hydraulic Conductivity of Soil with the Double-Tube Method," Proceedings, Soil Science Society of America, Vol. 28, 1965, pp. 19-23.

21. Bouwer, H., "Unsaturated Flow in Groundwater Hydraulics," Journal, Hydraulic Division of ASCE, HY5, 1964, pp. 121-144.

22. Bouwer, H., "Rapid Field Measurement of Air Entry Value and Hydraulic Conductivity of Soil as Significant Parameters in Flow System Analysis," Water Resources Research, American Geophysical Union, Vol. 2, 1966, pp. 729-738.

23. Bouwer, H., "Field Measurement of Saturated Hydraulic Conductivity in Initially Unsaturated Soil," Publication No. 70, International Association for Scientific Hydrology, 1967, pp. 243-251.

24. Bouwer, H., "Planning and Interpreting Soil Permeability Measurements," Journal, Irrigation and Drainage Division, American Society of Civil Engineers, No. IR3, 1969, pp. 391-402.

25. Bouwer, H. and Jackson, R. D., "Determining Soil Properties," Drainage for Agriculture, American Society of Agronomy, Inc., Madison, Wisconsin, 1974, pp. 611-672.

26. Bouwer, H., and Rice, R. C., Journal, Irrigation and Drainage Division, American Society of Civil Engineers, IR4, December, 1968, pp. 481-492.

27. Brooks, R. H. and Reeve, R. C., "Measurement of Air and Water Permeability of Soils," Transactions, American Society of Agricultural Engineers, Vol. 2, 1959, pp. 125-126, 128.

28. Bruce, R. R. and Klute, A., "The Measurement of Soil Moisture Diffusivity," Proceedings, Soil Science Society of America, Vol. 20, 1956, pp. 458-462.

29. Brutsaert, W., "Some Methods of Calculating Unsaturated Permeability," Transactions, American Society of Agricultural Engineers, Vol. 10, 1967, pp. 400-404.

30. Burgy, R. H. and Luthin, J. N., "A Test of the Single and Double Ring Types of Infiltrometers," Transactions, American Geophysical Union, Vol. 37, 1956, pp. 189-191.

31. Burmister, D. M., "Principles of Permeability Testing of Soils," Permeability of Soils, Special Technical Publication 163, American Society for Testing and Materials, 1954, pp. 3-26.

32. Cedergren, H. R., Seepage, Drainage and Flow Nets, John Wiley and Sons, New York, 1967.

33. Cedergren, H. R., Drainage of Highway and Airfield Pavements, John Wiley and Sons, New York, 1974.

34. Cedergren, H. R., /KOA, "Appendix A - Literature Review Abstracts," Development of Guidelines for the Design of Pavement Subdrainage Systems, Phase I, Final Technical Report, March, 1971.

35. Cedergren, H. R., Arman, J. A., and O'Brien, K. H., Development of Guidelines for the Design of Subsurface Drainage Systems for Highway Pavement Structural Sections, Report No. FHWA-RD-73-14, Federal Highway Administration, February, 1973.

36. Chaplin, J. B. F., "Rapid Determination of Permeability in Porous Rock," Report of Investigations 6098, U. S. Bureau of Mines, 1962, 9 pp.

37. Childs, E. D. and Collis-George, N., "Permeability of Porous Materials," Proceedings, Royal Society (London), Vol. 201A, 1950, pp. 392-405.

38. Childs, E. C., "Measurement of Hydraulic Permeability of Saturated Soil In Situ I. Principles of a Proposed Method," Proceedings, Royal Society (London), Vol. 215, 1952, pp. 525-535.

39. Childs, E. C., Cole, A. H. and Edwards, D. H., "The Measurement of the Hydraulic Permeability of Saturated Soil In Situ II," Proceedings, Royal Society (London), Vol. 216, 1953, pp. 72-89.

40. Christiansen, J. E., "Effect of Entrapped Air Upon the Permeability of Soils," Soil Science, Vol. 50, 1944, pp. 355-365.

41. Christiansen, J. E., Firemen, M. and Allison, L. E., "Displacement of Soil-Air by CO_2 for Permeability Tests," Soil Science, Vol. 61, 1946, pp. 355-360.

42. Chu, T. Y. and Humphries, W. K., Investigation of Roadway Drainage as Related to Performance of Flexible Pavements, Final Report, College of Engineering, University of South Carolina, August, 1974.

43. Corey, A. T., "Measurement of Water and Air Permeability in Saturated Soil," Proceedings, Soil Science Society of America, Vol. 21, 1957, pp. 7-10.

44. Denisov, N. Ya., "The Concept of the Percolation Coefficient and the Methods of its Determination," Selected Sections from Engineering Geology and Hydrogeology, (Moscow), Israel Prog. for Sci. Trans. 1960, pp. 9-66.

45. DeWiest, R. J. M., Geohydrology, John Wiley and Sons, New York, 1965.

46. Dirksen, D., "Measurement of Hydraulic Conductivity by Means of Steady, Spherically Symmetric Flows," Proceedings, Soil Science Society of America, Vol. 38, No. 1, 1974, pp. 3-8.

47. Donnan, W. W. and Aronovici, W. S., "Field Measurement of Hydraulic Conductivity," Journal, Irrigation and Drainage Division, American Society of Civil Engineers, Vol. 87, No. IR2, 1961, pp. 1-13.

48. Evans, D. D. and Kirkham, D., "Measurement of the Air Permeability of Soil In Situ," Proceedings, Soil Science Society of America, Vol. 14, 1949, pp. 65-73.

49. Evans, D. D., Kirkham, D. and Frevert, R. K., "Infiltration and Permeability in Soil Overlying an Impermeable Layer," Proceedings, Soil Science Society of America, Vol. 15, 1950, pp. 50-54.

50. Fishel, V. C., "Further Tests of Permeability Under Low Hydraulic Gradients," Transactions, American Geophysical Union, Vol. 16, 1935, pp. 499-503.

51. Free, G. R. and Palmer, V. J., "Interrelationship of Infiltration, Air Movement and Pore Size in Graded Silica Sand," Proceedings, Soil Science Society of America, Vl. 5, 1940, pp. 390-398.

52. Frevert, R. K., "Development of a Three Dimensional Electric Analogue with Application to Field Measurement of Soil Permeability Below the Water Table," Unpublished Ph.D. Thesis, Iowa State College, Ames, Iowa, 1948.

53. Frevert, R. K. and Kirkham, D. A., "Field Method for Measuring the Permeability of Soil Below a Watertable," Proceedings, Highway Research Board, Vol. 28, 1948, pp. 433-442.

54. Gardner, W. R. and Miklich, F. J., "Unsaturated Conductivity and Diffusivity Measurements by a Constant Flux Method," Soil Science, Vol. 93, 1962, pp. 271-274.

55. Gerard, C. J., Influence of Antecedent Soil Moisture Suction on Saturated Hydraulic Conductivity of Soils," Proceedings, Soil Science Society of America, Vol. 38, 1974, pp. 506-509.

56. Glover, R. E., "Flow from a Test Hole Located Above Groundwater Level," Engineering Monograph 8, U. S. Bureau of Reclamation, 1953, pp. 69-71.

57. Golder, H. Q. and Gass, A. A., "Field Tests for Determining Permeability of Soil Strata," Special Technical Publication 322, American Society for Testing and Materials, 1962, pp. 29-46.

58. Grover, B. L., "Simplified Air Permeameters for Soil in Place," Proceedings, Soil Science Society of America, Vol. 19, 1955, pp. 414-418.

59. Harr, M. E., Groundwater and Seepage, McGraw Hill, New York, 1962.

60. Haynes, J. H. and Yoder, E. J., "Effects of Repeated Loading on Gravel and Crushed Stone Base Material Used in the AASHO Road Test," Highway Research Record No. 39, Highway Research Board, 1963.

61. Hillel, D. and Gardner, W. R., "Measurement of Unsaturated Conductivity and Diffusivity by Infiltration Through an Impeding Layer," Soil Science, Vol. 109, 1970, pp. 149-153.

62. Hillel, D., Krentos, V. D. and Stylianou, Y., "Procedure and Test on an Internal Drainage Method for Measuring Soil Hydraulic Characteristics In Situ," Soil Science, Vol. 114, 1972, pp. 395-400.

63. Hvorslev, M. J., "Time Lag and Soil Permeability In Groundwater Observations," Bulletin 36, Waterways Experiment Station, U.S. Corps of Engineers, 1951, 37 pp.

64. Johnson, A. I., "Selected References on Permeability," Special Technical Publication 163, American Society for Testing and Materials, 1955, pp. 131-136.

65. Johnson, A. I., "A Field Method for Measurement of Infiltration," Water Supply Paper 1544-F, U. S. Geological Survey, 1963, 27 pp.

66. Johnson, A. I., "Suggested Method of Test for Infiltration Rate in Field Using Double-Ring Infiltrometers," Special Technical Publication 479, American Society for Testing and Materials, 1970, pp. 187-191.

67. Johnson, A. I. and Richter, R. C., "Selected Bibliography on Permeability and Capillarity Testing of Rock and Soil Materials," Permeability and Capillarity of Soils, ASTM STP 417, 1967, pp. 176-210.

68. Johnson, H. P., Frevert, R. K. and Evans, D. D., "Simplified Procedure for the Measurement and Computation of Soil Permeability Below the Water Table," Agricultural Engineering, Vol. 33, 1952, pp. 283-289.

69. Kirkham, D., "Proposed Method for Field Measurement of Permeability of Soil Below the Water Table," Proceedings, Soil Science Society of America, Vol. 10, 1945, pp. 58-68.

70. Kirkham, D., "Measurement of the Hydraulic Conductivity of Soil in Place," Special Technical Publication 163, American Society for Testing and Materials, 1955, pp. 80-97.

71. Kirkham, D. and Van Bavel, C. H. M., "Theory of Seepage into Auger Holes," Proceedings, Soil Science Society of America, Vol. 13, 1948, pp. 75-82.

72. Klute, A., "Some Theoretical Aspects of the Flow of Water in Unsaturated Soils," Proceedings, Soil Science Society of America, Vol. 16, 1952, pp. 144-148.

73. Klute, A., "The Determination of the Hydraulic Conductivity and Diffusivity of Unsaturated Soils," Soil Science, Vol. 113, 1972, pp. 264-276.

74. Klychnikov, V. M., "A Device for Determining the Permeability of Soils to Water Under Field Conditions," Pochvovedenie (Russia), No. 9, 1952, pp. 851-859.

75. Lambe, T. W. and Whitman, R. V., Soil Mechanics, John Wiley and Sons, New York, 1969.

76. Lang, S. W., "Pumping Test Methods for Determining Aquifer Characteristics," Special Technical Publication 417, American Society for Testing and Materials, 1967, pp. 35-55.

77. Li, W. H., Bock, P. and Benton, G. S., "A New Formula for Flow into Partially Penetrating Wells in Aquifers," Transactions, American Geophysical Union, Vol. 35, No. 5, 1954, pp. 805-812.

78. Liebmann, G., 1950, "Solution of Partial Differential Equations With a Resistance Network Analogue," British Journal of Applied Physics, Vol. 1, pp. 92-103.

79. Livneh, M. and Shklarsky, E., "Permeability Tests for Directions of Flow Parallel and Perpendicular to the Direction of Compaction," Proceedings, 2nd S. E. Asian Conference on Soils Engineering, Singapore, 1970.

80. Luthin, J. N. and Kirkham, D., "A Piezometer Method for Measuring Permeability of Soil in Situ Below a Water Table," Soil Science, Vol. 68, 1947, pp. 349-358.

81. Maasland, M. and Kirkham, D., "Theory and Measurement of Anisotropic Air Permeability in Soil," Proceedings, Soil Science, Vol. 18, No. 4, 1955, pp. 395-400.

82. Maasland, M. and Haskew, H. C., "The Auger Hole Method of Measuring the Hydraulic Conductivity of Soil and its Application to Tile Drainage Problems," Transactions, 3rd International Commit. Irrig. Drain. Congr., Vol 3, 1957, pp. 8.69-8.114.

83. Mansur, C. I., "Laboratory and In Situ Permeability of Sand," Transactions, American Society of Civil Engineers, Vol. 123, 1958, pp. 868-882.

84. Mansur, C. I. and Dietrich, R. I., "Pumping Test to Determine Permeability Ratio," Proceedings, American Society of Civil Engineers, Vol. 91, No. SM4, Part 1, 1965, pp. 151-183.

85. Matsuo, S., Honmachi, Y. and Akai, K., "A Field Determination of Permeability," Proceedings, 3rd International Conf. Soil Mech. and Found. Engr., Switzerland, Vol. 1, 1953, pp. 268-271.

86. Maytin, I. L., "A New Field Test for Highway Shoulder Permeability," Proceedings, Highway Research Board, Vol. 41, 1962, pp. 109-124.

87. McAdam, J. L., "Report to the London Board of Agriculture," 1920.

88. Milligan, V., "Field Measurement of Permeability in Soil and Rock," State of the Art Paper, Proceedings, ASCE Conference on In Situ Measurement of Soil Properties, Vol. II, N. C. State University, 1975, pp. 3-36.

89. Mittal, H. K. and Morgenstern, N. R., "Parameters for the Design of Tailings Dams," Canadian Geotechnical Journal, Vol. 12, 1975, pp. 235-261.

90. Moore, T. V., "The Determination of Permeability from Field Data," Proceedings, American Petroleum Institute, Vol. 14, No. 4, 1933, pp. 4-13.

91. Moulton, L. K. and Seals, R. K., In Situ Determination of Permeability of Bases and Subbases, Phase I, Interim Report, Report No. FHWA-RD-78-21, Federal Highway Administration, December, 1977, 104 pp.

92. Muskat, M., The Flow of Homogeneous Fluids Through Porous Media, J. W. Edwards, Publisher, Ann Arbor, 1946.

93. Nelson, R. W., "In-Place Measurement of Permeability in Heterogeneous Media 1. Theory of a Proposed Method," Journal of Geophysical Research, Vol. 65, 1960, pp. 1753-1765.

94. Nelson, R. W., "In-Place Measurement of Permeability in Heterogeneous Media 2. Experimental and Computational Considerations," Journal of Geophysical Research, Vol. 66, 1962, pp. 2469-2478.

95. Nielsen, D. R., Biggar, J. W. and Erh, K. T., "Spatial Variability of Field-Measured Soil-Water Properties," Hilgardia, Vol. 42, 1973, pp. 215-270.

96. O'Flaherty, C. S., Highways, Edward Arnold Publishers, London, 1967.

97. Oglesby, C. H. and Hewes, L. I., Highway Engineering, John Wiley and Sons, New York, 1954.

98. Olson, T. C. and Swartzendruber, D., 1960, "Model Study of the Double Ring Infiltrometer in Layered Systems," Proceedings, 7th International Congress on Soil Science, Vol. 1, 1960, pp. 441-447.

99. Onodera, T., "Determination of Permeability by Pumping from a Spherical Well," Publication No. 44, International Assn. Sci., Hydrology, 1957, pp. 212-218.

100. Pillsbury, A. F. and Appleman, D., "Factors in Permeability Changes of Soils and Inert Granular Material," Soil Science, Vol. 50, 1945, pp. 115-123.

101. Polubarinova-Kochina, P. Ya., Theory of the Motion of Ground Water, Gostekhizdat, Moscow, 1952.

102. Rasmussen, W. and Lauritzen, L. W., "Measuring Seepage from Irrigation Canals," Agricultural Engineering, Vol. 34, 1953, pp. 326-329, 331.

103. Reeve, R. C. and Jensen, M. C., "Piezometers for Groundwater Flow Studies and Measurement of Subsoil Permeability," Agricultural Engineering, Vol. 30, No. 9, 1949, pp. 435-438.

104. Reeve, R. C. and Kirkham, D., "Soil Anisotropy and Field Methods for Measuring Permeability," Transactions, American Geophysical Union, Vol. 32, 1951, pp. 582-590.

105. Reeve, R. C., Luthin, J. N. and Donnan, W. W., "Drainage Investigation Methods," Monograph 8, American Society of Agronomy, 1957, pp. 395-459.

106. Richards, L. A., Chairman, "Report of the Subcommittee on Permeability and Infiltration," Proceedings, Soil Science Society of America, Vol. 16, 1952, pp. 85-88.

107. Richards, L. A. and Richards, P. L., "Radial-Flow Cell for Soil Water Measurements," Proceedings, Soil Science Society of America, Vol. 26, 1962, pp. 515-518.

108. Ridgeway, H. H., "Pavement Permeability and Drainage," Ph.D. Dissertation, University of Connecticut, June, 1975.

109. Robinson, A. R. and Rohwer, Carl, "Measuring Seepage from Irrigation Channels," Technical Bulletin 1203, U. S. Department of Agriculture, 1959, 82 pp.

110. Rose, C. W., Stern, W. R. and Drummond, J. E., "Determination of Hydraulic Conductivity as a Function of Depth and Water Content for Soil In Situ," Australian Journal of Soil Research, Vol. 3, 1965, pp. 1-9.

111. Schmid, W. E., "The Permeability of Soils and the Concept of a Stationary Boundary Layer," Proceedings, American Society for Testing and Materials, 1957, pp. 1195-1218.

112. Schmid, W. E., "Field Determination of Permeability by the Infiltration Test," Special Technical Publication 417, American Society for Testing and Materials, 1967, pp. 142-158.

113. Sides, J. P., "In Situ Determination of Soil Permeability," M. S. Thesis, School of Engineering and Applied Science, Princeton University, 1966, 74 pp.

114. Slaughter, G. H., Evaluation of Design Methods for Subsurface Drainage Facilities for Highways, Final Report, GDOT Research Project No. 6901, Georgia Department of Transportation, 1973.

115. Smiles, D. E. and Youngs, E. G., "A Multiple-Well Method for Determining the Hydraulic Conductivity of a Saturated Soil In Situ," Journal of Hydrology, Vol. 1, 1963, pp. 279-287.

116. Smith, T. W., Cedergren, H. R., and Reyner, C. A., "Permeable Materials for Highway Drainage," Highway Research Record No. 68, 1964.

117. Smith, W. O. and Stallman, R. W., "Measurement of Permeabilities in Groundwater Investigations," Special Technical Publication 163, American Society for Testing and Materials, 1955, pp. 98-122.

118. Snell, A. W. and Van Schilfgaarde, J., "Four Well Method of Measuring Hydraulic Conductivity of the Soil," Transactions, American Society of Agricultural Engineers, Vol. 7, 1965, pp. 83-87.

119. Strohm, W. E., Nettles, E. H., and Calhoun, C. C., Jr., "Study of Drainage Characteristics of Base Course Materials," Highway Research Record No. 203, Highway Research Board, 1967, pp. 8-28.

120. Szily, Joseph, "Permeability Device for Sand Samples," Proceedings, First International Conference of Soil Mechanics and Foundation Engineering, Cambridge, Mass., Vol. III, 1936, pp. D-24 to D-26.

121. Talsma, T., "Comparison of Field Methods of Measuring Hydraulic Conductivity," Trans. Cong. Irrig. Drainage IV, Vol. 6, 1960, pp. C145-C156.

122. Talsma, T., "Some Aspects of Three-Dimensional Infiltration," Australian Journal of Soil Research, Vol. 8, 1970, pp. 179-184.

123. Todd, D. K., Ground Water Hydrology, John Wiley and Sons, New York, 1963.

124. Uhland, R. E. and O'Neal, A. M., "Soil Permeability Determinations for Use in Soil and Water Conservation," Technical Paper 101, U. S. Dept. of Agriculture, Soil Conservation Service, 1951, 36 pp.

125. U. S. Army Corps of Engineers, "Appendix VII: Permeability Tests," Laboratory Soils Testing, EM1110-2-1906, Nov. 30, 1970, pp. VII-1-VII-27.

126. U. S. Bureau of Reclamation, "Field Permeability Test (Well Permeameter Method)," Designation E-19, Earth Manual, 1st Ed. U. S. Bureau of Reclamation, 1960, pp. 546-562.

127. U. S. Bureau of Reclamation, "Field Permeability Tests in Bore Holes," Designation E-18, Earth Manual, 1st Ed., U. S. Bureau of Reclamation, 1960, pp. 541-546.

128. Van Bavel, C. H. M. and Kirkham, D., "Field Measurement of Soil Permeability Using Auger Holes," Proceedings, Soil Science Society of America, Vol. 13, 1948, pp. 90-96.

129. Wang, F. C. Hassan, N. A. and Franzini, J. B., "A Method of Analyzing Unsteady, Unsaturated Flow in Soils," Journal of Geophysical Research, Vol. 69, No. 12, 1964, pp. 2569-2577.

130. Watson, K. K., "An Instantaneous Method for Determining the Hydraulic Conductivity of Unsaturated Porous Materials," Water Resources Research, Vol. 2, 1966, pp. 709-715.

131. Watson, K. K., "The Measurement of the Hydraulic Conductivity of Unsaturated Porous Materials Using a Zone of Entrapped Air," Proceedings, Soil Science Society of America, Vol. 31, 1967, pp. 716-721.

132. Weaver, A. S., "Determination of Permeability of Granular Soil by Air Subjected to a Decreasing Pressure Differential," Special Technical Publication 163, American Society for Testing and Materials, 1955, pp. 123-130.

133. Wenzel, L. K., 1942, "Methods for Determining Permeability of Water Bearing Materials," Water Supply Paper 887, U. S. Geological Survey, 1942, pp. 20-50, 71-117.

134. Whisler, F. D., Klute, A. and Peters, D. B., "Soil Water Diffusivity from Horizontal Infiltration," Proceedings, Soil Science Society of America, Vol. 32, 1968, pp. 6-11.

135. Wilkinson, W. B., "Constant Head In Situ Permeability Tests in Clay Strata," Geotechnique, Vol. 18, No. 2, 1968, pp. 172-194.

136. Winger, R. J., "In-Place Permeability Tests and Their Use in Subsurface Drainage," Proceedings, Internat. Commiss. on Irrig. and Drainage, 4th Congr., Madrid, Spain, 1960.

137. Youngs, E. G., "An Infiltration Method of Measuring the Hydraulic Conductivity of Unsaturated Porous Materials," Soil Science, Vol. 97, 1964, pp. 307-311.

138. Zanger, C. N., "Theory and Problems of Water Percolation," Engineering Monograph 8, U. S. Bureau of Reclamation, 1964, 75 pp.

APPENDIX A

Design, Construction and Operation Details of Laboratory Test Areas

Design of Test Areas (Subtask B-1)

General Physical and Operational Features of the Subsystems

Based on the criteria summarized in the previous sections as well as certain physical and equipment limitations, a laboratory permeability testing system was designed that consisted of two independent sets of three cells and their associated hydraulic circulation and saturation/underdrainage subsystems. The specific system and subsystem features and characteristics are described in the following sections. In addition, the rationale for the various characteristics of the system and subsystems is discussed.

Individual cell subsystem. A cell having internal dimensions of 5 feet (1.52 m) x 6 feet (1.83 m) in plan by 4 1/2 feet (1.37 m) deep was selected on the basis of providing sufficient space to minimize boundary effects, allow simulation of typical pavement sections, and still not exceed the lifting capacity of the overhead crane. The actual plan area of the simulated pavement section was reduced to 5 feet (1.52 m) x 5 feet (1.52 m) to provide two 6 inch (152.4 mm) sections at either end of the test specimen for a pervious screen and water reservoir. The two water reservoirs were utilized to control the hydraulic head at either end of the specimen in order to maintain steady sheet flow. To provide adequate structural stability for the various handling and loading conditions as well as minimize construction complexities, a 6 inch (152.4 mm) wall and base slab thickness was selected. Thus, the outside plan dimension of the cell was 6 feet (1.83 m) x 7 feet (2.13 m). The 5 foot (1.52 m) cell height, or 4 1/2 foot (1.37 m) internal height, was selected to permit the simulation of a pavement section consisting of a maximum of three 18 inch (457.2 mm) layers. A network of pipes was incorporated into the base slab to provide a mechanism for saturation and underdrainage of the pavement section. Both an inlet and outlet were provided for the saturation/underdrainage pipe network. In addition, two 3 inch

(76.2 mm) conduits were provided for both the upstream and downstream water reservoirs in the cell. A schematic drawing of an individual cell illustrating the features described above was presented earlier in Figure 8.

On the basis of available resources, costs, project requirements, and personnel expertise it was decided to construct the cells of reinforced concrete. Steel requirements (size, quantity, and placement) were based on current ACI Code recommendations, conservatively estimated loads, and the elastic method of analysis. Special attention was given to reinforcing steel placement in an attempt to prevent cracking under all possible handling and operational conditions. Reinforcement placement details were presented in an earlier report (91).

Special steel channel sections were designed and fabricated for placement in the vertical walls of the cell as illustrated in Figure 8. These channels supplied the guideway for the pervious metal grates utilized to contain the simulated pavement section adjacent to the upstream and downstream water pools. The retaining screens consisted of a commercially available steel walkway grating 1 1/2 inch (38.1 mm) x 3/16 inch (4.76 mm) @ 10.3 lb/ft^2 (50.3 kg/m^2). Anchors were also embedded in the walls of the cells to provide lifting points for handling and positioning.

Based on a consideration of the hydraulic requirements of the various layer thicknesses and permeability combinations, as well as equipment limitations and material handling needs, it was decided to construct two three-cell laboratory permeability systems with independent hydraulic circulation systems. Thus, a total of six cells having the characteristics previously discussed were constructed. As discussed in the immediately following section, the major difference in the two independent systems was the hydraulic pumping and measurement systems.

Hydraulic circulation subsystem. Based on the range of base and subbase layer thicknesses, from 3 inches (76.2 mm) to 18 inches (457.2 mm), and permeabilities, from 10 cm/sec to 10^{-4} cm/sec, to be considered, quantities of flow ranging from less than 1 gpm (6.31×10^{-5} m^3/sec) to as much as 100 gpm (6.31×10^{-3} m^3/sec) were possible. To minimize water quantity as well as supply and equipment requirements, it was decided that a closed-loop hydraulic circulation system would be utilized for each of the three cell test systems. Although it was decided that each cell in the three cell system should be capable of independent operation, simultaneous operation of all the cells was also a possibility. Thus, a maximum pumping requirement of 300 gpm (1.89×10^{-2} m^2/s) was established for the high permeability cell system (HPCS). To make use of available equipment, the maximum pumping capacity for the low permeability cell system (LPCS) was limited to 50 gpm (3.16×10^{-3} m^3/s). Another consideration in the decision to utilize two independent cell systems was the precision and accuracy of conventional, low-cost flow measurement equipment. On this basis, magnetic drive mainline flow meters (Lucern Multijet) were selected for use in the HPCS whereas a manual method of flow measurement was developed for the LPCS.

Each hydraulic circulation system consisted of a pump, a sump tank, constant head tanks, a pipe network, and a flow measurement system (flow meters or manual method). The pipe network was designed to accommodate the estimated quantities of flow, permit independent or coupled cell operation, provide a means of coarse-flow adjustment, and permit recirculation of water. Upstream and downstream constant head tanks were provided for each cell in order to maintain a constant differential head condition across the simulated pavement base or subbase layer.

Saturation/underdrainage subsystem. An independent network of 1 inch (25.4 mm) diameter pipes at approximately 8 inch (203.2 mm) centers was provided in the base of each cell for use in saturating

and/or underdraining the pavement section. The pipes were embedded in the base and placed perpendicular to the direction of flow so as to minimize the potential for piping. The pipe network was a flow-through system so it could be flushed and saturated before use. A tank was attached to the pipe network to supply water for saturation of any portion of the simulated pavement section.

Physical and Operational Features of the Test Cell Systems

As stated earlier, both a low and high permeability laboratory testing system were designed to satisfy the objectives of the project and meet the previously listed design, construction, and operational criteria. Both systems were composed of the three major subsystems described above: i.e., individual cell, hydraulic circulation, and saturation/underdrainage. The basic cell and hydraulic configuration that is common to both systems is illustrated schematically in Figure 9, which was presented earlier. Because the size and operational characteristics of the two systems differ somewhat, they will be discussed separately in the following sections.

High permeability cell system. This system will permit a maximum of 300 gpm (1.89×10^{-2} m^3/s) flow through all the cells (i.e., one cell can have a maximum of 300 gpm (1.89×10^{-3} m^3/s) flow when the other two cells are not operative) and a minimum of 35 gpm (2.21×10^{-3} m^3/s) flow through the first soil layer in any cell. The second condition is due to the requirement of the flow meters (the flow meters have upper and lower range within which they are accurate). The system is such that either one or more cells can be operated at a time. The flow is measured automatically by the flow meter installed on the outlet line from the cell.

The pump suction line is 2 1/2 inch (63.5 mm) diameter and the discharge line is a 2 inch (50.8 mm) diameter line. All the other piping is 3 inch (76.2 mm) diameter.

Both upstream and downstream constant head tanks are made from 55 gallon (0.208 m^3) barrels. In the upstream constant head tank, existing 2 inch (50.8 mm) diameter openings in the base of the barrels are used for inlets from the pump. Two 3 inch (76.2 mm) diameter openings are provided in the barrels, one for discharge into the cell and the other for overflow to the sump tank. In the downstream constant head tank, existing 2 inch (50.8 mm) and 1 inch (25.4 mm) diameter openings are blocked and two 3 inch (76.2 mm) diameter openings are provided, one to receive discharge from the cell and the other for overflow leading to the sump tank. The overflow pipes in the constant head tanks are exchangeable so that 3 inch (76.2 mm) diameter pipe sections of the appropriate length can be installed to keep the water levels at the desired elevations. The constant head tanks are placed on pedestals formed by 8 inch (203.2 mm) x 8 inch x 8 inch concrete blocks.

Low permeability cell system. This system will permit a maximum flow of 30 gpm (1.89×10^{-3} m^3/s) through all the cells (i.e., one cell can have maximum of 30 gpm (1.89×10^{-3} m^3/s) flow when the other two cells are not operative). In this system, one cell has an independent return pipe of 2 inches (50.8 mm) diameter to the sump tank whereas the other two cells have a combined return pipe of 2 inches (50.8 mm) diameter to the sump tank. The cell with independent return pipe has a maximum capacity of 30 gpm ($1.89 \times 10^{-3} m^3/s$) flow when the other two cells are not operative.

The flow is measured manually in this system. Two valves are provided by introducing a 'tee' in the return piping. When a measurement is to be made, one valve is closed to stop water returning to the sump tank while the other valve is opened to receive water in a measuring container. When high flow is introduced in the first cell (where the return to the sump tank is independent), measurement can be made by introducing a flow meter in the return piping.

The pump suction line is 1 1/2 inch (38.1 mm) diameter and the discharge line is 1 inch (25.4 mm) in diameter. All the other piping is 2 inch (50.8 mm) diameter. The piping is such that one or more cells can be operated at one time. All the piping is PVC Schedule 40 with the exception of the pump suction pipe which is galvanized.

Both upstream and downstream constant head tanks are made from 55 (0.208 m^3) gallon barrels. In the upstream constant head tank, existing 1 inch (25.4 mm) and 2 inch (50.8 mm) diameter openings are used to receive discharge from the pump and to discharge into the cell, respectively. An additional 2 inch (50.8 mm) diameter opening was provided for overflow. In the downstream constant head tank, the existing 1 inch (25.4 mm) diameter opening is blocked but two 2 inch (50.8 mm) diameter openings are provided for inflow and overflow, respectively. All the other arrangements are the same as the high permeability cell system.

Summary. Although the two cell systems are physically and operationally almost the same, certain differences do exist. The physical differences are summarized in Table 8 which itemizes the various component characteristics and sizes. Detailed drawings of the high and low permeability test cell systems, including bills of materials, are included in Figures 30 and 31, and 32 and 33, respectively. Both drawings represent the "as-built" systems.

Construction of Test Areas (Subtask B-2)

Fabrication of the Individual Test Cells

The conventional method of constructing a reinforced concrete tank in stages, with construction joints, was rejected to minimize the potential for leakage and to avoid elaborate waterproofing measures. Instead, the tank was constructed using a single concrete pour, thus eliminating the need for joints. To accomplish this, each tank was poured in an inverted position (i.e., the base on top). Three days after the pour, the side form work was removed, and the

Table 8. Design Summary

Component	Low Permeability Cell System	High Permeability Cell System
Concrete Cell	6' (1.83 m) x 5' (1.52 m) x 4.5' (1.39 m) inside; Wt. 1300 lbs (5895.7 kg)	6' (1.83 m) x 5' (1.52 m) x 4.5' (1.39 m) inside; Wt. 1300 lbs (5895.7 kg)
Pump	Brown and Sharpe Model No. 70886-8 RF 110 V Single Phase 0.50 H.P., 55 gpm (3.47×10^{-3} m^3/s)	Peerless Pump Model C 620 AM 3 Phase, 200 V 3 H.P., 400 gpm (2.52×10^{-2} m^3/s)
Pump Suction Pipe(1)	1 1/2" (38.1 mm) Diameter	2 1/2" (63.5 mm) Diameter
Pump Discharge Pipe	1" (25.4 mm) Diameter	2" (50.8 mm) Diameter
Concrete Cell Inlet and Outlet Pipes	2" (50.8 mm) Diameter	3" (76.2 mm) Diameter
Return Piping	2" (50.8 mm) Diameter	3" (76.2 mm) Diameter
Underdrainage Piping	1" (25.4 mm) Diameter	1" (25.4 mm) Diameter
Constant Head Tanks	55-gal. (0.208 m^3) barrels	55-gal. (0.208 m^3) barrels
Saturation Tank	55-gal. (0.208 m^3) barrels	55-gal. (0.208 m^3) barrels
Sump Tank	100-gal. (0.375 m^3) trough type tank, 4' (1.22 m) x 2' (0.61 m) x 2' (0.61 m) inside	272-gal. (1.030 m^3) trough type tank, 8' (2.44 m) x 2.6' (0.76 m) x 2' (0.61 m) inside
Flow Measurement	Manual	Lucern 2-Inch (50.8 mm) Multijet Magnetic Water-meter and/or Manual

(1) Galvanized steel pipe. All other piping is PVC Schedule 40.

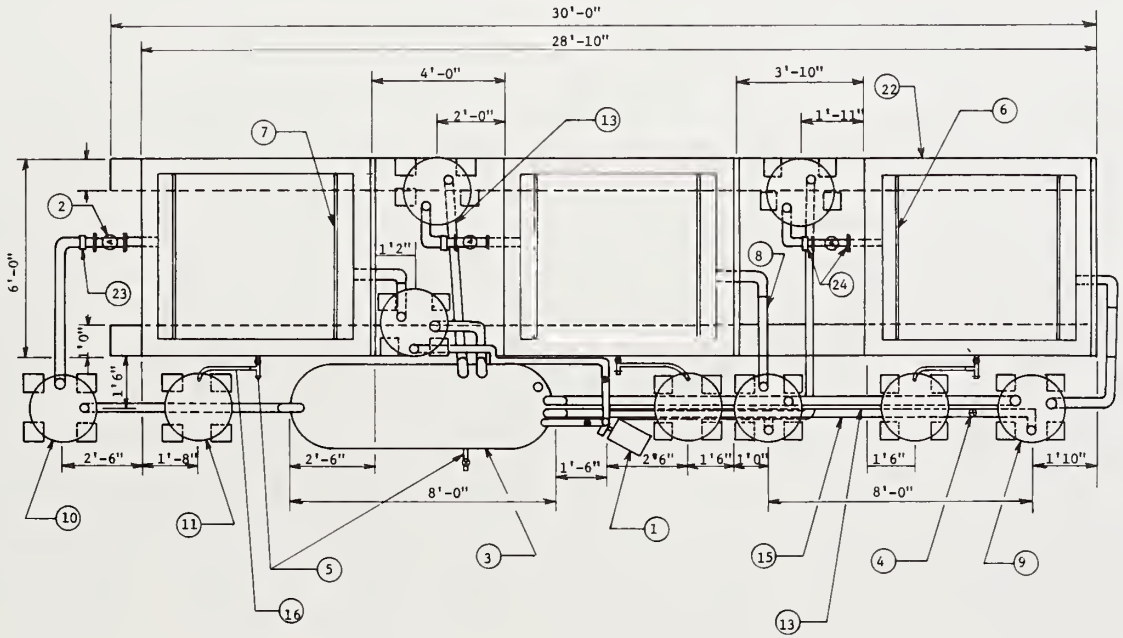

Figure 30. Plan View and List of Materials for High Permeability Cell System

Note: 1 ft. = 0.3048 m
1 in. = 25.4 mm

Item	Qty.	LIST OF MATERIALS
1	1	Peerless Pump Model No. C620 AM 3500 RPM 300 GPM @ 5' Head Closed Coupled to Standard Hydraulic Institute Nema 'C' Face Motor
2	3	2-inch Lucern Multijet Magnetic Watermeter
3	1	Sump Tank-272 Gallon - 2 1/2'x2'x8'
4	4	2" Gate Valve on 2" Discharge line as shown
5	7	3/4" Gate Valve on Drain Pipes (3/4" Dia.)
6	6	Steel Gratings 4'-2"x5'-1"x3/4"
7	-	Filter Cloth-Capacity 10 CMS/SEC
8	3	3" I.D. Flexible Plastic Hose with 2 hose clamps
9	3	Constant Head Tank - Upstream
10	3	Constant Head Tank - Downstream
11	3	Saturation Tank
12	3	Underdrainage Systems
13	70'	3" Dia. Pipe - PVC Schedule 40
14	16"	2 1/2" Dia. Suction Pipe - Galvanized with union connection
15	30'	2" Dia. Discharge pipe - PVC Schedule 40
16	3	3/4" I.D. Rubber Hose 3' lgh with 2 hose clamps
17	2	12" x 12" H Beam 30'-0" long
18	6	9"x12"x10' Oak Beams
19	6	1 3/4"x3 1/2" x 6" Wooden Blocks
20	110	8"x8"x8" Conc. Hollow Blocks
21	3	Concrete Cells 5'x6'x7' outside Dim.
22	3	3" Galvanized pipe unions
23	6	3" Galvanized pipe nipples fully threaded

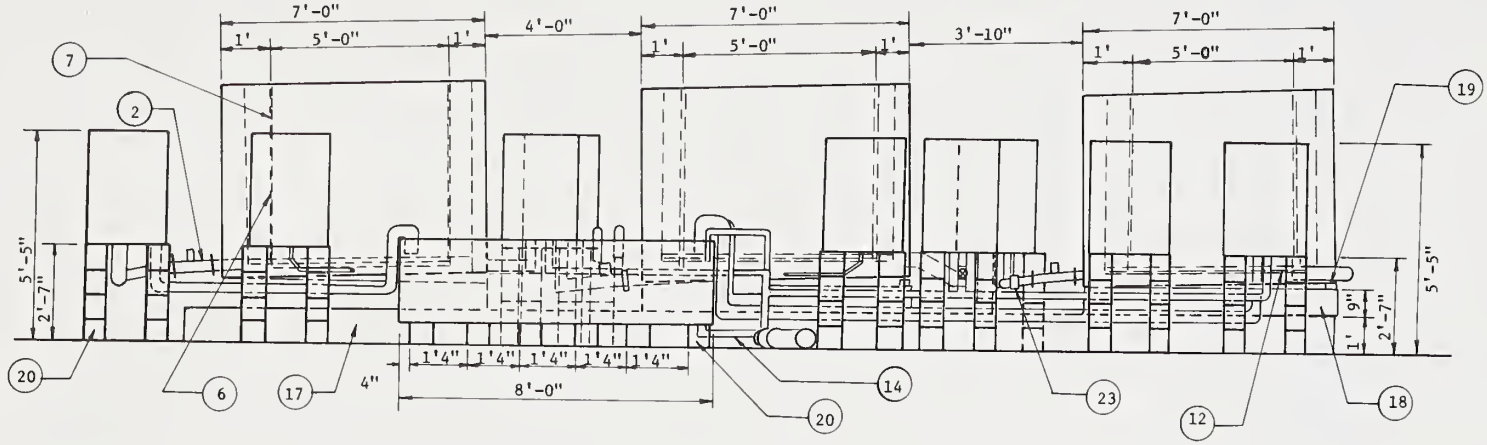

Figure 31. Elevation of High Permeability Cell System

Note: 1 ft. = 0.3048 m
1 in. = 25.4 mm

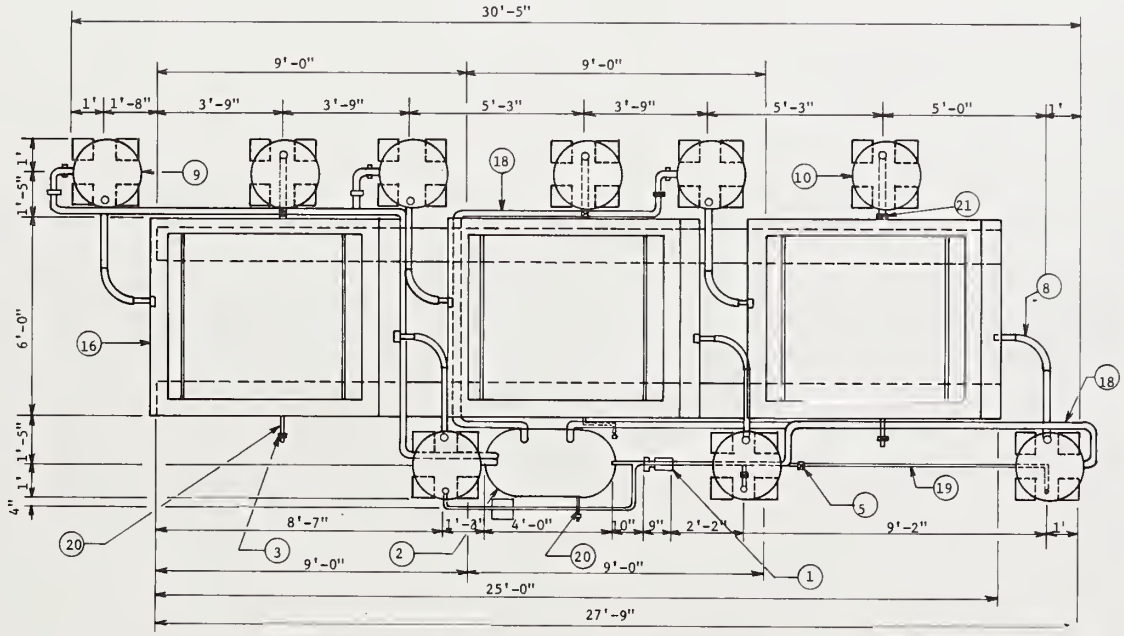

Note: 1 ft. = 0.3048 m
1 in. = 25.4 mm

Figure 32. Plan View and List of Materials for Low Permeability Cell System

Item	Qty.	LIST OF MATERIALS
1	1	Pump 1/4 HP, 45 GPP, 110V Single Phase
2	1	Sump Tank 2' x 2' x 4', 100 Gallons
3	4	3/4" Gate Valve on Drain Pipes
4	6	2" Gate Valve on Downstream return pipe (2")
5	4	1" Gate Valve on pump discharge pipe (1")
6	6	Steel Gratings Coated with Anti-rust Paint
7	-	Filter Cloth-Capacity 10^{-1} CMS/SEC.
8	6	2 1/8" Radiator Hose with 2 Clamps
9	6	Constant Head Tank, 3U/S, 3D/S
10	3	Saturation Tank
11	3	Underdrainage System
12		Wooden Wedge to Level Concrete Cell
13	6	2"x6"x8' Wooden Batten
14	2	15"x12"x1" H Beam
15		8"x8"x8" Conc. Hollow Blocks to Form Supports
16		Concrete Cell 5'x6'x5' Inside
17		2 1/2" Dia. Suction Pipe-Galvanized
18		2" Return Pipe (PVC)
19		1" Dia. Pump Discharge (PVC)
20		3/4" Dia. Drain Pipe
21		1" Gate Valve
22	3	3"x2 3/4"x2'-3" Wooden Batten

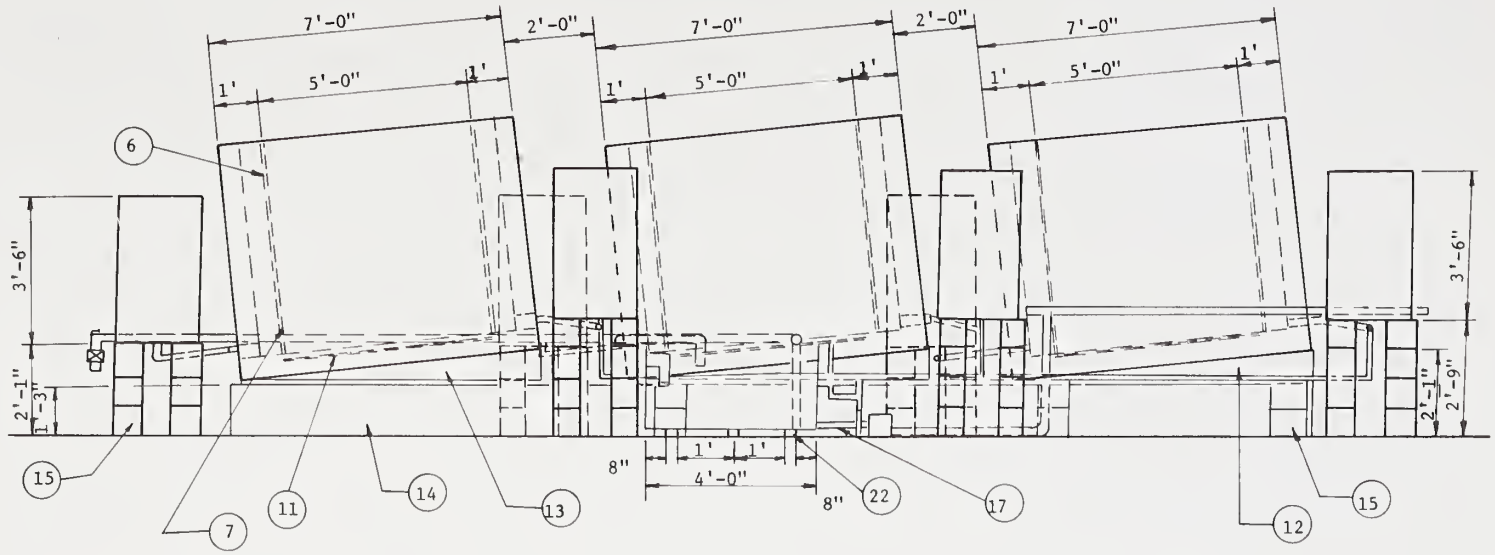

Figure 33. Elevation View of Low Permeability Cell System

Note: 1 ft. = 0.3048 m
1 in. = 25.4 mm

cell was turned over and placed on its base. The central form work "box", which consisted of four separate sides and a top, was then removed. The forms were constructed of 3/4 inch (19.1 mm) plywood braced by 2 inch (50.8 mm) x 4 inch (101.6 mm) and 2 inch (50.8 mm) x 6 inch (152.4 mm) framing. Because of the nature and size of the cell, considerable time was required for the design, construction, and subsequent modification of the form work.

In addition to the placement of reinforcement, the grating channels, anchors, inlet/outlet pipes, and saturation/underdrainage pipe networks had to be positioned in the form work.

The portland cement concrete mixture utilized for fabrication of the cells was designed to have low shrinkage and good placement characteristics and achieve a strength of approximately 3,000 psi (2.109 x 10^6 kg/m^2) in three days. The 3,000 psi (2.109 x 10^6 kg/m^2) compressive strength permitted the cells to be handled at the end of a three day curing period. Thus, after the external forms were stripped, the cells were inverted using a 10 ton (9071.8 kg) capacity overhead crane and the anchors provided in the sides of the cells.

At some later time, the cells were tested for leakage by maintaining them full of water for a three-day period. The only leakage that was observed under these conditions was a minor amount around a 3 inch (76.2 mm) diameter inlet pipe. Stoppage of this leakage was accomplished by applying an epoxy-based sealing compound to the affected areas. Following the leakage tests, the cells were coated with two applications of a commercially available waterproofing compound, "SAHARA." The purpose of this coating was two-fold: (a) to minimize any potential leakage through the cell walls and (b) to create a rough surface texture on the walls of the cell to minimize piping potential. After painting and water testing of the cells, 1/2 inch (12.7 mm) diameter holes were drilled at approximately 6 inch (152.4 mm) centers in the saturation/underdrainage pipe network cast into the base of the cell.

To permit gravity return flow from the downstream constant head tank to the sump tank, the three individual cells in a system were placed on two steel beams. The two steel beams were covered with wood to minimize the potential edge cracking of the cells when they are tilted in conjunction with permeability testing.

Hydraulic Circulation System

After the constant head and saturation tanks were fitted with the appropriate connections, they were positioned and placed on pedestals consisting of 8 inch (203.2 mm) concrete blocks. The sump tank and pump were placed in positions at floor level to minimize space, connection, and piping requirements. The hydraulic circulation pipe system was then fabricated for the established positions of the tanks and cells. As indicated in Table 8, the pipe sizes varied with pump size and the relative permeability of the pavement section to be investigated. Special consideration was given to the pipes and connections between the constant head tanks and the cells to insure sufficient flexibility when the tanks are tilted. The majority of the piping and connections utilized to fabricate the hydraulic circulation system pipe network was PVC Schedule 40. However, because of certain supply deficiencies, some galvanized steel fittings were used in lieu of PVC. Brass valves were utilized throughout both test cell systems. Following completion of the fabrication of the hydraulic circulation system, the operation of the system was checked by pumping water through it. Any leakage noted during the pumping test was corrected and checked again for satisfactory performance.

Figures 34 and 35 are photographs of the low permeability cell system. Similarly, Figures 9, 36, and 37 are photographs of the high permeability cell system. Figure 38 illustrates the grating detail which is common to both systems.

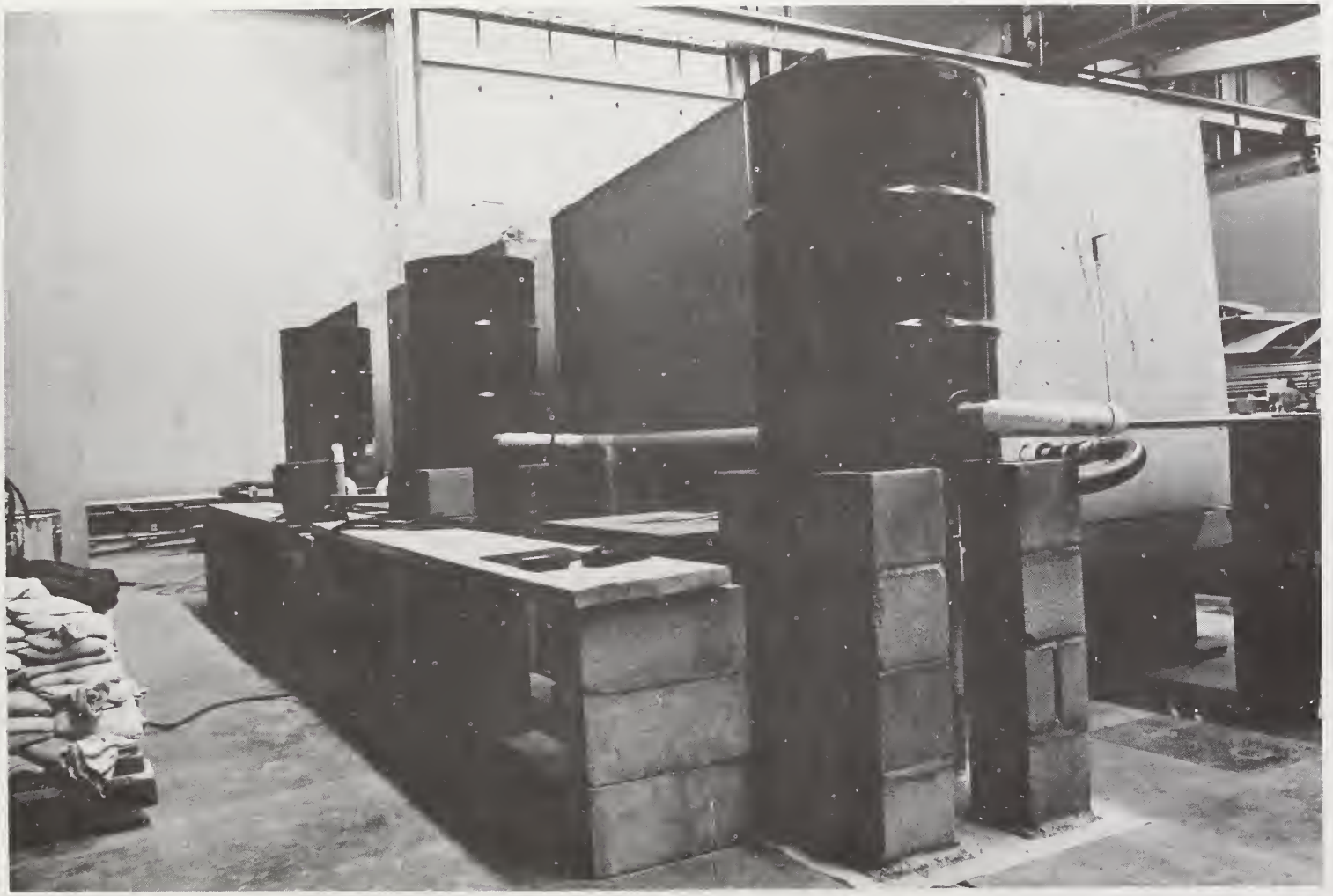

Figure 34. Overall View of Low Permeability Cell System Showing Cells and Upstream Constant Head Tanks

Figure 35. Saturation and Downstream Constant Head Tanks

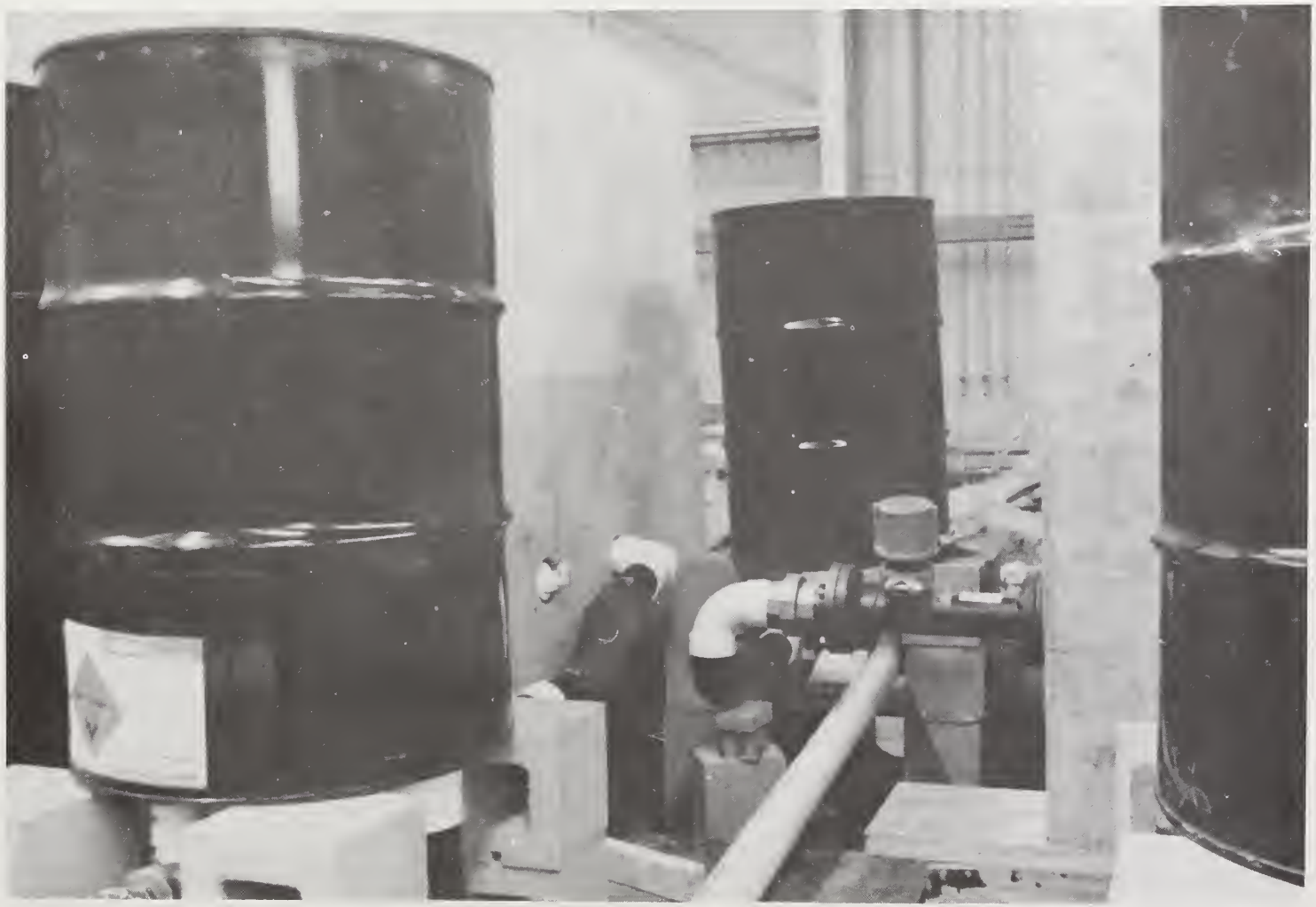

Figure 36. Detail of Upstream and Downstream Constant Head Tanks for High Permeability Cell System.

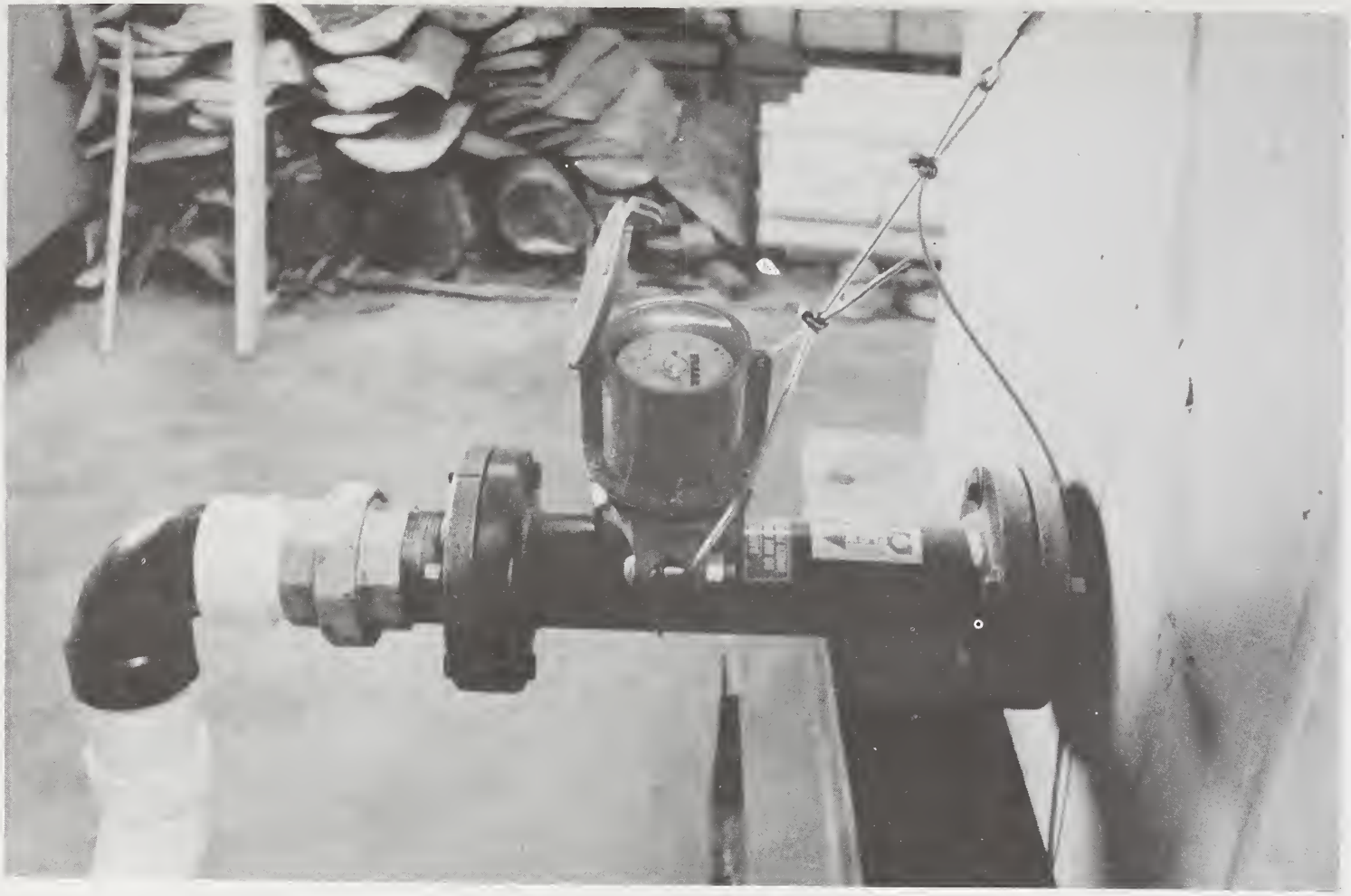

Figure 37. Detail of Flow Meter Used for Flow Rate Determination In High Permeability Cell System

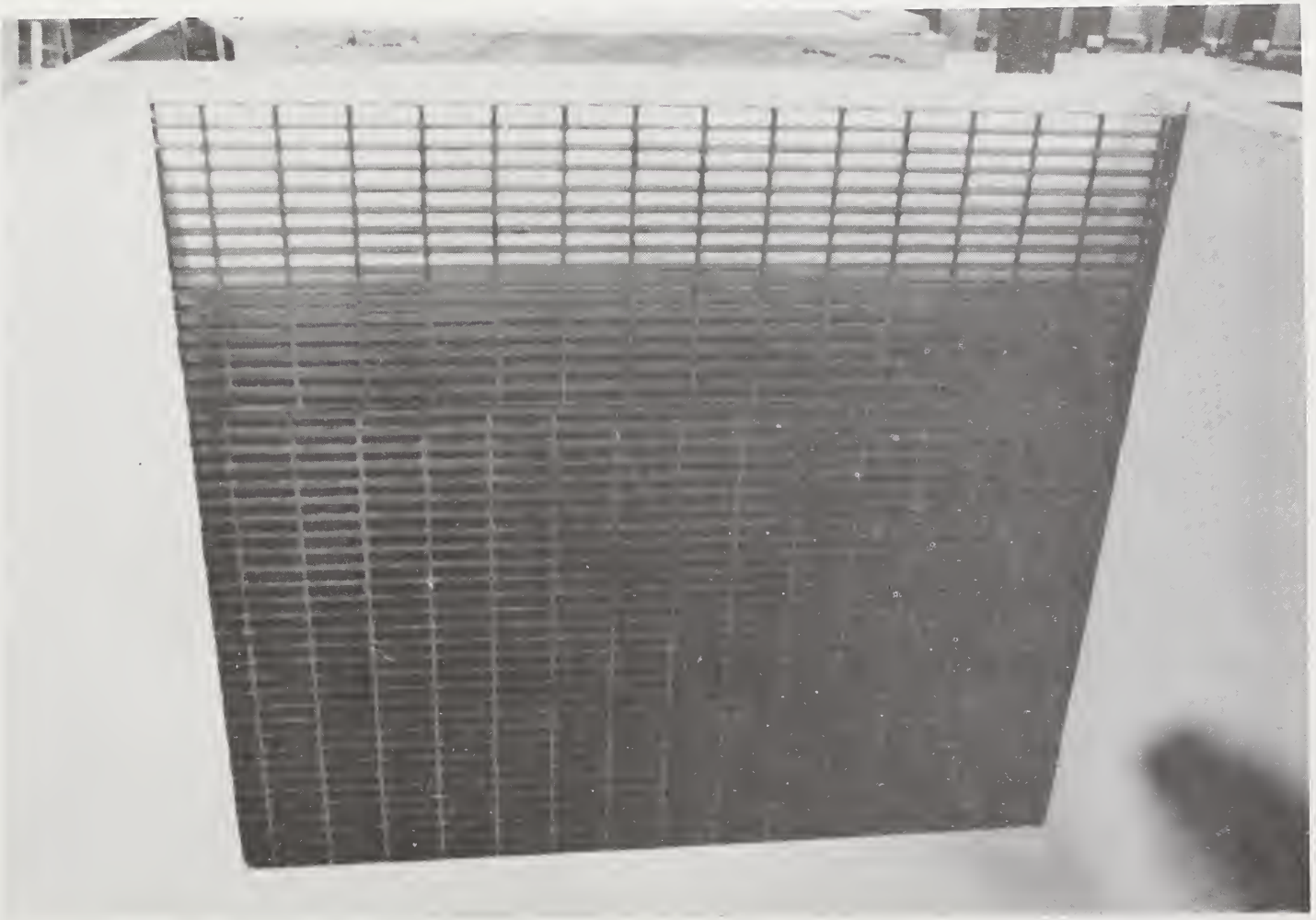

Figure 38. Detail of Metal Walkway Grating Used to Contain Simulated Pavement Section in Cell.

Operation of the System

Prior to utilizing the cell systems for testing purposes, their operation was checked to insure satisfactory performance under anticipated operating conditions. At different flow rates, established by adjusting the sump return valve, the water level in the downstream constant head tank was monitored for fluctuation. Although little fluctuation was noted, several desirable modifications/additions to the system were identified. Firstly, at peak flow in the LPCS it was observed that the constant head tank outlet had a tendency to surge (i.e., periodically inundate the overflow pipe). This problem was solved using a bell-mouth overflow pipe. Secondly, to obtain more precise measurements of the upstream and downstream pressure heads, piezometer tubes were installed at both the inlet and outlet reservoirs of the individual cells.

Operation of the cell system for determination of the permeability of various layers of a pavement system is accomplished in the following steps:

1. With tank in a horizontal position, place and compact soil/aggregate layers in the simulated pavement section to desired thicknesses and densities.
2. Tilt tank to desired grade to produce uniform sheet flow at appropriate hydraulic gradient under operating conditions.
3. Saturate simulated pavement section by upward flow of water from the saturation/underdrainage system.
4. Install upstream and downstream overflow pipe sections at required elevations.
5. Establish steady state flow conditions through the layer(s) by adjusting sump return valve and monitoring upstream and downstream piezometric levels.
6. Determine the quantity of flow through the soil/aggregate layer(s) using the manual method for the LPCS or the flow

meters or manual method for the HPCS.

7. Repeat steps 4 through 7 for additional layers. For multi-layer systems, the flow through each additional layer must be determined from the total quantity of flow and the quantity of flow through the previous layer(s).

The soil/aggregate is uniformly placed in the cell using a concrete hopper bucket adapted for use with typical base and subbase materials. Because of the physical characteristics of the cell, the layer is enclosed on two sides by the walls of the cell and on two sides by the steel walkway gratings. As necessary, filter fabric[1] and/or wire mesh (1/4 inch (6.35 mm) square openings) is utilized between the layer and the grating to prevent the loss of material through the upstream and downstream gratings. Compaction of the layer is accomplished by multiple passes of a Model PCS-30 Homelite Plate Compactor purchased for use in the project. Density determinations of the in place layer may be based on the weight and volume of the as compacted layer and/or by use of a nuclear moisture-density gage.

After flushing air from the saturation/underdrainage pipe network, water from the saturation tank is permitted to flow upward through the layer to produce an essentially saturated condition. The flow conditions during this process are carefully monitored to insure that piping and/or disturbance of the layer does not occur. Once the appropriate saturation process has been completed, the valve to the saturation tank is closed to prevent any flow into or from that system.

---

[1] Mirafi(TM) 140 Fabric, Celanese Fibers Marketing Company, New York.

To produce uniform sheet flow through the pavement layer at the appropriate hydraulic gradient, the tank is tilted to the desired position with wooden chocks. The tank is tilted by use of the overhead crane and the lifting anchors embedded in the cell walls. A surveying level is utilized to establish the appropriate elevations of the upstream section of the cell as well as for the overflow pipes in the upstream and downstream constant head tanks. In addition, the level is used to determine the average thickness of the compacted soil/aggregate layer(s).

Once the pump is started to initiate flow through the system, the upstream and downstream piezometric levels are monitored to verify the establishment of steady state flow conditions. Coarse adjustment of the required quantity of flow can be accomplished by use of the sump return valve provided in the hydraulic circulation system. Fine adjustment of the flow quantity is automatically accomplished by the overflow pipe in the upstream constant head tank. The appropriate hydraulic gradient is maintained by properly positioned overflow pipes in both the upstream and downstream constant head tanks.

After steady state flow conditions are established, the quantity of flow is determined by the manual method for the LPCS and by flow meters or the manual method for the HPCS. On the LPCS, valves are appropriately located to permit collection of flow passing through the downstream CHT overflow pipe. A sufficient number of flow measurements are taken to insure satisfactory accuracy. The flow meters in the hydraulic circulation system of the HPCS will be utilized to determine the steady state flow quantity for the high permeability tests. In addition to instantaneous flow quantities, the flow meters also permit determination of accumulated flow quantities. Thus, a more accurate determination of the average quantity of flow is possible.

In testing a multi-layered system, the testing must progress from bottom to top in sequence. In that way, the quantity of flow

passing through each preceding layer or combination of layers will be known. Based on this information plus the physical dimensions of the layers and the hydraulic gradient, the average horizontal coefficient of permeability for each layer can be calculated using the following equation:

$$k_n = \frac{q_n}{i\ A_n}$$

where k_n = the coefficient of permeability of the layer under consideration,

q_n = the flow rate through the layer under consideration = $q-q_{n-1}$,

i = hydraulic gradient, and

A_n = area of layer under consideration = thickness of layer (T_n) x width of layer (B).

As indicated above, the value of the flow rate for the layer under consideration (q_n) is calculated using the following equation:

$$q_n = q-q_{n-1}$$

where q = the total flow rate through the section undergoing steady state sheet flow and

q_{n-1} = the total flow rate through the preceding layer or layers.

Thus,

$$q = \sum_{i=1}^{n} q_i$$

and

$$q_{n-1} = \sum_{i=1}^{n-1} q_i$$

where n = number of layers undergoing steady state sheet flow for a given test.

APPENDIX B

Design and Construction Details For Prototype Field Permeability Test Device

Reservoir and Pressure Subsystem

As indicated above, the reservoir and pressure system consists of the fresh water supply tanks, a salt water supply tank, and a pressure source (Figure 15).

The fresh water supply tanks provide the source of water for saturating the base or subbase and establishing steady state flow during permeability testing. These tanks were constructed from two 55 gallon (0.208 m^3) steel drums, which are supported on a timber frame as shown in Figure 39. The tanks are connected at the bottom by a 3/4 inch (19.05 mm) galvanized pipe manifold to a single 1/2 inch (12.7 mm) O.D. plastic tubing, which constitutes the main water supply line. This water supply line is provided with a shut-off valve. One of the tanks is equipped with a water level indicator consisting of 1/4 inch (6.35 mm) O.D. plastic tubing which is connected to the pressure source. The tanks are also provided with gasketed caps that can be removed so that the water supply system can operate under atmospheric pressure if desired.

The salt water (electrolyte) supply tank, which is constructed from 6 inch (152.4 mm) O.D. plexiglass tubing with a 1/4 inch (6.35 mm) wall thickness, is supported on an adjustable frame made of 1 1/4 inch (31.75 mm) x 1 1/4 inch (31.75 mm) x 1/8 inch (3.18 mm) steel angles. The salt water tank and its supporting frame are shown in Figure 40. The adjustable frame permits the tank to be raised or lowered so that the salt water level is the same as the fresh water level during testing. The 1/2 inch (12.7 mm) O.D. plastic outlet tubing from the tank is provided with a shut-off valve. The top of the salt water tank is connected to the pressure source with 1/4 inch (6.35 mm) O.D. plastic tubing.

The pressure source consists of cylinder of nitrogen equipped with a coarse pressure regulator. Fine pressure control is provided by an additional pressure regulator in the plastic line between the

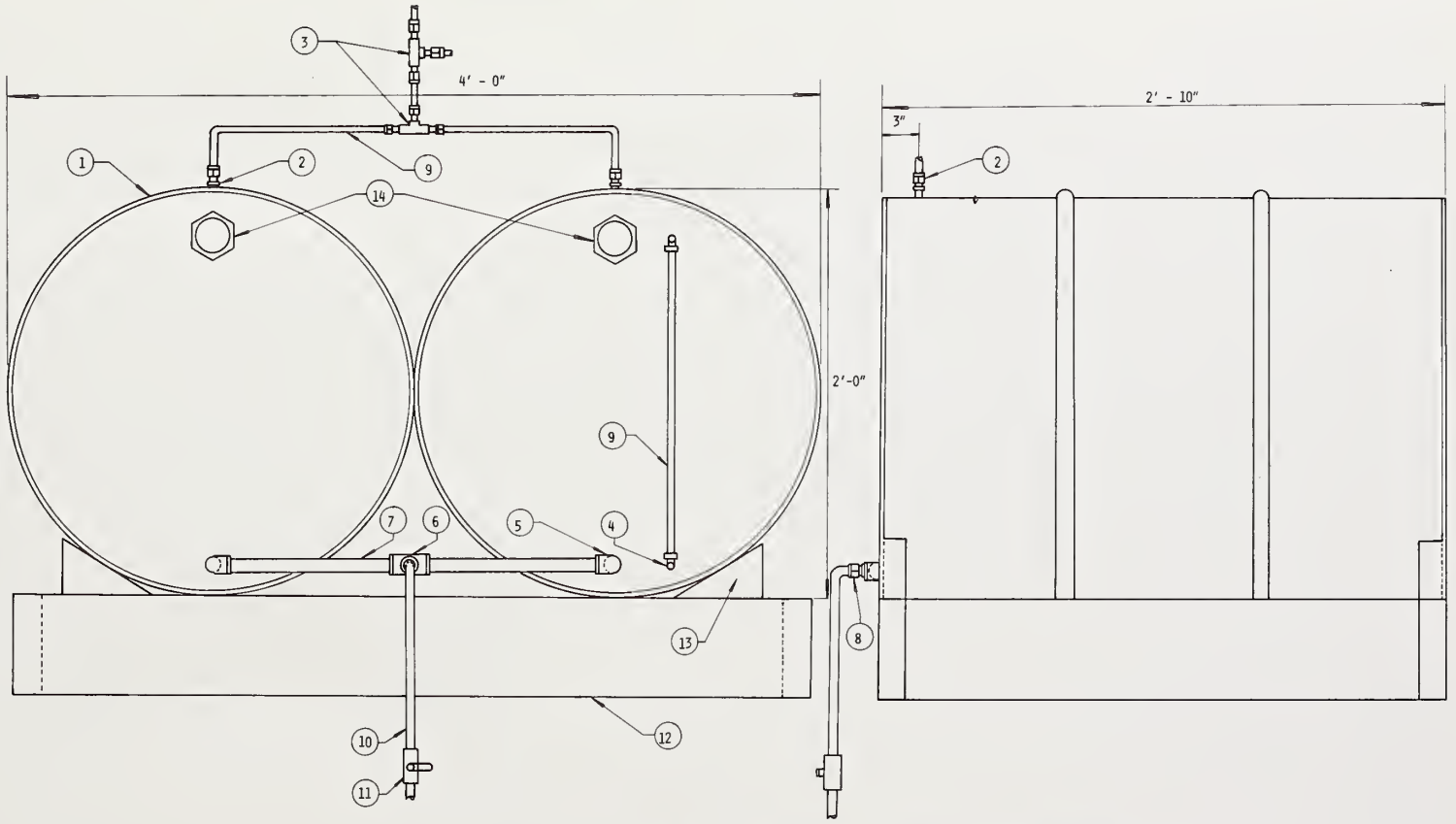

NOTE: 1 FT. = 0.3048 METER
1 IN. = 25.4 MILLIMETERS

ITEM	LIST OF MATERIALS	ITEM	LIST OF MATERIALS
1	55 GALLON DRUM	8	3/4" MALE TO 1/2" O.D. TUBE REDUCER
2	SWAGELOK CAT. NO. B-400-1-2	9	1/4" O.D. PLASTIC TUBING
3	SWAGELOK CAT. NO. B-400-3	10	1/2" O.D. PLASTIC TUBING
4	SWAGELOK CAT. NO. B-400-2-2	11	BRASS SHUT-OFF VALVE
5	3/4" PIPE 90° STREET ELBOW	12	2" x 6" TIMBER
6	3/4" PIPE TEE	13	2" TIMBER BLOCK
7	3/4" GALVANIZED PIPE	14	CAPS WITH RUBBER GASKETS

Figure 39. Fresh Water Tanks.

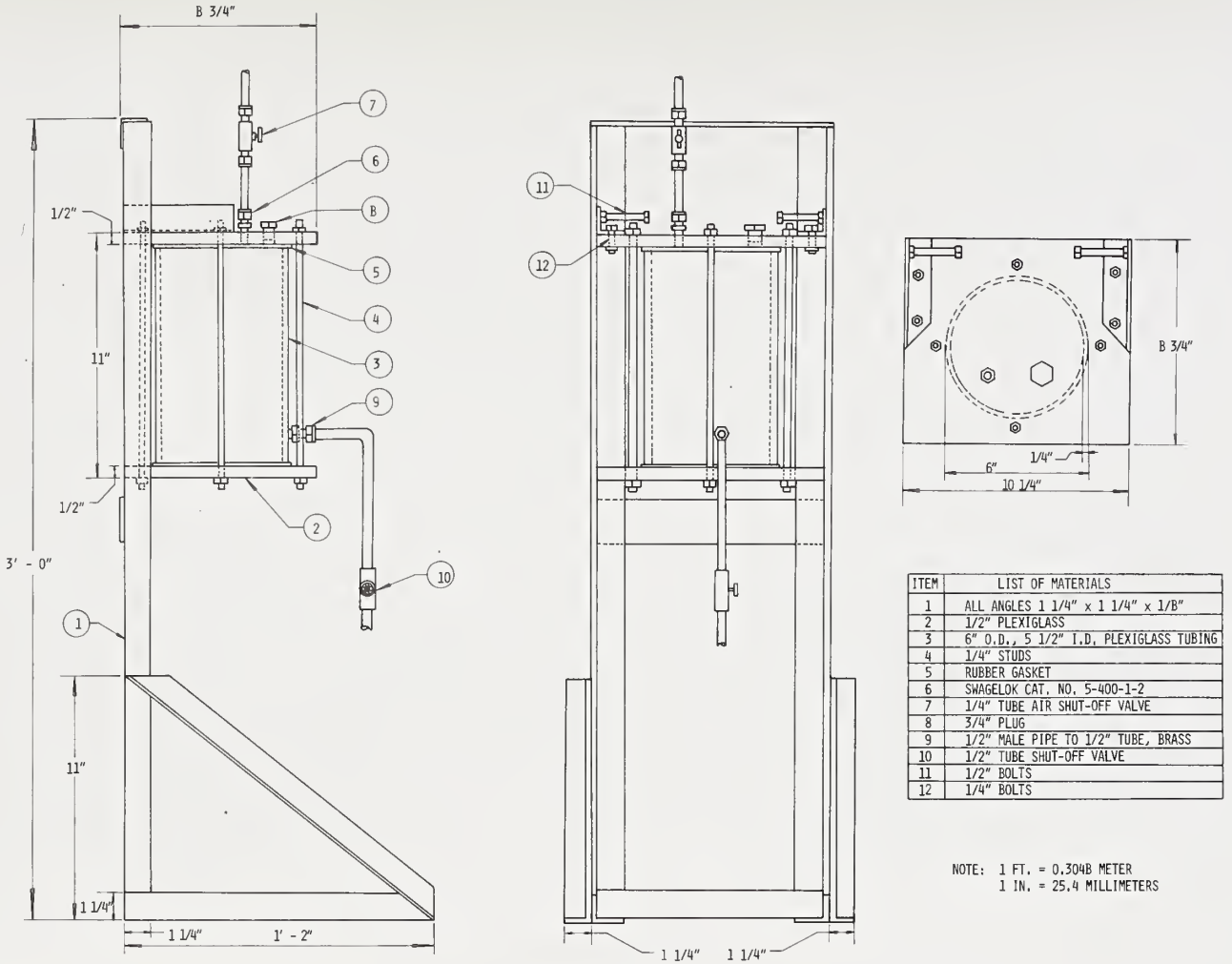

ITEM	LIST OF MATERIALS
1	ALL ANGLES 1 1/4" x 1 1/4" x 1/8"
2	1/2" PLEXIGLASS
3	6" O.D., 5 1/2" I.D. PLEXIGLASS TUBING
4	1/4" STUDS
5	RUBBER GASKET
6	SWAGELOK CAT. NO. 5-400-1-2
7	1/4" TUBE AIR SHUT-OFF VALVE
8	3/4" PLUG
9	1/2" MALE PIPE TO 1/2" TUBE, BRASS
10	1/2" TUBE SHUT-OFF VALVE
11	1/2" BOLTS
12	1/4" BOLTS

NOTE: 1 FT. = 0.3048 METER
1 IN. = 25.4 MILLIMETERS

Figure 40. Salt Water Tank

nitrogen tank and the water supply tanks.

Control and Measurement Subsystem

The Control and Measurement Subsystem, which is shown schematically in Figure 16, consists of the hydraulic controls, the electrical sensing system, and the pressure sensing system. The details of the system are shown in Figure 41.

The hydraulic controls on the water supply line consist of a three-way valve and a fine adjustment valve. The three-way valve provides for shut off of the water supply or access to either the fresh water supply or the salt water supply. The fine adjustment valve, as the name implies, provides for precise control of the water supply to the water injection probe. The fresh water and salt water inlets and outlet tubing are provided with quick-connect couplings for rapid connection to the other subsystems of the FPTD.

Each of the two electrical sensing circuits consists of a rechargeable battery, toggle switch, variable resistor, and DC microammeter with connecting wire and phono plug. The variable resistor allows for the adjustment of the response of the microammeter, and the phono plug provides for the connection of the sensing circuit to the electrodes in the sensing probes. The on-off switch allows the sensing circuits to be opened after microammeter deflection during testing to avoid overloading and damaging the microammeters.

The pressure sensing system, which is used to determine the head difference between the pressure taps contained in the sensing probes, consists of a Dwyer manometer with 1/4 inch (6.35 mm) O.D. plastic supply lines.[1] Each of the manometer supply lines is

---

[1] It was originally anticipated that the head loss between sensing probes would be measured using Capsuhelic Differential Pressure Gages, manufactured by Dwyer Instruments, Inc. However, these gages proved to be unreliable for long term use, and they were abandoned in favor of the more reliable manometer system.

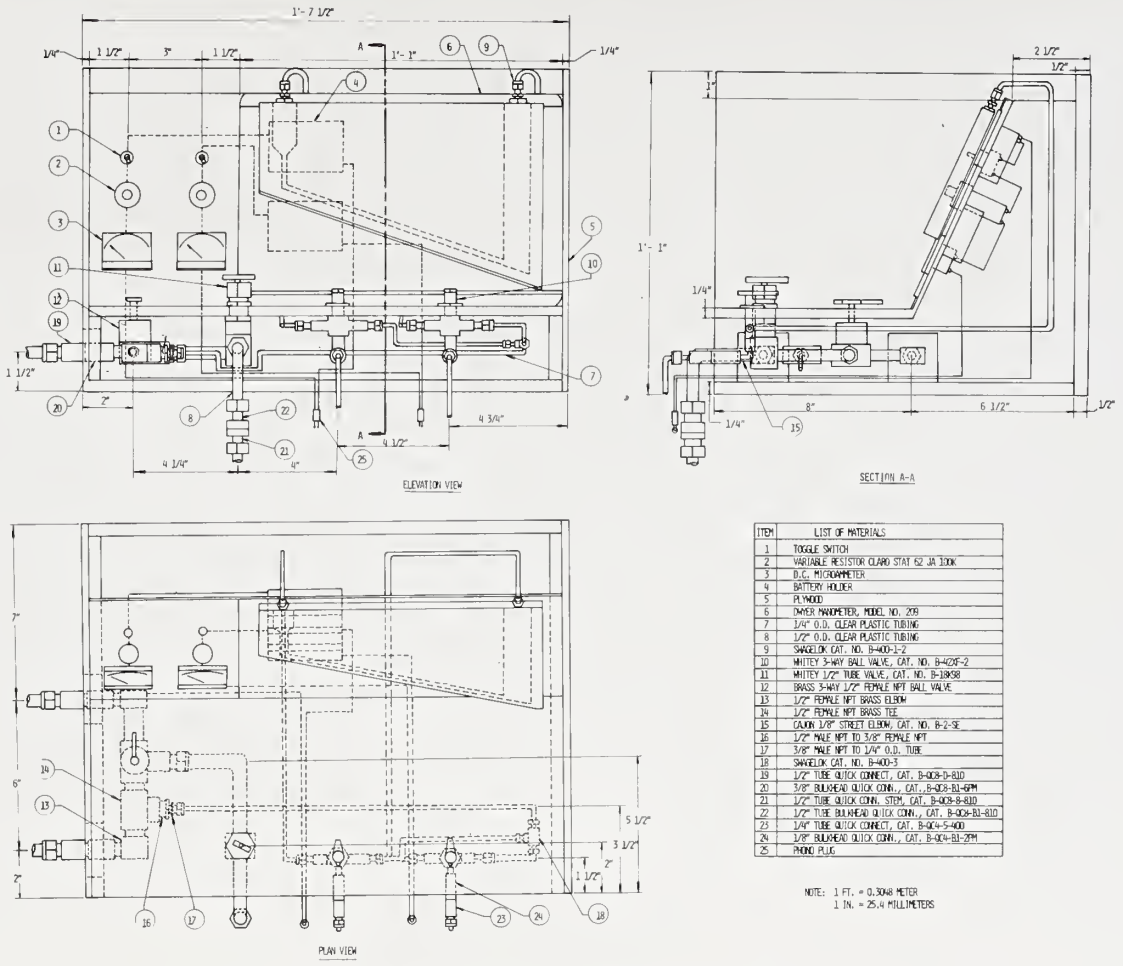

ITEM	LIST OF MATERIALS
1	TOGGLE SWITCH
2	VARIABLE RESISTOR CLAROSTAT 62 JA 100K
3	D.C. MICROAMMETER
4	BATTERY HOLDER
5	PLYWOOD
6	DWYER MANOMETER, MODEL NO. 209
7	1/4" O.D. CLEAR PLASTIC TUBING
8	1/2" O.D. CLEAR PLASTIC TUBING
9	SWAGELOK CAT. NO. B-400-1-2
10	WHITEY 3-WAY BALL VALVE, CAT. NO. B-4ZDF-2
11	WHITEY 1/2" TUBE VALVE, CAT. NO. B-18RS8
12	BRASS 3-WAY 1/2" FEMALE NPT BALL VALVE
13	1/2" FEMALE NPT BRASS ELBOW
14	1/2" FEMALE NPT BRASS TEE
15	CAJON 1/8" STREET ELBOW, CAT. NO. B-2-SE
16	1/2" MALE NPT TO 3/8" FEMALE NPT
17	3/8" MALE NPT TO 1/4" O.D. TUBE
18	SWAGELOK CAT. NO. B-400-3
19	1/2" TUBE QUICK CONNECT, CAT. B-QC8-D-810
20	3/8" BULKHEAD QUICK CONN., CAT., B-QC8-B1-6PM
21	1/2" TUBE QUICK CONN. STEM, CAT. B-QC8-B-810
22	1/2" TUBE BULKHEAD QUICK CONN., CAT. B-QC6-B1-810
23	1/4" TUBE QUICK CONNECT, CAT. B-QC4-5-400
24	1/8" BULKHEAD QUICK CONN., CAT. B-QC4-B1-2PM
25	PHONO PLUG

Figure 41. Control and Measurement Subsystem

interconnected with the fresh water supply line and provided with a three-way valve to permit shut-off or flushing of the manometer lines to remove entrapped air if encessary. The manometer supply lines are equipped with quick-connect couplings for rapid connection to the pressure tap lines on the sensing probes. The sloping position of the manometer, shown in Figure 41, was established so that the manometer would be direct reading on the attached scale up to 3 inches (76.2 mm) of water with the blue indicator fluid provided. This makes it critical that control and measurement subsystems be level during testing. Thus, this unit has been provided with level indicator bubbles so that its position can be properly adjusted during setup prior to testing.

Plate and Probe Subsystem

As indicated earlier, the plate and probe system consists of the horizontal plate, the water injection probe and the sensing probes. Two versions of the 18 inch (457.2 mm) diameter aluminum plate are shown in Figure 42. Both versions are equipped with a central port, through which the water injection probe is inserted, and radially located ports through which the sensing probes can be inserted. The original plate was recessed on the bottom to permit the placement of a soft rubber seal between the surface of the plate and the base or subbase. However, during field evaluation of the FPTD, some difficulty was encountered occasionally with the development of piping at the interface between the plate and the base or subbase. In an effort to avoid this difficulty, a revised plate was prepared with annular projections as shown in Figure 42.

The water injection probe, shown in Figure 43, simply consists of 1/2 inch (12.7 mm) O.D. copper tubing with a pointed steel tip. It is equipped with 1/4 inch (6.35 mm) diameter holes located on 3/8 inch (19.05 mm) centers. During testing, the probe is oriented so that these holes point in the direction of the row of plate ports,

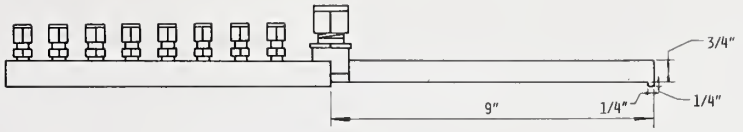

ORIGINAL PLATE

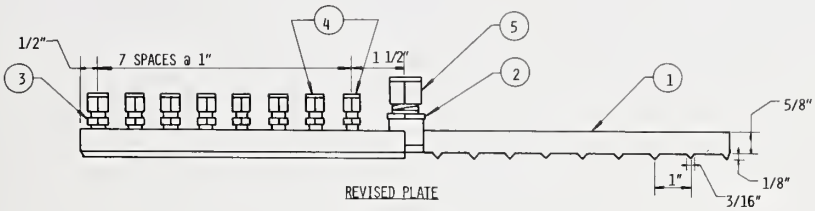

REVISED PLATE

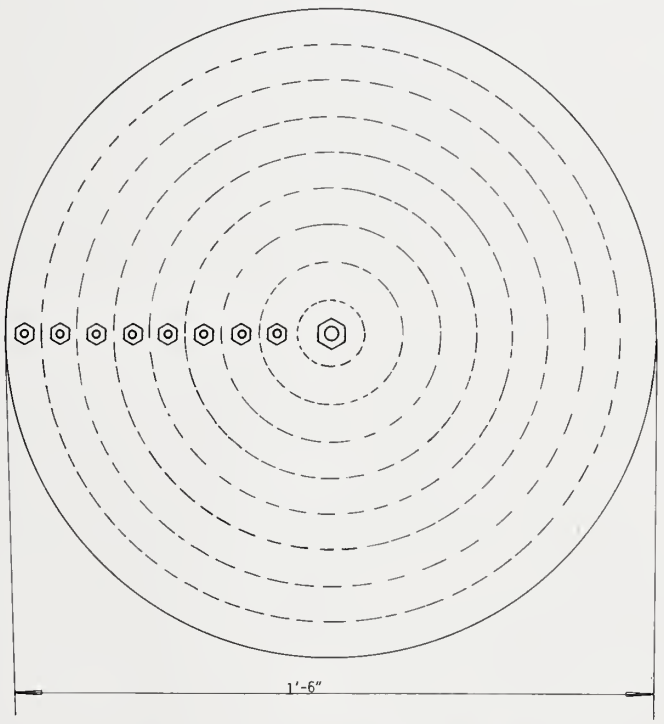

NOTE: 1 FT. = 0.3048 METER
1 IN. = 25.4 MILLIMETERS

ITEM	LIST OF MATERIALS
1	ALUMINUM PLATE
2	SWAGELOK CAT. NO. 13-810-1-12
3	SWAGELOK CAT. NO. B-400-1-2
4	SWAGELOK CAT. NO. B-402-1, OR
4	SWAGELOK CAT. NO. 400-P
5	SWAGELOK CAT. NO. B-812-1

Figure 42. Original and Revised Plates

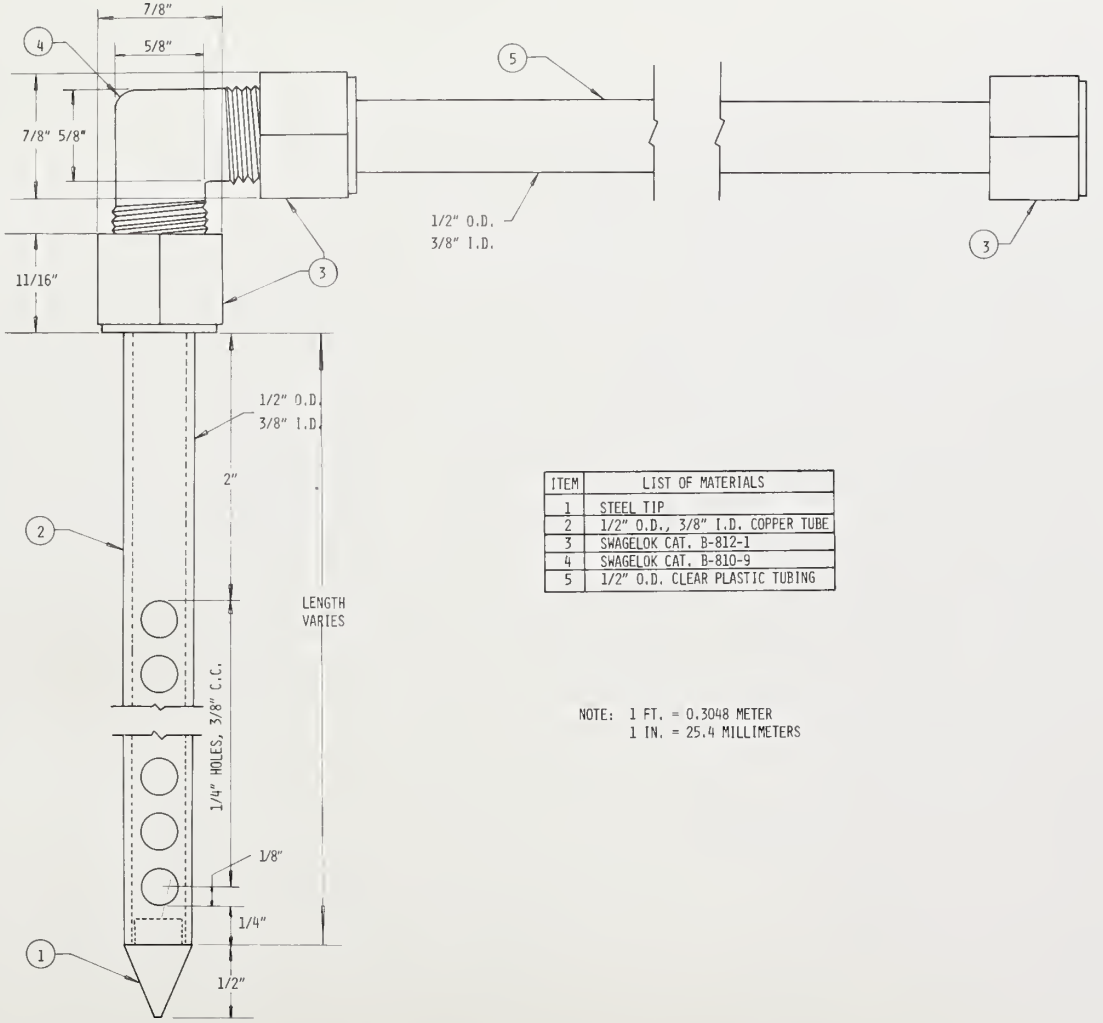

ITEM	LIST OF MATERIALS
1	STEEL TIP
2	1/2" O.D., 3/8" I.D. COPPER TUBE
3	SWAGELOK CAT. B-812-1
4	SWAGELOK CAT. B-810-9
5	1/2" O.D. CLEAR PLASTIC TUBING

NOTE: 1 FT. = 0.3048 METER
1 IN. = 25.4 MILLIMETERS

Figure 43. Water Injection Probe

i.e., in the direction of testing. Water injection probes were made in several different lengths to suit the geometry of the test situation.

The sensing probes, detailed in Figure 44, were constructed from 1/4 inch (6.35 mm) O.D. stainless steel tubing with a brass tip. The tip contains four 3/32 inch (2.38 mm) diameter ports to permit the access of water to the manometer for head measurement. A two wire electrode is brought down through the sensing probe and secured in the tip with epoxy. The sensing probes were made in various lengths to suit the geometry of the test situation.

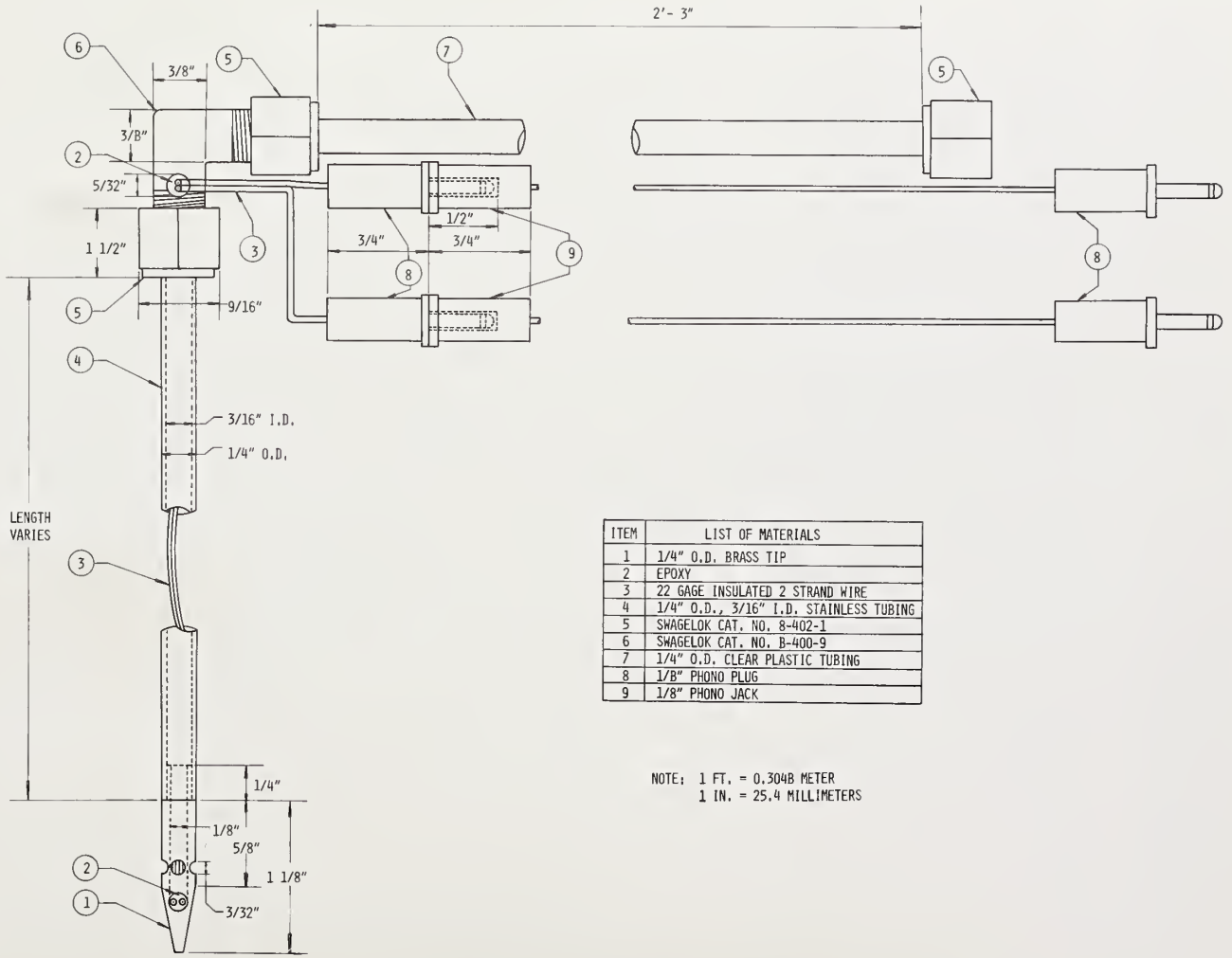

ITEM	LIST OF MATERIALS
1	1/4" O.D. BRASS TIP
2	EPOXY
3	22 GAGE INSULATED 2 STRAND WIRE
4	1/4" O.D., 3/16" I.D. STAINLESS TUBING
5	SWAGELOK CAT. NO. 8-402-1
6	SWAGELOK CAT. NO. B-400-9
7	1/4" O.D. CLEAR PLASTIC TUBING
8	1/8" PHONO PLUG
9	1/8" PHONO JACK

NOTE: 1 FT. = 0.3048 METER
1 IN. = 25.4 MILLIMETERS

Figure 44. Sensing Probe

* U.S.G.P.O. 629-017/1302-2198

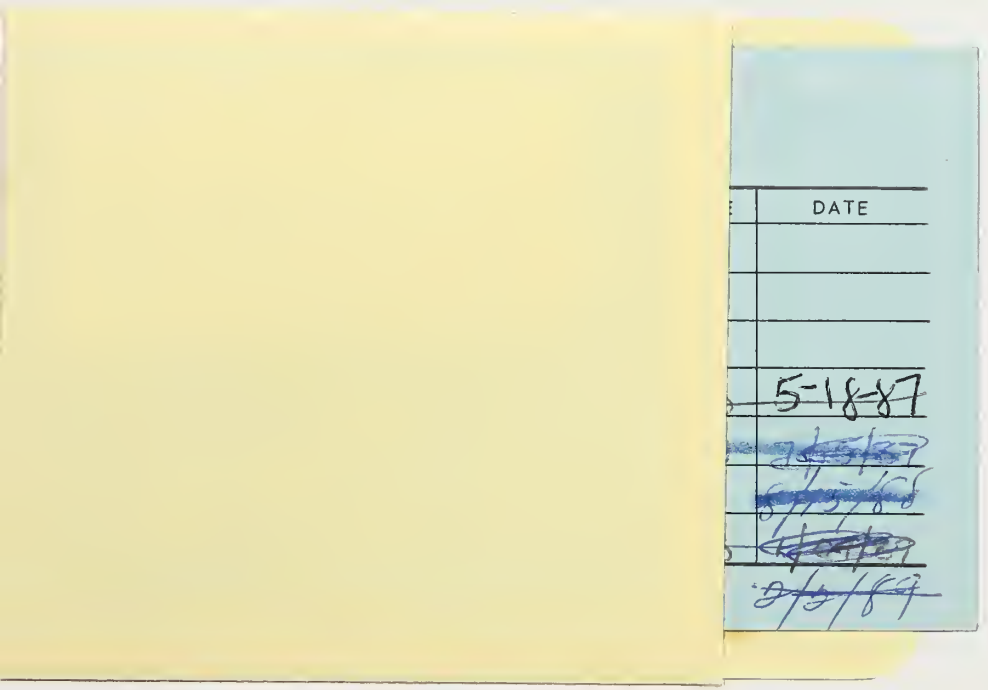
DATE
5-18-87

FEDERALLY COORDINATED PROGRAM OF HIGHWAY RESEARCH AND DEVELOPMENT (FCP)

The Offices of Research and Development of the Federal Highway Administration are responsible for a broad program of research with resources including its own staff, contract programs, and a Federal-Aid program which is conducted by or through the State highway departments and which also finances the National Cooperative Highway Research Program managed by the Transportation Research Board. The Federally Coordinated Program of Highway Research and Development (FCP) is a carefully selected group of projects aimed at urgent, national problems, which concentrates these resources on these problems to obtain timely solutions. Virtually all of the available funds and staff resources are a part of the FCP, together with as much of the Federal-aid research funds of the States and the NCHRP resources as the States agree to devote to these projects.*

FCP Category Descriptions

1. Improved Highway Design and Operation for Safety

Safety R&D addresses problems connected with the responsibilities of the Federal Highway Administration under the Highway Safety Act and includes investigation of appropriate design standards, roadside hardware, signing, and physical and scientific data for the formulation of improved safety regulations.

2. Reduction of Traffic Congestion and Improved Operational Efficiency

Traffic R&D is concerned with increasing the operational efficiency of existing highways by advancing technology, by improving designs for existing as well as new facilities, and by keeping the demand-capacity relationship in better balance through traffic management techniques such as bus and carpool preferential treatment, motorist information, and rerouting of traffic.

3. Environmental Considerations in Highway Design, Location, Construction, and Operation

Environmental R&D is directed toward identifying and evaluating highway elements which affect the quality of the human environment. The ultimate goals are reduction of adverse highway and traffic impacts, and protection and enhancement of the environment.

4. Improved Materials Utilization and Durability

Materials R&D is concerned with expanding the knowledge of materials properties and technology to fully utilize available naturally occurring materials, to develop extender or substitute materials for materials in short supply, and to devise procedures for converting industrial and other wastes into useful highway products. These activities are all directed toward the common goals of lowering the cost of highway construction and extending the period of maintenance-free operation.

5. Improved Design to Reduce Costs, Extend Life Expectancy, and Insure Structural Safety

Structural R&D is concerned with furthering the latest technological advances in structural designs, fabrication processes, and construction techniques, to provide safe, efficient highways at reasonable cost.

6. Prototype Development and Implementation of Research

This category is concerned with developing and transferring research and technology into practice, or, as it has been commonly identified, "technology transfer."

7. Improved Technology for Highway Maintenance

Maintenance R&D objectives include the development and application of new technology to improve management, to augment the utilization of resources, and to increase operational efficiency and safety in the maintenance of highway facilities.

---

* The complete 7-volume official statement of the FCP is available from the National Technical Information Service (NTIS), Springfield, Virginia 22161 (Order No. PB 242057, price $45 postpaid). Single copies of the introductory volume are obtainable without charge from Program Analysis (HRD-2), Offices of Research and Development, Federal Highway Administration, Washington, D.C. 20590.